Äspö Hard Rock Laboratory

Äspö Task Force on modelling of groundwater flow and transport of solutes

Discrete fracture network flow and transport modelling at the rock block scale: Task 6D, 6E, 6F and 6F2.

William Dershowitz

Aaron Fox

Glori Lee

Mick Van Fossen

Golder Associates, Inc.

Masahiro Uchida

JNC Tokai

November 2005

SKB

**Äspö Hard Rock
Laboratory**

Äspö Hard Rock Laboratory

Äspö Task Force on modelling of groundwater flow and transport of solutes

Discrete fracture network flow and transport modelling at the rock block scale: Task 6D, 6E, 6F and 6F2.

William Dershowitz
Aaron Fox
Glori Lee
Mick Van Fossen
Golder Associates, Inc.

Masahiro Uchida
JNC Tokai

November 2005

Abstract

The JNC/Golder team has developed discrete fracture network (DFN) approaches for modelling solute transport in fractured rocks with multiple immobile zones. This approach provides significant advantages, including its ability to directly model the geometry and transport pathways, and the variation of transport properties along those pathways. Immobile zones are particularly important for solute transport at the long time scales of radioactive waste repository safety assessment.

This report presents a series of simulations carried out by JNC/Golder for the Äspö Modelling Task Force, Tasks 6D through 6F. These tasks looked at solute transport at experimental (Task 6D) and performance assessment (Task 6E) time scales in a synthetic rock block containing well defined fractures. Due to the complicated nature of transport in the fracture network, Tasks 6F and 6F2 were defined to study transport in a simpler geometry, under similar boundary conditions.

The JNC/Golder team carried out all of these simulations using a channel network discretization of the project reference 200 m scale deterministic discrete fracture network (DFN). The channel network was developed by utilizing rectangular cross-section pipe elements to connect fracture intersections on fracture planes. Each pipe element was assigned transport and immobile zone properties corresponding to the hydrostructural and microstructural reference model used by the project. The JNC/Golder simulations demonstrated the importance of assumptions regarding fracture type and complexity for PA time scale solute transport. They also demonstrated that assumptions regarding fracture orientation and size are of lesser importance.

Sammanfattning

Ett team från JNC/Golder har utvecklat ett koncept baserat på diskreta spricknätverk (DFN) för modellering av transport av lösta ämnen i sprickigt berg med multipla immobila zoner. Konceptet erbjuder flera betydelsefulla fördelar såsom möjligheten att direkt modellera geometrier och transportvägar och variationen av transportegenskaper utmed dessa transportvägar. Immobila zoner är speciellt viktiga för transport av lösta ämnen för de tidsskalor som är av intresse för säkerhetsanalysen för slutförvaring av kärnbränsle.

Denna rapport presenterar en serie av simuleringar som har utförts av JNC/Golder inom Äspö Task Force för modellering av grundvattenströmning och ämnestransport. Modelleringsuppgifterna är i detta fall Task 6D till och med 6F. Dessa modelleringsuppgifter inriktar sig på transport av lösta ämnen i experimentell skala (Task 6D) och säkerhetsanalysskala (Task 6E) för en syntetisk bergblocksmodell med väldefinierade sprickor. Eftersom problemet med transport i spricknätverk är av komplicerad natur, inriktade sig Task 6F och 6F2 på enklare geometrier under liknande randvillkor som ovan.

Teamet från JNC/Golder utförde samtliga simuleringar med hjälp av ett kanalnätverk som baserades på det referensspricknätverk (DFN), en deterministisk modell i 200-metersskalan, som definierats för projektet. Kanalnätverket byggdes upp av rörelement, med rektangulärt tvärsnitt, som kopplar ihop sprickkorsningar i sprickplanen. Varje rörelement tilldelades transportegenskaper och egenskaper för immobil zon i enlighet med projektets hydrostrukturella och mikrostrukturella referensmodell. JNC/Golder-simuleringarna påvisade vikten av de antaganden som görs angående typ av sprickor och angående sprickornas komplexitet för transport i säkerhetsanalysskala. Det visades även att antaganden om sprickorientering och sprickstorlek är av mindre vikt.

Contents

List of Tables

List of Figures

1 Introduction

1.1 Background

Solute transport in discrete fracture networks is a key aspect of repository safety. As a result, detailed approaches have been developed for analysis and simulation of DFN solute transport for both performance assessment (PA) and repository site characterization (SC). These approaches can be quite different, and Task 6 seeks to bridge the gap between PA and SC type models. Task 6 is focused on the 50 to 100m scale, which is the scale of many SC experiments, and also a key scale for geosphere barriers in the JNC repository program.

1.2 Objectives

The JNC/Golder team's objectives for Task 6 are as follows:

- Identify key assumptions needed for long term prediction in PA and identify less important assumptions in PA

- Identify the most significant PA model components of a site.

- Prioritize assumptions in PA modelling and demonstrate a rationale for simplifications in PA-models by parallel application of several PA models of varying degree of simplification.

- Provide a benchmark for comparison of PA and SC models in terms of PA measures for radionuclide transport at PA temporal and spatial scales

- Establish how to transfer SC models using site characterization data to PA models, i.e., how to simplify SC models into PA models in a consistent manner

1.3 Outline of report

The JNC/Golder report of Task 6F simulation results is structured as follows:

- Chapter 2 summarizes the various model tasks and methodologies assigned during each phase of Task 6.

- Chapter 3 describes the basic JNC/Golder discrete-fracture network / channel network (DFN-CN) modelling approach. This chapter includes a mathematical description of both the flow and transport models, as well as the JNC/Golder team's implementation of the Task 6C microstructural and fracture complexity models.

- Chapter 4 describes the JNC/Golder methodology, implementation, and results for Task 6D.

- Chapter 5 describes the JNC/Golder methodology, implementation, and results for Task 6E.

- Chapter 6 describes the JNC/Golder methodology, implementation, and results for Task 6F and 6F2.

- Chapter 7 presents the general conclusions of the JNC/Golder modelling team for Task 6, and includes our recommendations for future work.

2   Modelling Tasks

2.1   Task 6D – Block scale transport on a tracer test time scale

The fracture geometry, transport properties, and boundary conditions for Task 6D were specified by Elert and Selroos (2002). This section provides a summary of these specifications, with a description of how specific features of the specification were implemented in each of the JNC/Golder modelling efforts.

Task 6D was designed to be carried out at site characterization time and spatial scales. The time scale for Task 6D was specified as the time scale over which the TRUE-BS project, Phase C2 tracer test was carried out, extended to included additional, more strongly sorbing tracers. The simulations described here were therefore carried out to 10^8 seconds (3.2 years). This allowed for recovery of even the most strongly sorbing tracers simulated.

The spatial scale for Task 6D can be defined by (a) the scale of the model, which was a 200 m block, (b) the Euclidian distance between injection and withdrawal sections (17.6 m), (c) the estimated fracture network path length between the injection and withdrawal sections (66 m). For DFN simulations, there are several pathways through the fracture network, with lengths varying from 50 to over 100 m.

2.2   Task 6E – Block scale transport on a PA time scale

Task 6E (Elert and Selroos, 2004b)was designed to move the Task 6D transport conceptual models to a reference set of performance assessment (PA) time scales and boundary conditions. Sensitivity studies similar to those conducted during Task 6D were to be completed. JNC/Golder Task 6E simulations were performed at the 200 meter TRUE block scale, as defined in the Task 6C semi-synthetic hydrostructural model report (Dershowitz et. al., 2002). With tracer source sections near the center of the 200 meter block, Euclidian distances ranged from 10 – 100 meters, while transport pathway lengths were typically in the 50 – 200 meter range, depending on sink location.

JNC/Golder Task 6E simulations were run with observation windows of years to decades, with total simulation durations of 100 million (1.0×10^8) years. Temporal resolution was slightly greater near the beginning of the tracer tests (to adequately capture early-time behaviors) and slightly less near the end of the simulations.

The fracture network geometries, transport properties, and boundary conditions for Task 6E were constrained by Elert and Selroos (2004b) in a draft modelling specification. Additional performance metrics, such as the computation of water residence time distributions and pathway β-factors, were completed as specified in Elert and Selroos (2004a).

2.3   Task 6F – PA Benchmark

Task 6F originated as a response to concerns aired during the September 2003 Task 6 Workshop. Specifically, the combination of a complex fracture network model (the Task 6C DFN) with a series of conceptually and mathematically different models made the comparison and analysis of results between teams very difficult. It was decided at that meeting to perform a series of 'test-bench' style simulations within a simplified DFN network. The goal of Task 6F was to produce a model simple enough to facilitate direct comparisons between modelling teams.

Task 6F utilized the fracture complexity, geologic structure assignment, and the microstructural model from the Task 6C report (Dershowitz et al., 2002). Flow and transport were simulated in a single Type I (fault) and a single Type II (joint) structure, using several tracers from the Task 6E experiment. The boundary conditions, model specifications, and performance metrics for the Task 6F experiment were presented in Elert and Selroos (2004c). The experiment was performed at Site Characterization (SC) temporal (0.1 – 10 years) and spatial (10 – 100 m) scales, with DFN background fractures based on those encountered in the TRUE Block Scale volume (Task 6C report: Dershowitz et al., 2002).

2.4   Task 6F2 - Sensitivity study

Task 6F2 consisted of a series of additional model studies designed to further evaluate aspects of the Task 6E and 6F DFN models. The primary goal of Task 6F2 was to further constrain the differences between the Task 6 results produced by the various modelling teams, as well as continuing to assess the sensitivity of Task 6 models to changes in assumptions and parameters.   The detailed scope of the sensitivity studies were left to the individual modelling teams; however a list of suggested topics was presented in the Task definition (Elert and Selroos, 2004d).

The JNC/Golder team elected to test the effect of the geometry of the flow system (specifically, the discretization process from DFN to CN) on tracer transport within a low-complexity feature. The study was conducted at the same spatial and temporal scales as Task 6F, and used Task 6F Model Cases A1 (Structure 1S) and A2 (Stucture 4S) as the model basis.

3 General Task 6 Conceptual Models

Most of the JNC/Golder modelling efforts during the Task 6 program have utilized the FracMan discrete fracture network modelling software components

- FracWorks XP (discrete fracture network generation and geometry)

- MAFIC (finiite element flow),

- PAWorks (transport pathways identification), and

- LTG (Laplace Transform Galerkin solute transport with multiple immobile zones).

The underlying mathematics and physics of the conceptual models implemented in these codes are described within this section.

Initial discrete fracture network models were built using FracWorks XP. The discrete fracture networks created by FracWorks XP are composed of three-dimensional polygonal elements. These elements were transformed to a three-dimensional network of one-dimensional, rectangular cross-section pipe elements (a 'channel network') utilizing PAWorks. The discretization process is described in detail in Section 3-1, and in the PAWorks/LTG software manual (Dershowitz et al., 2000). A summary of the general PAWorks approach is presented below as Figure 3-2. Solute transport and retention was simulated using the LTG software package.

3.1 JNC/Golder Flow Model

Flow was modeled using 1D pipe element networks and the FracMan/MAFIC code. The MAFIC flow model is described in Miller et al. (2001). In this model, each of the fracture intersections are considered to be line segments ("traces"). These segments, along with the edges of the polygonal fractures, are then used to discretize the fractures to either 1D or 2D finite elements. When discretizing a DFN to 2D elements, the fractures are transformed into triangular finite elements conditioned to match the edges of the fracture and the intersection traces. When discretizing a DFN to 1D (pipe) elements, the pipes are defined to provide connections between the intersection traces, which maintaining the same flow area between the fracture traces (Figure 3-1). The discretization process is described in detail in Dershowitz et al. (2000).
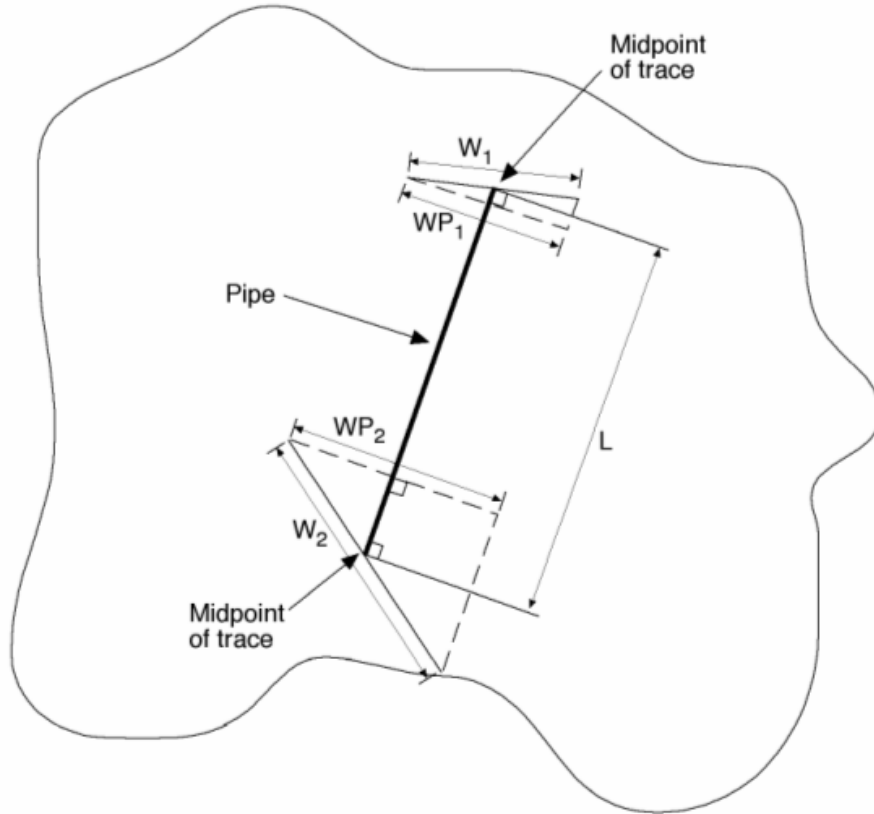
Figure 3-1. *Discretization of rectangular pipe elements between fracture intersection traces.*

Realistic fracture pattern

3D pipe connectivity topology

Finite element fow solution defines heads and flows in network

Graph theory identification of non-reentrant path between sources and sinks

Graph theory identification of non-reentrant path between sources and sinks

Approximate calculation of conductor properties and head fields among conductors

Pathway effective flow and transport properties

Output of pathways and geochemical properties to solute transport code LTG

Figure 3-2. *The general PAWorks approach to flow and transport within a 1D channel network approximation of a 3D discrete-fracture network. Figure from Dershowitz et al. (2000).*

3.1.1 Processes Considered

The flow model considers advective flow only. Advection is modeled as Darcy flow in rectangular cross-section pipes.

3.1.2 Mathematical Description

The mathematical description of flow modelling in MAFIC is taken from Miller et al, (2001). Using continuum principles of mass balance, the diffusivity equation which describes flow can be written as (Bear, 1972):

$$\frac{\partial}{\partial x_i}[\frac{\rho}{\mu}k_{ij}(\frac{\partial P}{\partial x_i}+\rho g\frac{\partial z}{\partial x_j})] = \rho(\alpha+\phi\beta)\frac{\partial P}{\partial t}-q$$

Equation 3-1

where:

x_i	=	coordinate directions (L)
ρ	=	fluid density (M/L^3)
μ	=	fluid viscosity (M/LT)
k_{ij}	=	permeability (absolute) (L^2)
P	=	fluid pressure (M/LT^2)
g	=	gravitational acceleration (L/T^2)
z	=	vertical direction (upward) (L)
α	=	pore compressibility (LT^2/M)
Φ	=	porosity
β	=	fluid compressibility (LT^2/M)
q	=	source term (M/T)
t	=	time (T)

For nearly incompressible fluid (e.g., water), and for flow in two dimensions (e.g., in a fracture), the mass-conservation of equation (3-1) can be simplified to a volume-conservation equation:

$$S\frac{\partial h}{\partial t}-K\overline{\nabla}^2 h = q$$

Equation 3-2

where:

S	=	Fracture Storativity (dimensionless)
h	=	Hydraulic head (L)
T	=	Fracture Transmissivity (L^2/T)
q	=	Source/Sink Term (L/T)
t	=	Time (T)
$\overline{\nabla}^2$	=	Two-dimensional Laplace Operator

3.1.3 Numerical Implementation

MAFIC uses a Galerkin finite element solution scheme to approximate the solution for Equation 3-1. The finite element approximation to the diffusivity equation in two dimensions is given by:

$$\sum_{m=1}^{N}\left[\int_R (T_{nm}\overline{\Delta}\xi_n \bullet \overline{\Delta}\xi_m \, dR)\, h_m\right] + \sum_{m=1}^{N}\left[\int_R (S_{nm}\xi_n\xi_m \, dR)\frac{dh_m}{dt}\right] = \int_R q\,\xi_n \, dR \quad n = 1,2,...N \quad \textbf{\textit{Equation 3-3}}$$

where:

T	=	fracture transmissivity (L^2 /T)	
S	=	fracture storativity (dimensionless)	
q	=	source flux, volume per unit area (L/T)	
ξ	=	linear or quadratic basis function	
R	=	element area (L^2)	
h	=	nodal hydraulic head (L)	
t	=	time (T)	
N	=	number of nodes	

For the present study, flow modelling was carried out using a three-dimensional network of rectangular cross-section pipe elements generated from the base discrete-fracture network model.

3.2 JNC/Golder LTG Transport Model

Solute transport was simulated using the Laplace Transform Galerkin method, as implemented in PAWorks / LTG (Dershowitz et al., 2000). Radionuclide transport occurred within a three-dimensional channel network composed of one-dimensional pipe elements, with multiple immobile zones working in parallel to simulate rock and structural interactions.

3.2.1 Processes Considered

Solute transport modelling with the PAWorks and LTG packages considers the following processes:

- advection
- dispersion (longitudinal only)
- diffusion (to immobile zones)
- sorption (in immobile zones)
- surface sorption (onto fracture mineral coatings)

Radionuclide decay and non-equilibrium chemical processes were not considered in Task 6 simulations.

3.2.2 Mathematical Description

This section describes the mathematical basis of the FracMan/PAWorks Laplace Transform Galerkin (LTG) solute transport model. This text is from Dershowitz et al (2000). The model topology is illustrated in Figure 3-3. The LTG transport solution is carried out assuming steady-state flow. A second-order approach is used to describe the diffusive mass transfer of a solute between the groundwater in a pipe and the multiple immobile porosity zones attached to it, the advective-dispersive transport of solute species n in a pipe network is given by:

$$A\left[R_n(\ell)\frac{\partial C_n}{\partial t} + q(\ell)\frac{\partial C_n}{\partial \ell} - \frac{\partial}{\partial \ell}D_{l_n}(\ell)\frac{\partial C_n}{\partial \ell} + R_n(\ell)\lambda_n C_n - R_{n-1}(\ell)\lambda_{n-1}C_{n-1}\right]$$

$$\pm \sum_{\ell'}\dot{M}\,\delta(\ell-\ell') + \sum_{\ell^*}Q(C_n - C_n^*)\delta(\ell-\ell^*) + \sum_{im=1}^{IM}P_{im}\theta_{im}D_{im}\frac{\partial C_n^{im}}{\partial w}\bigg|_{w=0} = 0$$

Equation 3-4

where:

n	=	nuclide index [-]
im	=	immobile zone class number (note: if desired $_{im}$ can equal 0) [-]
IM(ℓ) =		total number of immobile zones attached to pipe ℓ [-]
A(ℓ) =		pipe cross-sectional area [L^2]
Rn(ℓ) =		retardation factor [-]
q (ℓ) =		specific discharge ($\equiv$ Pipe velocity v) [L/T]
$D_{\ell_n}(\ell)$ =		dispersion coefficient = $\alpha v + D_n^o$ [L^2/T]
α	=	pipe longitudinal dispersivity [L],
D_n^o	=	free-solution diffusion coefficient [L^2/T]
λ_n	=	decay constant [1/T]
$\dot{M}$ (t)	=	internal solute mass source/sink [M/T]
Q	=	external fluid source/sink [L^3/T]
$\delta(\ell-\ell')$ =		Dirac delta [1/L]
$\delta(\ell-\ell^*)$ =		Dirac delta [1/L]
P_{im}	=	block surface area per unit length of matrix (equivalent to the effective perimeter of immobile zone $_{im}$) [L]
D_{im}	=	matrix effective diffusion coefficient [L^2/T]
θ_{im}	=	immobile zone porosity for immobile zone $_{im}$
Cn	=	pipe concentration [M/L^3]
C_n^*	=	concentration of injectate in external fluid source [M/L^3]

C_n^{im}	=	immobile zone concentration [M/L^3]
ℓ	=	distance along interconnected pipe network [L]
ℓ'	=	location of solute mass source/sink [L]
ℓ^*	=	location of external fluid source/sink [L]
w	=	distance perpendicular to plane of fracture [L]
t	=	time [T]

It should be noted that if there is no flow along a particular pipe within the network (i.e. $q(l) = 0$), then the model allows for diffusive transport along the length of this pipe. It should also be pointed out that if fluid is withdrawn at a resident concentration, $C_n^* = C_n$, then the term involving Q in (1) vanishes. If the injectate concentration $C_n^* = 0.0$, then this term accounts for the dilution effect of the injection of solute-free water.
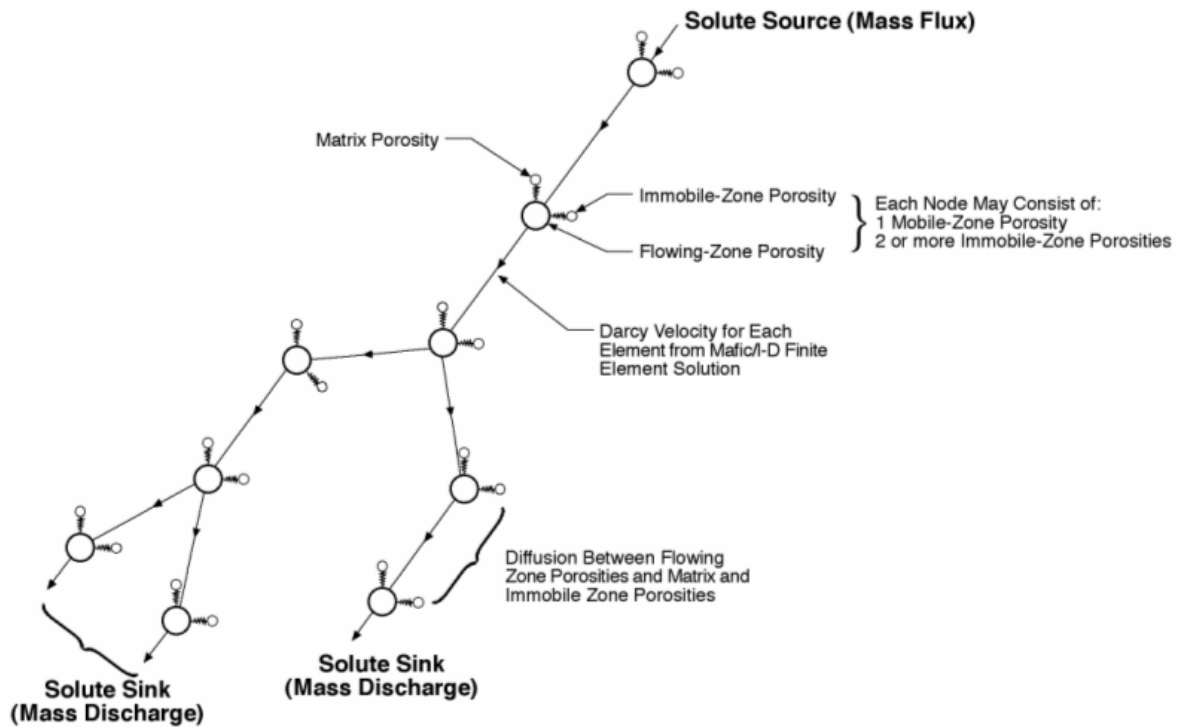
Figure 3-3. Topology of LTG Solution (from PAWorks/LTG manual).

The initial concentrations of all species within the domain are assumed to be zero in the current version of LTG. Boundary conditions may be either of the Dirichlet-type where the input concentration history of each species is a specified function of time, or of the Cauchy-type where the advective input mass flux can be prescribed as a function of time at the origin of a pipe on the boundary of the domain. Mathematically, these boundary conditions are described by:

Dirichlet: $Cn = C_n^o(t)$ on Γ **Equation 3-5**

Cauchy: $A(\ell)q(\ell)C_n^o(t) = A(\ell)\left[q(\ell)C_n(\ell,t) - D_{\ell_n}(\ell)\dfrac{\partial C_n}{\partial \ell}\right]$ on Γ **Equation 3-6**

where C_n^o is the specified concentration for species n. LTG also allows the concentration or flux rate (e.g. mol/yr) to be specified at an interior point.

3.2.2.1 Immobile Zone

Conceptually, tracer retention within a channel network model discretized from a DFN is modeled through the use of immobile zones within the transport code LTG. Figure 3-4 describes the conceptual model that relates immobile zone structure to the geometry of the host DFN fracture. In order to represent the diffusive exchange of solute mass between the pipes and any on the *im* immobile zones attached to them, LTG uses a second-order approach described by:

$$\theta_{im}\left(im,\ell\right)R_n^{im}\left(im.\ell\right)\frac{\partial C_n^{im}}{\partial t} - \frac{\partial}{\partial w}\theta_{im}\left(im,\ell\right)D_{im}\frac{\partial C_n^{im}}{\partial w}$$

Equation 3-7

$$+ \theta_{im}\left(im,\ell\right)R_n^{im}\left(im,\ell\right)\lambda_n C_n^{im} - \theta_{im}\left(im,\ell\right)R_{n-1}^{im}\left(im,\ell\right)\lambda_{n-1}C_{n-1}^{im} = 0$$

where:

$\theta_{im}\left(im,\ell\right)$ = porosity for immobile zone "*im*" attached to pipe "ℓ" [-]

$R_n^{im}\left(im,\ell\right)$ = retardation factor for immobile zone "*im*" attached to pipe "ℓ" [-]

C_n^{im} = concentration in matrix [M/L^3]

D_{im} = matrix effective diffusion coefficient [L^2/T]

= $D_n^0\,\tau$

D_n^o = free-solution diffusion coefficient [L^2/T]

τ = tortuosity [-]
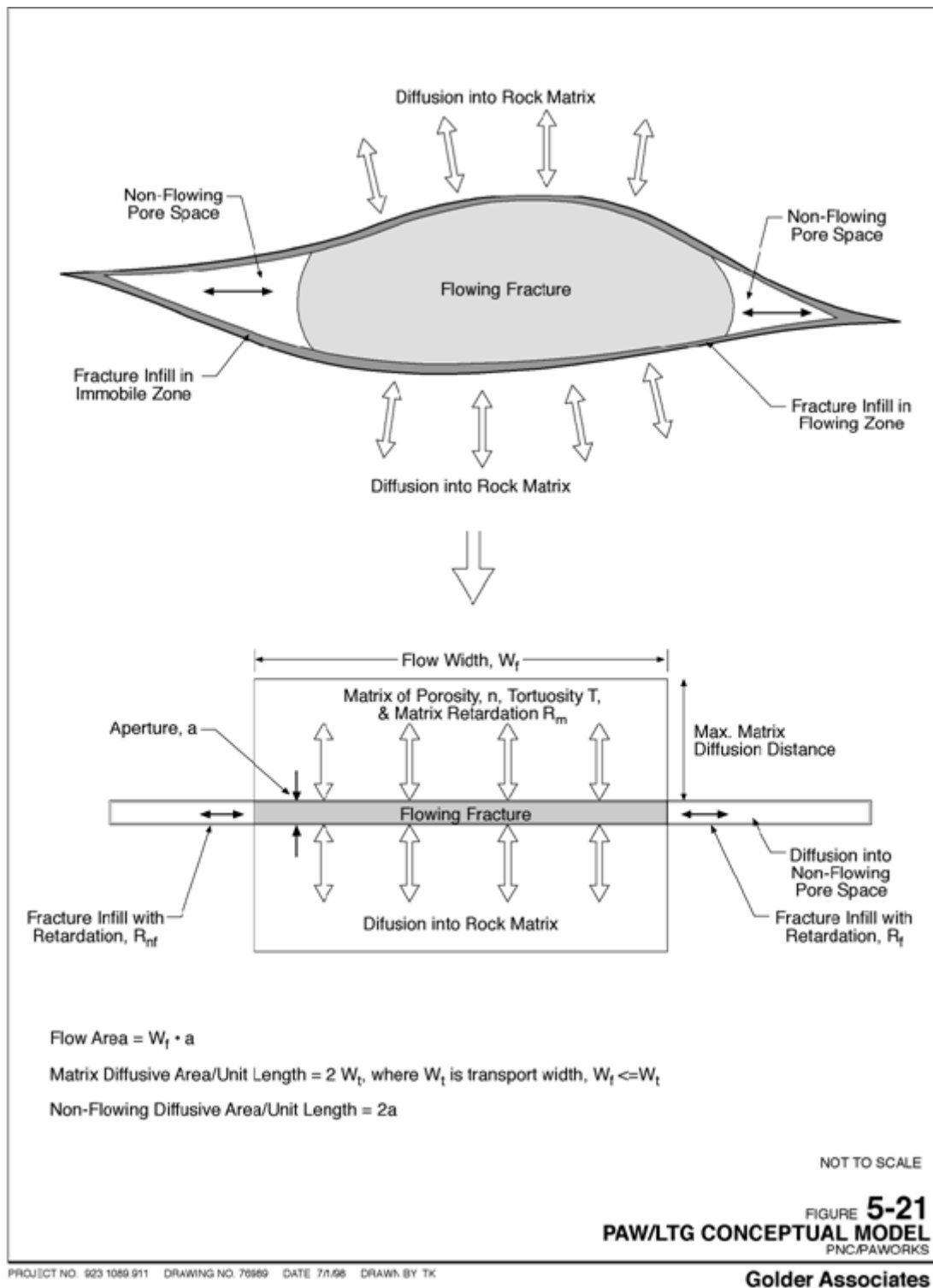
Figure 3-4. *PAWorks / LTG conceptual model of solute retention inside immobile zones surrounding pipes in a 1D channel-network model (PAWorks/LTG manual).*

If a particular immobile zone is fluid-filled, such as within an immobile water zone attached to a pipe within a fracture plane, then the immobile zone porosity, θ_{im}, would equal 1.0.

3.2.3   Transport Model Solution Parameters

The JNC/Golder team's transport model, as implemented in the LTG software package, describes nuclide transport in a one-dimensional channel network in terms of the following parameters:

- Geometric parameters for flow channel area (for each rectangular cross-section pipe): length L, width W, transport aperture e, and pipe velocity v;

- Immobile zone material parameters (for each immobile zones): Volumetric sorption coefficient K_d, porosity n, and material bulk density ρ;

- Immobile zone geometric parameters (for each immobile zone and each 1D CN pipe): immobile zone material thickness t, diffusion perimeter p, and transport aperture e.

3.3   JNC/Golder Tracer Rentention Conceptual Model

3.3.1   The Task 6C Microstructural Model

A key component of the Task 6C modelling effort was the development of a microstructural framework for characterizing the complexity inherent in geological structures. The microstructural model incorporates the ideas of:

- Fractures as larger-scale zones of deformation (parallel joint sets, multiple fracture planes)

- Areas of enhanced porosity and permeability due to the destruction of the host rock (cataclasite, fault gouge, alteration by hydrothermal fluids)

- Variability in mineralogy of materials (host rock, mineral infillings, gouge, cataclasite, and mylonite) in contact with groundwater within the fractures

Task 6 models incorporate the microstructural model by identifying two end-members of the realm of fracture structures; Type I structures are similar to classic geologic faults, where brittle deformation (gouge formation) occurs within a zone of pre-existing ductile deformation (cataclasite / mylonite). Figure 3-5 illustrates an example Type I geologic structure. Type II structures are characteristic of joints with little to no indication of significant shear; however, a zone of hydrothermal alteration with fracture infill mineralization is present. Figure 3-6 illustrates a sample Type II geologic structure

Geologic structure type assignments in the Task 6 models were made according to the length probability models described in the Task 6C report. Inside the DFN, fractures are assigned to sets based on both their geologic types and their assigned geologic complexity factor. For example, a single 'set' of background fractures might consist of all Type II (joint) features with a complexity factor of 2. This aids in the post-processing necessary to simulate geologic complexity in the JNC/Golder transport model.

In addition, Task 6C models implement a reconceptualization of the geometry of many features in a fractured rock mass. Rather than existing as single planar features, a certain percentage of geologic structures are composed of series of smaller interconnected fractures. 'Fracture Complexity' was assigned to both deterministic and stochastic fractures as a function of fracture size in the Task 6C report (Dershowitz et al., 2003); the details of the complexity complex are summarized below in .
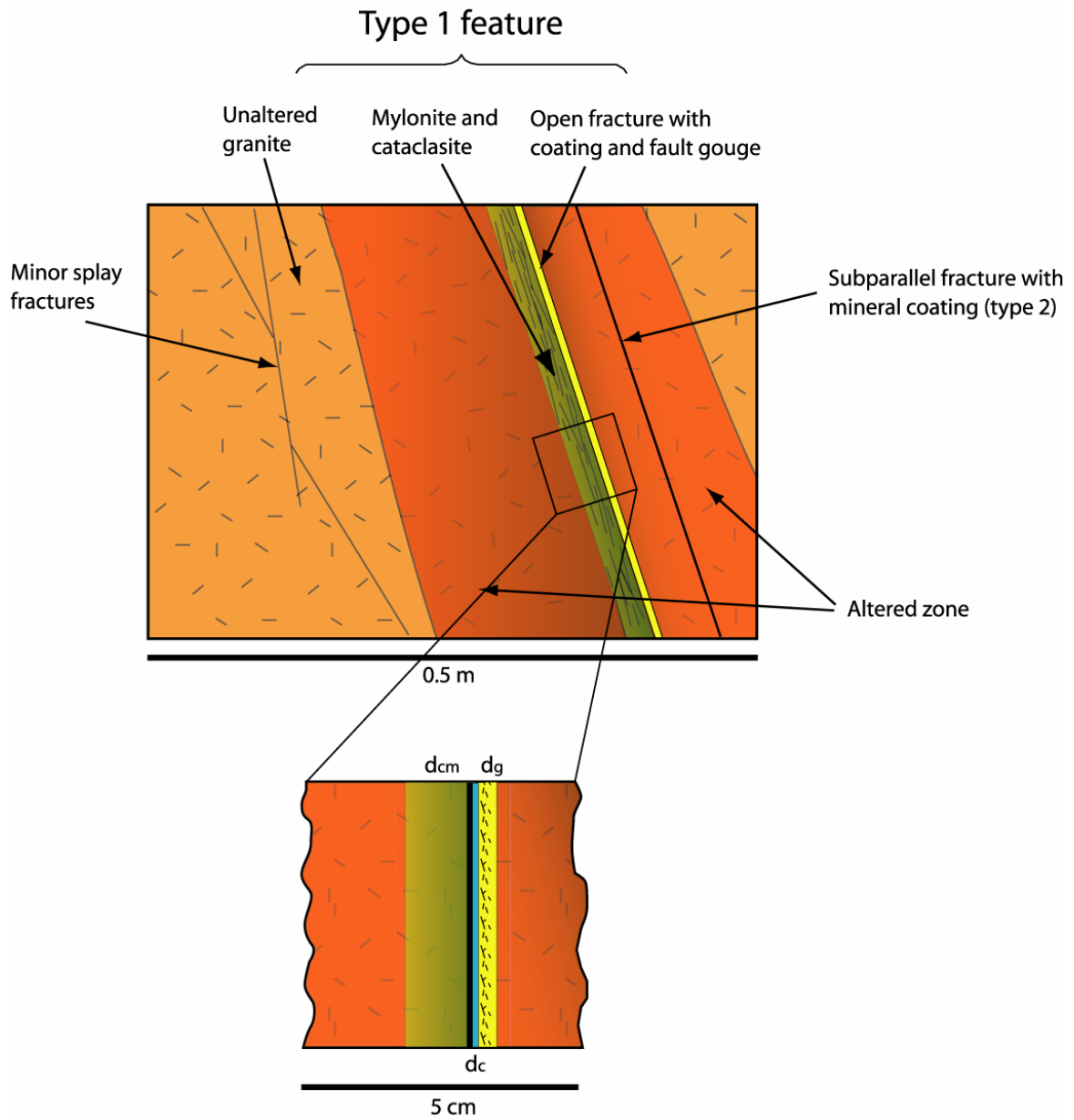
Figure 3-5. *Example Type I (Fault) geologic structure. This figure is from the Task 6C hydrostructural model report (Dershowitz et. al., 2003).*
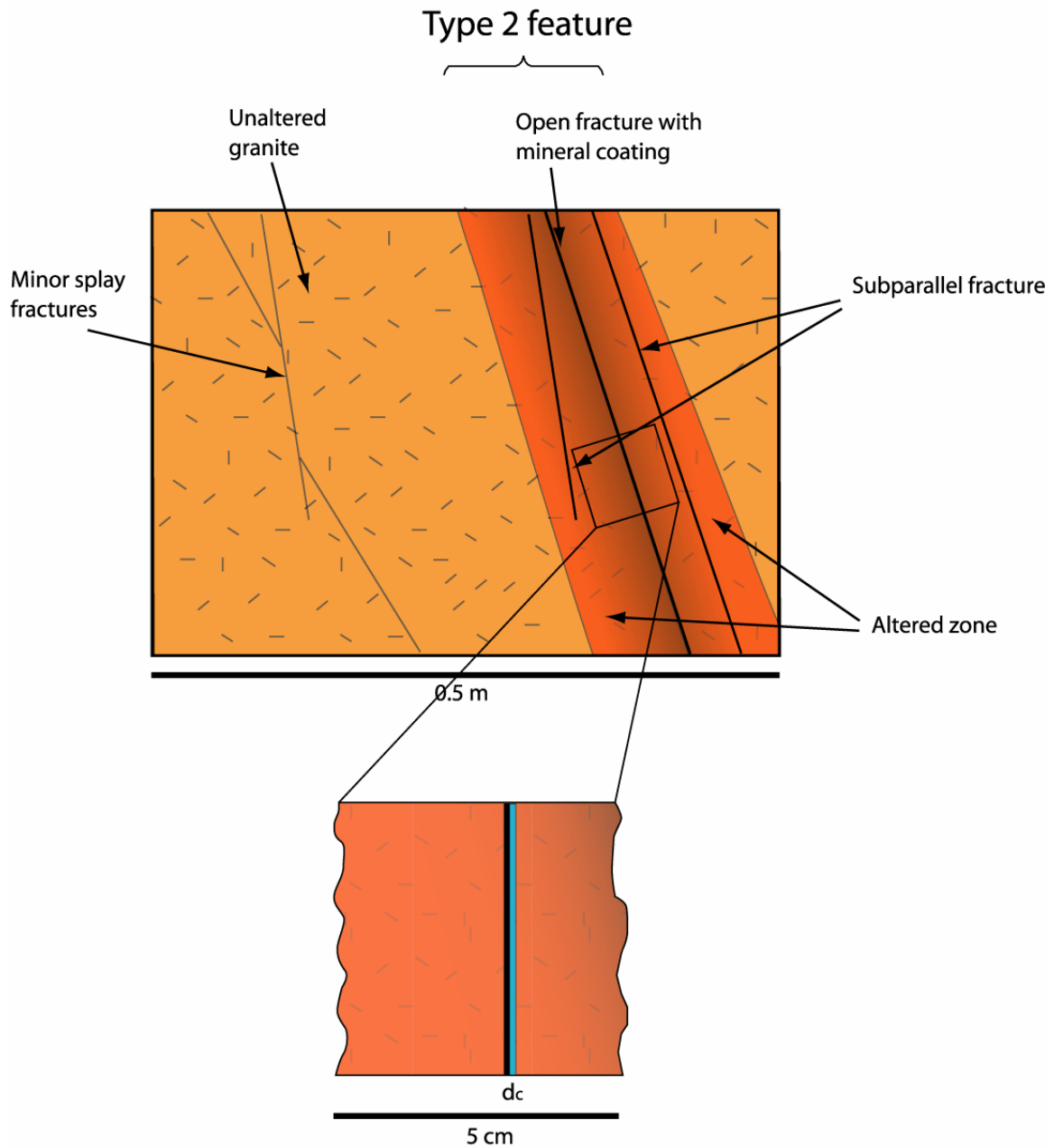
Figure 3-6. *Example Type II (Joint) geologic structure. This figure is from the Task 6C hydrostructural model report (Dershowitz et. al., 2002).*

Table 3-1. The definition of Complexity Factor for geologic structures (Task 6C report).

Complexity Factor	Number of (sub-parallel) conductive features/fractures per structure	Percent of primary geological structure type or combination of geological structure types (by area)
1	1	90-100%
2	1 to 2	70 to 100%
3	1 to 3	50 to 90%
4	3 to 10	50 to 90%
5	10+	50 to 90%

3.3.2 Geometrical Description of Pore Space

The pore space models used in the JNC/Golder Task 6 modelling efforts are those of the Type I and Type II geologic structures with fracture complexity, as described in the previous section. Pore spaces representing fault gouge, cataclasite / mylonite, fracture mineral coatings, altered wall rock, and fresh wall rock (Äspö diorite) were implemented as PAWorks/LTG immobile zones (described in Chapter 3.2.2.1). In PAWorks/LTG, immobile zones simulate mechanical and chemical transport processes by applying retardation factors to solute transport based on the zone properties. Fundamentally, mass is not 'lost' from a model to an immobile zone; the tracer is merely retarded to a point where it does not reach the specified sinks during the simulation duration.

The Task 6C microstructural conceptual model (Chapter 3.3.1) includes a combination of parallel and series immobile zones. The diffusion from the advective flow channel to the gouge and fracture coating is assumed to occur in parallel, while the diffusion from the fracture coating to the altered wall rock and intact rock is assumed to occur in series.

In the JNC/Golder implementation of the Task 6 modelling specification, diffusion and sorption were implemented as parallel processes within parallel immobile zones. Each process had access to the entire fracture flow wetted perimeter. It was recognized that this implementation would produce an over-estimate of diffusion. However, for the time scales involved, it was anticipated that this would not significantly over-estimate the amount of matrix diffusion and sorption within the rock mass, because the high porosity immobile zones (gouge, coating) would dominate during the short site characterization (SC) time periods. The effect should be noticeable, however, for strongly sorbing tracers over performance-assessment (PA) time scales.

Immobile zone properties were specified based on a specific combination of immobile zones for "Type 1" and "Type 2" structures. Immobile zones were assigned on a set-by-set basis; as such, fracture sets were grouped in the geologic model by geologic structure type (I or II). The description of the assignment of individual immobile zone properties (thickness, porosity, etc.) is described separately within the definition of each Task 6 modelling phase (6D, 6E, 6F, and 6F2) in later chapters.

3.3.3 Derivation of Transport Parameters

The JNC/Golder modelling team used Kd values as assigned in the specific task specifications (see Section 2); in general, Kd values were the same as those provided for TRUE Block Scale groundwater for Task 6D. Effective diffusivity (D_e) was based on the product of the formation factor F and the free-water diffusivity (D_w).

Surface sorption distribution coefficients (K_a) were calculated from the K_d values according to the following formula:

$$K_a = (K_d * \rho + n) * d$$

where d was the thickness of the fracture coating in meters, n was the porosity of the material within the immobile zone, and ρ was the bulk density of the material in kilograms per cubic meter. Unless otherwise specified in the Task-specific model description, surface sorption calculations assume a fracture infilling density of 2600 kg/m^3. K_a values were calculated on the fly in PAWorks as an immobile zone property, and, as such, vary from fracture set to set. Geologic material densities were either

estimated from past Task 6 experiments (Task 6D) or computed using mineralogical breakdowns specified in the Task 6C hydrostructural report (Dershowitz et al., 2002) and average chemical compositions of typical mineral end-members (Deer et al., 1966 and Kline & Hurlbut, 1993).

3.3.4   Implementation of Fracture Complexity

Geologic and structural complexity is implemented in the JNC/Golder channel network model through a post-processing modification of the immobile zone surface area in the 'downstream' network of pipes between sources and sink. These modifications take place after the flow solution and pathway identification has been made; retention effects are simulated solely within the transport code.

In the JNC/Golder Task 6 DFN-CN models, retention was modeled in immobile zones by increasing the effective surface area (and corresponding pore volume) available to diffusion and surface sorption. This was accomplished by multiplying the perimeter of the material-specific immobile zones by the complexity factor. For example, fractures of Complexity 2 had a diffusion perimeter of twice that of Complexity 1 fractures. The adjustement to pipe perimeter was made on an immobile zone by immobile zone basis; it was possible to simulate different perimeter adjustments to the same pipe for different immobile zone types.

In the Task 6 models, though conceptualized as a system of series flow and parallel flow processes, diffusion and sorption were implemented as parallel processes within parallel immobile zones. Each process had access to the entire fracture flow wetted perimeter. It was recognized that this implementation would produce an over-estimate of diffusion. However, for the time scales involved, it was anticipated that this would not significantly over-estimate the amount of matrix diffusion and sorption within the rock mass, because the high porosity immobile zones (gouge, coating) would dominate during the short timeframe of the site-characterization (SC) scale experiments.

4 Task 6D – Site Characterization Time Scale Simulations in a Rock Block

4.1 Modelling strategy

Task 6D was designed to study solute transport at site characterization (SC) time scales within a 200 m scale rock volume (TRUE Block) in which all fractures and their properties were predefined based on a semi-stochastic hydrostructural model created during Task 6C (Dershowitz et al., 2003). The strategy used for Task 6D was one of forward modelling. In this strategy, the JNC/Golder team directly incorporated the specified flow geometry, boundary conditions, and material properties specified in the Task 6C report into a discrete fracture network (DFN) model. The task simulations were designed to assess how well the geologic and hydraulic conceptual models developed during Task 6C would compare to in situ observations. The JNC/Golder Task 6D modelling effort was not a formal calibration exercise, but rather a test of the consistancy of the Task 6C hydrostructural model with the tracer test measurements of Task 6D.

The major focus of the JNC/Golder Task6 modelling was a Site Characterization style simulation (with associated sensitivity studies), carried out using FracMan software. For these simulations, the full 200 m scale TRUE Block was simulated using the discrete fracture network (DFN) approach, discretized to a one-dimensional channel-network (CN). Tracer transport and retention in the fracture network was solved using the Laplace Transform Galerkin method. Task 6D Performance measures were only calculated for the "Base Case" DFN transport simulations.

The JNC/Golder Task 6D simulations are subject to the following assumptions and constraints:

- Radioactive decay was not considered in the modelling, such that all concentrations reported are values which would be measured if there were no radioactive decay. This is equally true for tracer injection time histories and breakthrough curves. This is based on the Task 6D specification.

- Simulations were carried out up to a time of 1×10^8 hours or until a full recovery is obtained for all tracers. This is based on the Task 6D specification.

- The immobile zone conceptual model assumed a combination of immobile zones in parallel (grout, coating, and mylonite), and in series (coating-altered rock-intact rock). The implementation of this conceptual model assumes only immobile zones functioning simultaneously in parallel.

4.2 Model Implementation

4.2.1 Implementation of the Task 6C semi-synthetic hydrostructural model

The Task 6D specification requires that transport modelling be carried out within the 200-m scale "semi-synthetic" hydrostructural model developed within Task 6C (Dershowitz et al, 2003). The model combines (Figure 4-1)

- Deterministic structures directly identified in the Äspö TRUE Block Scale experiment and further codified in the Task 6C semi-synthetic hydrostructural model;

- Stochastic background fractures generated using FracMan software, based on analysis of Äspö data from the TRUE Block Scale rock volume and other portions of the laboratory.
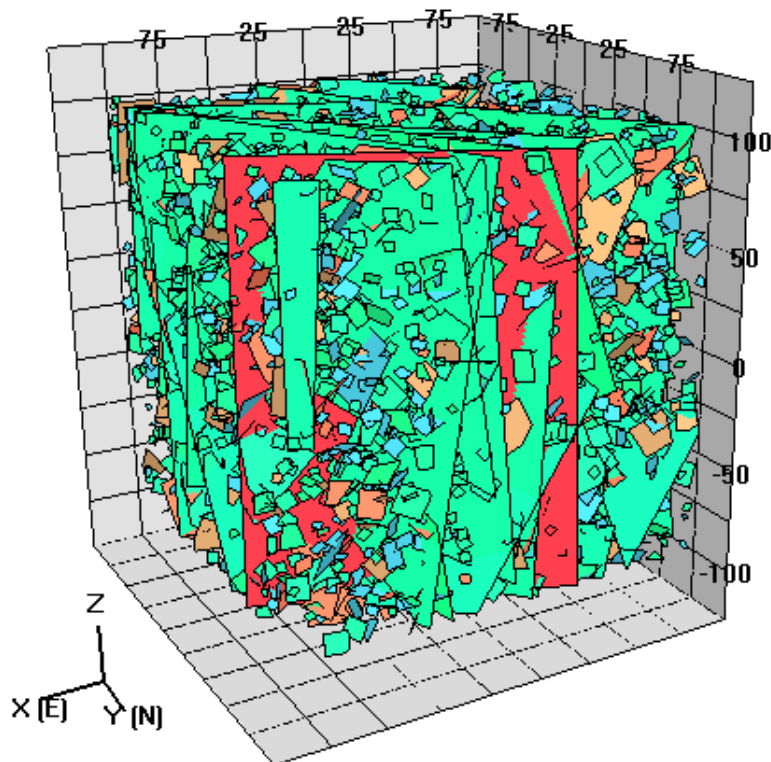
Figure 4-1. *Deterministic and background fractures in the 200-m block scale model. From Task 6C report (Dershowitz et al., 2003).*

The procedure for DFN model implementation was as follows:

1. Construct the Task 6C hydrostructural model as a three-dimensional discrete feature network (DFN) model using the FracWorks XP software package. This model included all deterministic, semi-synthetic, and background structures.

2. Convert the DFN into a one-dimensional pipe network model, using PAWorks/Genpipe. This pipe network was conditioned to match the connectivity of the DFN model, with pipe properties set to match the apertures and transmissivities of their host fractures. Pipes that did not connect to a head or flow boundary were removed from the system for computational efficiency

3. Apply the specified steady state flow boundary conditions through the MAFIC software package to obtain a nodal head and flux field. The resulting flow solution assigns an advective transport velocity to all pipes.

4. Convert the full channel network into a smaller mesh of just the "downstream" network of pipes between the defined tracer injection sources and sink. The new mesh is then exported this from PAWorks to the LTG solver. Immobile zone parameters are assigned to pipes based on set membership of their host fractures. Solute transport boundary conditions are also assigned at this stage.

5. Derive advective flow performance metrics (beta-factor and water residence time distributions) from transport pathways identified in PAWorks through a graph-theory traversal of the channel network.

6. Calculate τ and β values for the flow pathway that each particle took by dividing the travel time tw in each pipe by the pipe aperture e, and summing the result over the length of the pipe.

7. Simulate fracture complexity by altering the perimeters of pipes on a set-by-set basis in the LTG input files (IMMDATA.IN, GRID.IN). Pipes belonging to fractures of complexity 2 had the pipe perimeter available to transport processes doubled, while pipes belonging to fractures of complexity 3 had their perimeters tripled. Flow perimeters, and therefore pipe velocities, were unchanged.

8. Simulate solute transport using FracMan/LTG in the pipe network. This program reports fluxes, concentrations, and cumulative releases at user-specified trace planes and at specified head / flux boundaries (boreholes, constand head and constant flux edges).

9. Calculate additional performance measure statistics (breakthrough curves, t_5, t_{50}, t_{95}).

4.2.2 Task 6D Flow Model

The JNC/Golder Task 6D simulation efforts utilized the FracMan/PAWorks and MAFIC approaches, as described in Chapter 3.1. The end result was a 1D channel network discretized from the Task 6C semi-synthetic hydrostructural DFN model.

4.2.2.1 Boundary Conditions

Boundary conditions for the Task 6D were specified on 10 m scale panels for each of the faces of the TRUE Block Scale rock volume and provided in the Task 6C Data Delivery, These heads were implemented directly in the JNC/Golder DFN-CN model. The CN model assumes steady-state flow conditions; flow rates and tracer release points are described below in Table 4-1.

Table 4-1. Hydraulic and geometric parameters for tracer test C2 (Task 6D).

Parameter	Source Section KI0025F03:P7	Sink Section KI0023B:P6
Northing	7194.840	7186.294
Easting	1929.741	1914.628
Elevation	-476.100	-473.065
Injection Rate	1.67×10^{-7} m^3/s (10 ml/min)	--
Pumping Rate	--	3.25×10^{-5} m^3/s (1.95 l/min)
Cartesian Distance	17.6m	
DFN Path Length	66 m	
Structures Involved	20, 21, 22, 23	

4.2.3   Task 6D Transport Model

The goal of Task 6D was to simulate the TRUE Block Scale experiment "C2", described in Andersson et al. (2002b) and Andersson et al. (2001). Tracer test C2 tested a fracture network transport pathway composed of four major deterministic structures (23, 22, 20, and 21) within the TRUE Block Scale volume at the Äspö Hard Rock Laboratory. Table 4-1 details the parameters for tracer test C2. Coordinates in Table 2 2 are provided in the ÄSPÖ96 system. The Task 6D specification notes these injection and pumping rates have been corrected compared to the data given in Table 6.3 in the draft Task 6C report (2002-10-15).

The DFN model for the pore space considered only parallel immobile zones. Diffusion and retardation due to surface sorption were calculated in all immobile zones simultaneously, rather than in series, where a given species would have diffuse completely through a given structural element before gaining access to another element (i.e. material must diffuse through the fracture mineral coatings before it can diffuse into the cataclasite layer). Given the time scale of interest, the immobile zone for intact rock was not included in the simulations. Gouge, Cataclasite, Coating, and Altered Rock were considered as parallel immobile zones.

The C2 Experiment transport simulations described later in this chapter were completed using the assumption that all structures in the model had a complexity factor of 1; there was no post-processing adjustement to the pipe perimeter available for sorption and diffusion. Note that this assumption did not hold for the model sensitivity analysis.

4.2.3.1 Processes Considered

The transport parameter simulated in all Task 6 models are described in Chapter 3.2.1. The C2 experiement utilized the following tracers:

- non-sorbing (^{186}Re as perrhenate, ReO$_4^-$),

- slightly sorbing (^{47}Ca^{2+})

- moderately sorbing (^{131}Ba^{2+})

- strongly sorbing (^{137}Cs$^+$).

The Task 6D modelling scope specified that all modelling teams were to simulate the behavior of six tracers; ^{129}I$^-$, ^{47}Ca^{2+}, ^{137}Cs$^+$, ^{226}Ra, ^{99}Tc(IV) and ^{241}Am(III).

4.2.3.2 Parameters

The solute transport properties for "Type 1" and "Type 2" structures were provided in the Task 6D modelling specifications (Elert and Selroos, 2002). The values used in the JNC/Golder Task 6D simulations are based on these specifications.

Immobile zone properties are specified based on a specific combination of immobile zones for "Type 1" and "Type 2" structures. The thickness, formation factor F and porosity n are specified by immobile zone in Table 4-2 and Table 4-3, based on Dershowitz et al. (2003). Effective diffusivity (D_e) for a species is based on the product of the immobile zone formation factor (F) and the species free-water diffusivity (D_w).

Table 4-2. Immobile zone parameters for Type 1 (Fault) structures.

Rock type	Extent (cm)	Porosity (%)	Formation factor (–)
Intact wall rock	–	0.3	7.E-5
Altered zone	20	0.6	2.E-4
Cataclasite d_{cat}	2	1	5.E-4
Fault gouge d_g	0.5	20	5.E-2
Fracture coating d_c	0.05	5	6.E-3

Table 4-3. Immobile zones for Type II (Non-Fault) structures.

Rock type	Extent (cm)	Porosity (%)	Formation factor (–)
Intact wall rock	–	0.3	7.E-5
Altered zone	10	0.6	2.E-4
Fracture coating d_c	0.05	5	6.E-3

Table 4-4. Effective diffusivity (De) for various tracers used in the TRUE Block Scale and Task 6 experiments.

		Fracture Coating	Fault gouge	Cataclasite	Altered Zone	Unaltered wall rock
	Porosity (%)	5	20	1	0.6	0.3
	Formation factor, F	6.20E-03	5.60E-02	4.90E-04	2.20E-04	7.30E-05
	D_w (m^2/s)$^{A)}$	D_e (m^2/s)	D_e (m^2/s)	D_e (m^2/s)	D_e (m^2/s)	D_e (m^2/s)
HTO	2.13E-09	1.30E-11	1.20E-10	1.00E-12	4.70E-13	1.60E-13
I$^-$	2.00E-09	1.20E-11	1.10E-10	9.80E-13	4.40E-13	1.50E-13
Na$^+$	1.33E-09	8.30E-12	7.40E-11	6.50E-13	2.90E-13	9.70E-14
Mg^{2+}	7.05E-10	4.40E-12	3.90E-11	3.50E-13	1.50E-13	5.20E-14
K$^+$	1.96E-09	1.20E-11	1.10E-10	9.60E-13	4.30E-13	1.40E-13
Ca^{2+}	7.93E-10	5.00E-12	4.40E-11	3.90E-13	1.70E-13	5.80E-14
Rb$^+$	2.06E-09	1.30E-11	1.20E-10	1.00E-12	4.50E-13	1.50E-13
Sr^{2+}	7.94E-10	5.00E-12	4.40E-11	3.90E-13	1.70E-13	5.80E-14
Cs$^+$	2.07E-09	1.30E-11	1.20E-10	1.00E-12	4.50E-13	1.50E-13
Ba^{2+}	8.48E-10	5.30E-12	4.70E-11	4.20E-13	1.90E-13	6.20E-14
Ra^{2+}	8.89E-10	5.60E-12	5.00E-11	4.40E-13	1.90E-13	6.50E-14
Am(III)	5.95E-10	3.70E-12	3.30E-11	2.90E-13	1.30E-13	4.40E-14
Tc(IV)	5.00E-10	3.10E-12	2.80E-11	2.50E-13	1.10E-13	3.70E-14

Table 4-5. Volumetric sorption coefficients (Kd) for tracer species used during Task 6D.

	Fracture Coating K_d (m^3/kg)	Fault Gouge K_d (m^3/kg)	Cataclasite K_d (m^3/kg)	Altered Zone K_d (m^3/kg)	Intact wall rock K_d (m^3/kg)
I$^-$	0	0	0	0	0
Ca^{2+}	2.30E-04	7.10E-04	6.70E-05	8.80E-05	4.40E-05
Cs$^+$	5.20E-02	1.60E-01	1.50E-02	2.00E-02	1.00E-02
Ra2+	4.60E-02	1.40E-01	1.30E-02	1.80E-02	8.80E-03
Tc(IV)	2.00E-01	2.00E-01	2.00E-01	2.00E-01	2.00E-01
Am(III)	5.00E-01	5.00E-01	5.00E-01	5.00E-01	5.00E-01
Ba^{2+}	4.60E-03	1.40E-02	1.30E-03	1.80E-03	8.80E-04

Free water diffusivity for the Experiment C2 tracer Rhenium (ReO^{4-}) is assumed to be the same that the diffusivities of iodide (I$^-$) and pertechnetate (^{99}Tc) are the same as Iodine in Table 4-4, as recommended in the Task 6D specifications (Elert and Selroos, 2002). The volumetric sorption coefficients listed in Table 4-5 were also provided in the Task 6D specifications, and are based on the TRUE Block Scale groundwater chemistry.

Additional information provided to support K_d and tracer property values in as follows.

- The injection time history for ^{129}I$^-$ was assumed to be identical to that of ^{186}Re (Elert and Selroos, 2002).

- The injection time histories for ^{99}Tc and ^{241}Am(III) were assumed to be identical to that of ^{137}Cs^{2+} (Elert and Selroos, 2002).

- Sorption characteristics of ^{226}Ra^{2+} in TRUE Block Scale groundwater are obtained by multiplying the corresponding K_d-value of ^{131}Ba^{2+} by a factor of 10.

- For Tc(IV) and Am(III), hydrolysis combined with surface complexation is considered to be the major sorption mechanism. The influence of different mineral types and different water compositions are considered to be minor.

4.3   Model calibration

The goal of the JNC/Golder team in Task 6D was not to determine the single "correct" set of transport pathway properties for the fracture network, but rather, to study the relative significance of each of the transport assumptions provided in the rock block characterization. This is fundamentally a forward modelling approach, rather than a calibration approach. As such, no formal calibration was performed. Sensitivity studies are described later in this document.

4.4   Results

4.4.1   Flow

4.4.1.1 Drawdown in injection and pumping borehole

Model drawdowns were recorded assuming a steady-state flow field, and are presented below in Table 4-6.

Table 4-6. Simulated Drawdowns in JNC/Golder CN model during C2 simulation.

Borehole Packer Section	Initial Head (m)	Final Head (m)	Drawdown (m)
Source: KI0025F03:P7	-60.63	-61.95	1.32
Sink: KI0023B: P6	-61.65	-97.95	36.29

4.4.1.2 Water residence time distribution

The water residence time distribution for the JNC/Golder Task 6D channel network models was calculated using a tracer breakthrough curve for a Dirac pulse input source. A constant injection mass of $1.00 \times 10^{+8}$ Becquerel over a period of one hour was simulated. All immobile zones were turned off within the transport code to remove surface and matrix interaction effects (Elert and Selroos, 2004a). This resulted in an advection- and longitudinal dispersion-only breakthrough curve; it is not possible to disable longitudinal dispersion in the LTG code. A graphical display of the Task 6D water residence time distribution is presented below as Figure 4-2; formal time-series data was submitted as a Microsoft Excel® spreadsheet.
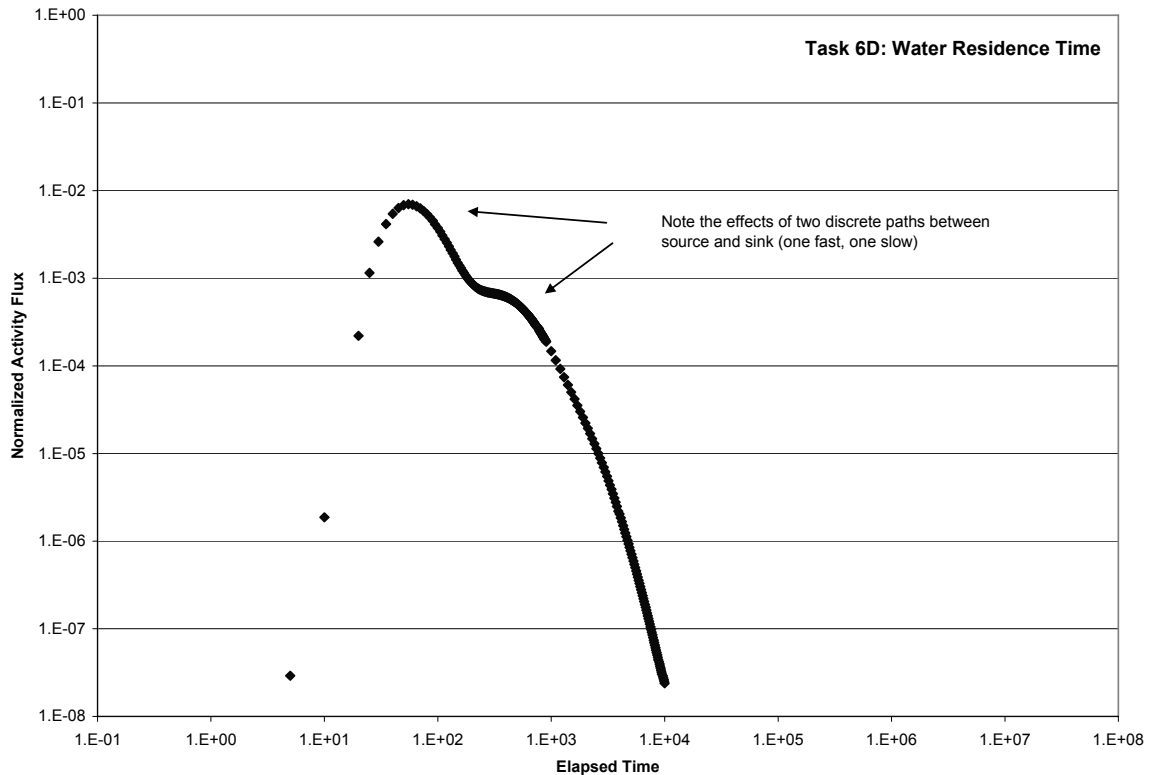
Figure 4-2. Water residence time distribution for JNC/Golder Task 6D CN model.

4.4.2 Transport

Transport modelling was accomplished using the LTG software package, which simulates advection, diffusion, dispersion, and sorption in one-dimensional (pipe) and three-dimensional (plate) fracture networks. The transport solutions presented below assume that all trans only Type I geologic structures (faults); no

4.4.2.1 β-factor

The β-factor is a parameter group specified by SKB that is a combined metric of the area available in a transport model to surface and matrix interactions, along with the time constant necessary for those interactions to occur (Elert and Selroos, 2004a).

β-factors were calculated using PAWorks-produced output files. As such, the values represent conditions only within the advective flow network; no immobile zones are included in the calculation, as they are only modelled within the transport code (LTG). The current JNC/Golder Task 6D model computes the β-factor using two methods:

1. Through PAWorks particle tracking trajectories. A β-factor is calculated for each pipe in a track by dividing the particle travel time for that segment by the fracture half-aperture. The β-values were then summed along the total particle track to provide an accurate count for the complete pathway.

40

2. Through PAWorks pathways identified using a weighted graph theory algorithm. For each pipe in a given pathway (75 total theoretical pathways), the flow wetted surface perimeter was divided by the product of the pipe area and the pipe velocity. All calculations assume a parallel-plate approximation for the network rather than a stream tube.

Figure 4-3 illustrates the relationship between travel time τ and the β-factor. The JNC/Golder simulation results suggested a power-law relationship between the two parameters, at least for the flow pathways defined for the C2 experiment. Pathway travel times range from approximately 100 hours to as long as 45,000 hours, with an average travel time of 648 hours. β-factor values ranged from 1×10^5 to 2×10^8 hours / meter, with a significant number of pathways falling between 1×10^6 and 1×10^7 hours per meter.
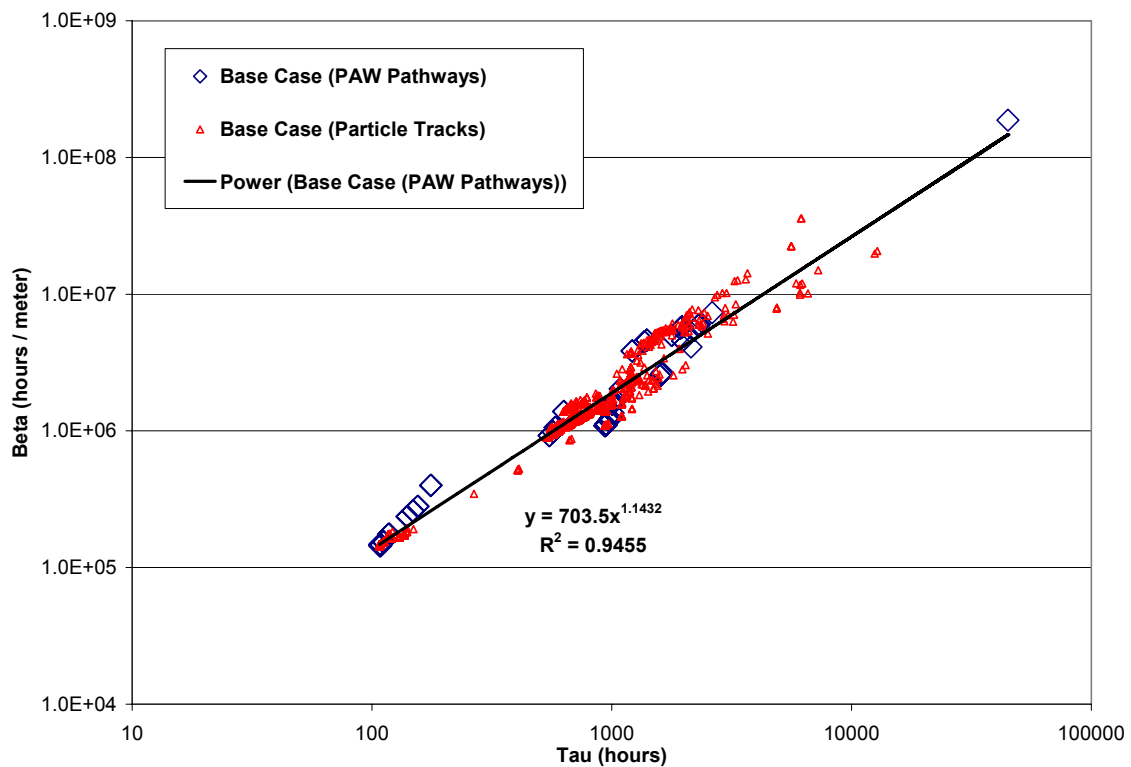
Figure 4-3. *Travel time (τ) versus β–factor distribution for Task 6D simulations of the C2 tracer experiment using the JNC/Golder channel network model.*

4.4.2.2 Breakthrough time history for the tracers

Breakthrough time series data was recorded for all six simulated tracers, and was included in as an Microsoft Excel® spreadsheet in a formal Task 6 delivery to SKB. Breakthrough curves for both the specified tracer injection histories (Figure 4-4) and for an assumed Dirac pulse input case (Figure 4-5) are presented below; breakthrough statistics for both model cases are contained in Table 4-7.

Table 4-7. Breakthrough statistics for JNC/Golder CN model simulations of the C2 tracer experiment.

Base-case (supplied injection time histories)				
Tracer	t_5 (hrs)	t_{50} (hrs)	t_{95} (hrs)	Maximum Release Rate (Bq/kg)
Re-186	160	500	7000	3410
Ca-47	500	1800	27,000	3.60
Cs-137	80,000	300,000	4,500,000	1.07
Ra-226	70,000	270,000	4,000,000	1.17
Tc-99	320,000	1,110,000	17,000,000	0.26
Am-241	800,000	2,960,000	43,000,000	0.105
Dirac Pulse Injection				
Tracer	t_5 (hrs)	t_{50} (hrs)	t_{95} (hrs)	Maximum Release Rate (Bq/kg)
Re-186	150	500	6000	1.8×10^{-3}
Ca-47	500	1800	27,000	4.86×10^{-4}
Cs-137	80,000	300,000	4,600,000	3.08×10^{-6}
Ra-226	70,000	270,000	4,100,000	3.36×10^{-6}
Tc-99	320,000	1,100,000	17,000,000	7.46×10^{-7}
Am-241	800,000	2,960,000	44,000,000	3.02×10^{-7}
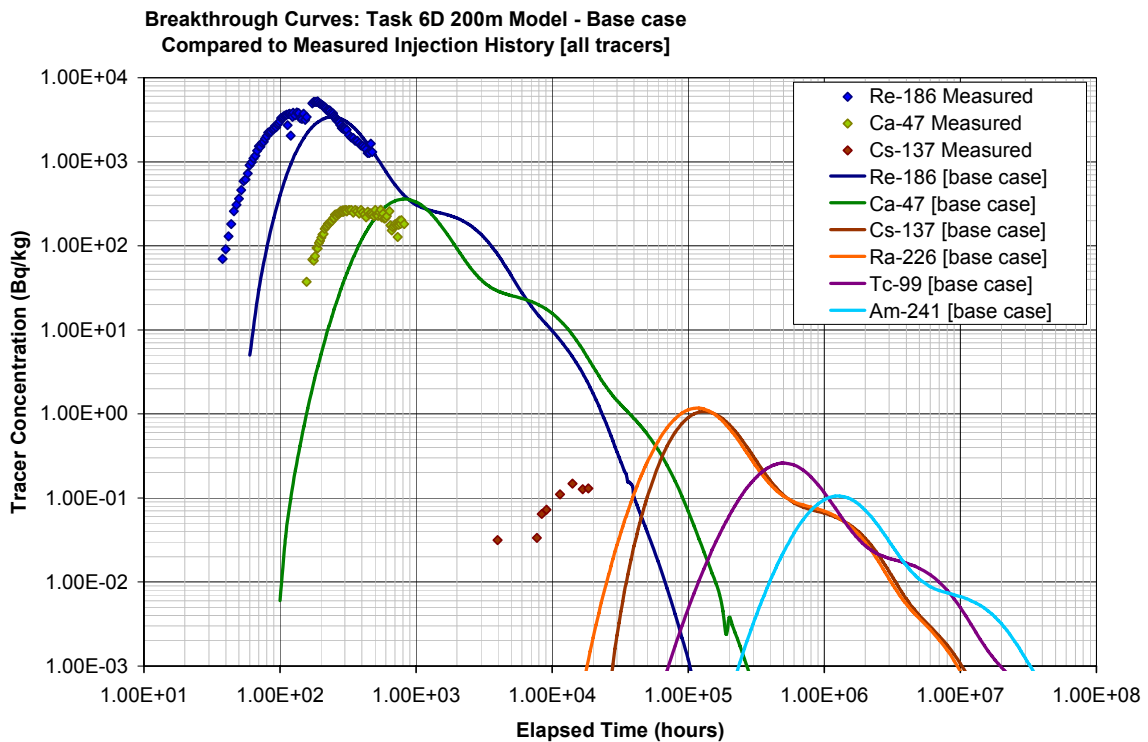
Figure 4-4. *Tracer breakthrough curves for Experiment C2 default model injection profiles using the JNC/Golder Task 6D channel-network model.*

42
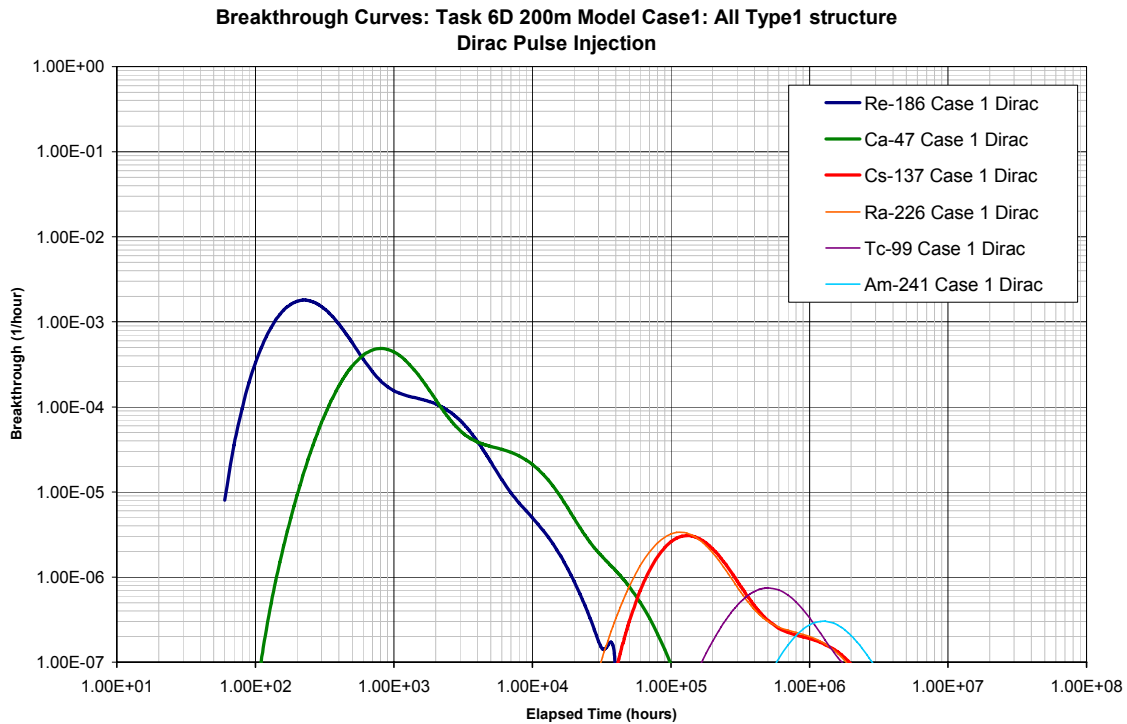
Figure 4-5. *Tracer breakthrough curves for Experiment C2 assuming Dirac pulse injection profiles using the JNC/Golder Task 6D channel-network model.*

4.4.2.3 Maximum release rate

Maximum release rates for all tracer cases (specified injection flux and Dirac pulse) are presented in Table 4-7.

4.5 Sensitivity analysis

A limited sensitivity analysis of the JNC/Golder Task 6D DFN-CN was conducted, with an emphasis on determining the effects of the various microstructural and hydrostructural parameters on tracer breakthroughs. Specifically, the sensitivity analysis addressed:

- The influence of the microstructural models (Type I versus Type II features),

- The influence of fracture complexity, and

- The geometry of the semi-stochastic background fracture network.

4.5.1 The Influence of Geological Structure type

The geological structure type of a fracture is important at the microstructural scale for assessing retention effects. The immobile zones that tend to react strongly at experimental time scales are those with higher porosity (cataclasite / mylonite) and reactive surface materials (fault gouge). These structures have the potential to dramatically increase both retention and retardation due to enhanced surface and matrix reactivity. In general and in the Task 6C conceptual models, these materials are found exclusively along Type II (fault) features.

The base case simulations were run using a mixture of Type 1 and Type 2 structures, as specified by the Task 6D modelling guidelines (Elert and Selroos, 2002). The two sensitivity studies consider the effect of converting all fractures to structure type 1, or converting all fractures to structure type 2.

Converting fractures to Structure Type 1 adds fault gouge and cataclasite to those fractures assigned to Structure Type 2. This would be expected to increase tracer retention, resulting in delayed breakthrough and a larger tailing effect. Converting all fractures to Type 2 removes the reactive materials and, in general, decreases the pore space available to sorption and diffusion processes. This change reduces the tracer retention, resulting in slightly earlier tracer breakthroughs with less-pronounced tailing.
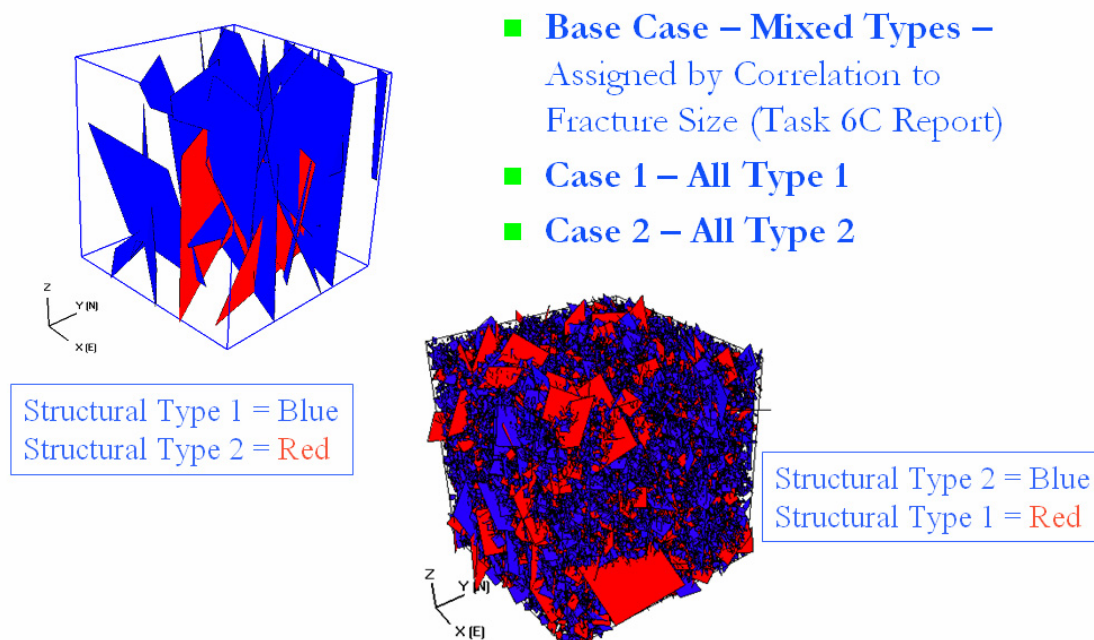
Figure 4-6. *Outline for Task 6D study of the sensitivity of tracer transport to geologic structure type.*

4.5.2 The influence of fracture complexity

The base case simulations described in Chapter 4.4 were run assuming that all modeled DFN structures possessed a complexity factor of one. This implies that every structure consists of only one fracture. In the Task 6C conceptual model, however, many of the major "Type 1" structures were considered to be composed of multiple smaller features, and were assigned a complexity factor of 2 or 3. A higher fracture complexity value corresponds to an increased available flow-wetted surface area, which can potentially have a dramatic effect on solute retention. Higher levels of complexity also correspond to mixtures of "Type 1" and "Type 2" immobile zones both on fracture surfaces, and between the different fractures which make up the structures.

There are two different conceptualizations of complexity that were available for implementation in the JNC/Golder Task 6D simulations. Case 1 focused on increasing the reactive surface area in proportion to the number of available fracture surfaces.

Case 2 focused on the effects of varying the geologic structure type of the smaller features that made up a larger Type I structure. This report only describes sensitivity results for the first Case; no modelling in support of Case 2 was performed. These cases are summarized below in Figure 4-7. All simulations used the injection time histories for the C2 Experiment; the effects of a Dirac pulse injection were not evaluated.

The sensitivity study consisted of two sets of simulations:

- The complexity factor of all structures (including background fractures) was set to 2. This effectively doubled the reactive surface area available for diffusion across the entire model.

- The complexity factor of all structures was set to 1, 2 or 3, as specified in the Task 6C hydrostructural model.
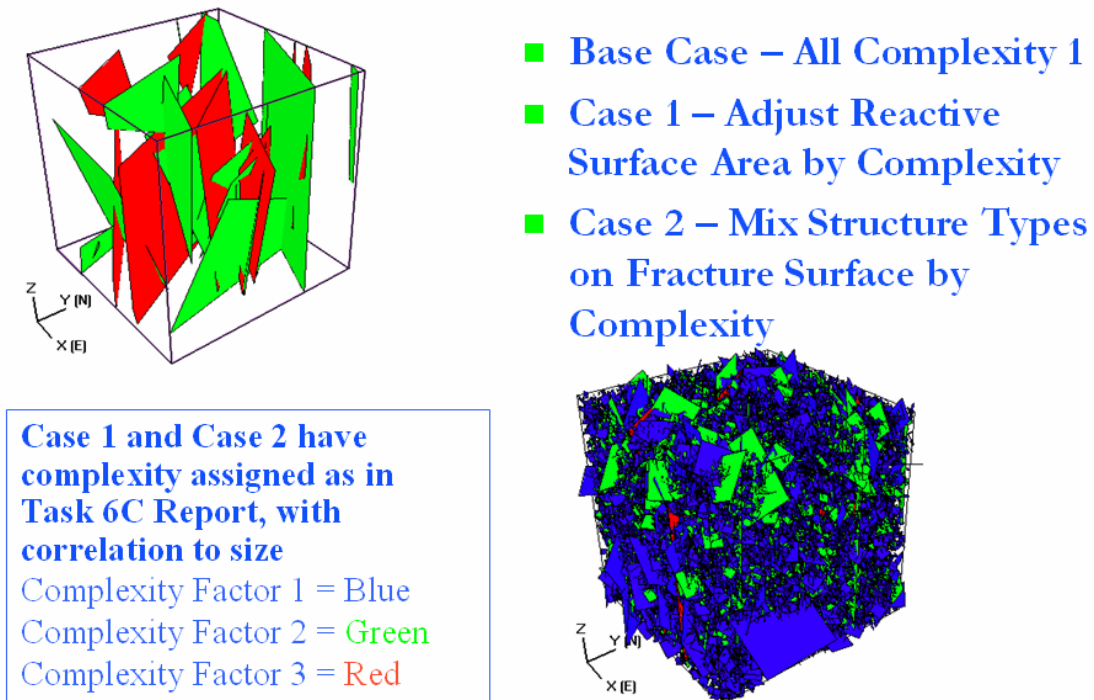
Figure 4-7. *Outline for Task 6D study of the sensitivity of tracer transport to fracture complexity factor.*

Results of these simulations are presented in Figure 4-8, Figure 4-9, Table 4-8, and Table 4-9. As expected, the implementation of fracture complexity as increased surface area available for reactive transport processes (sorption and diffusion) significantly increases retention. However, the increased retention provided by incorporating fracture complexity does not improve the fit between predicted and observed breakthrough data when simulating the C2 Experiment using the JNC/Golder Task 6D DFN-CN model. The increase in complexity factor also resulted in longer tracer tails and a delayed t_{95} statistic for most models.
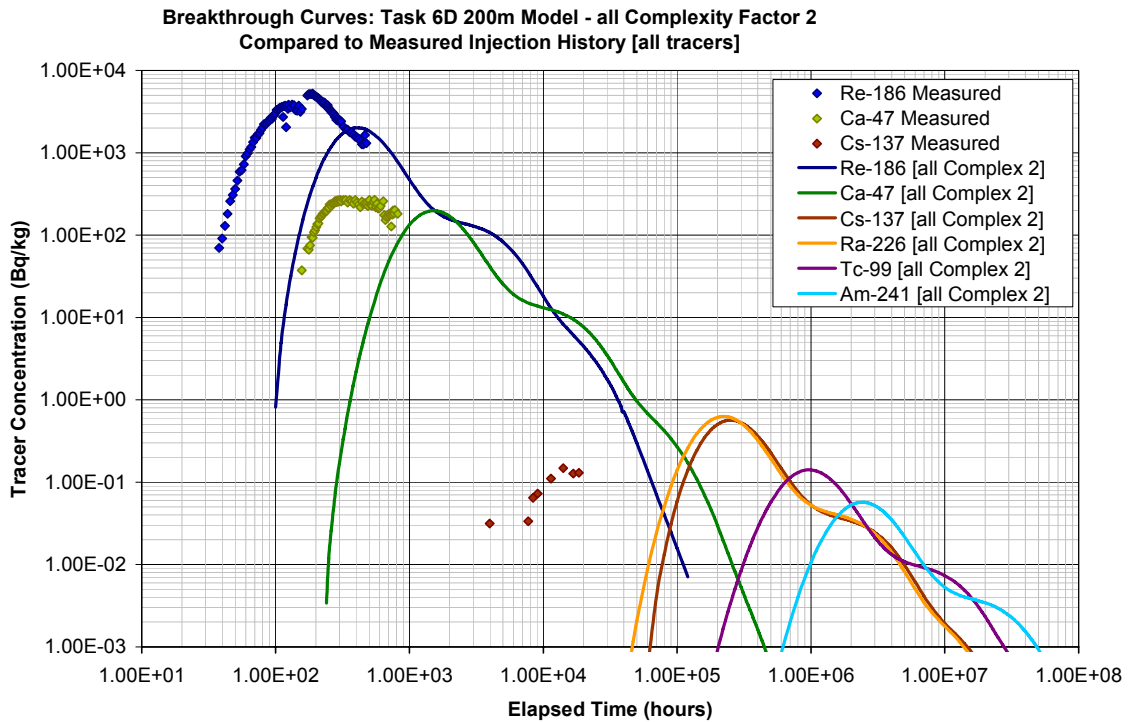
Figure 4-8. *Breakthrough curves for Experiment C2 simulations assuming all fractures assigned a complexity factor of 2.*
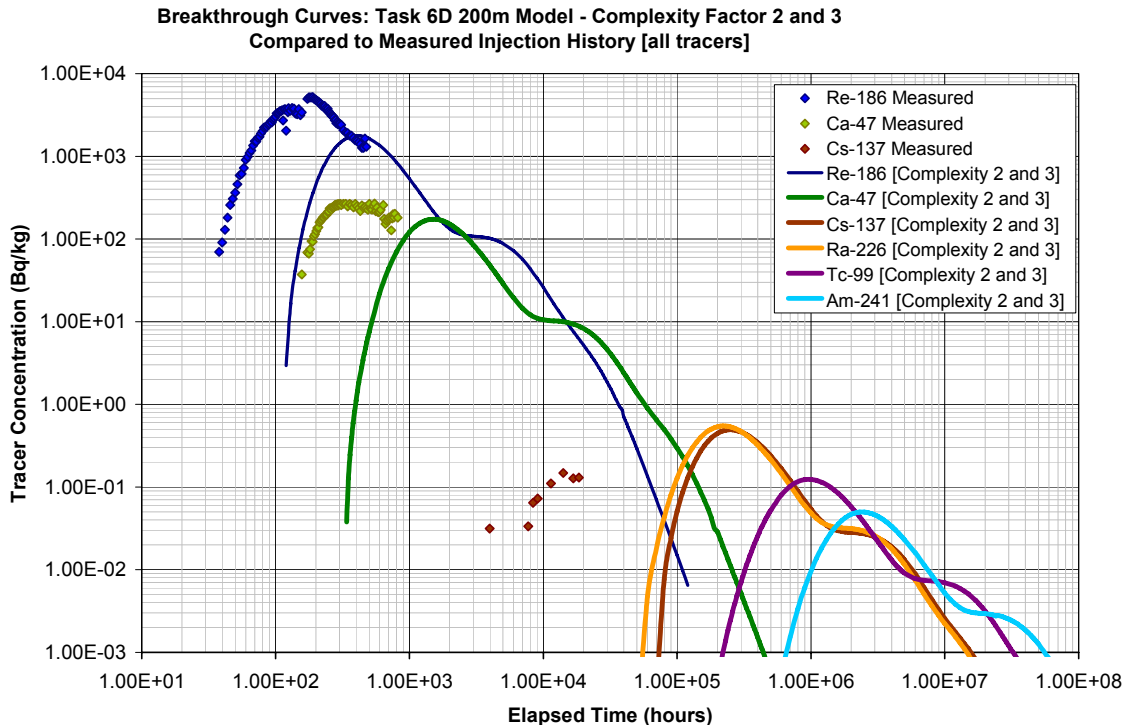
Figure 4-9. *Breakthrough curves for Experiment C2 simulations assuming deterministic fracture complexity assignments as presented in the Task 6C report (mix of Complexity 2 and 3 features).*

Table 4-8. Breakthrough statistics for Experiment C2 simulations assuming all fractures assigned a complexity factor of 2.

C2 Experiment: All fractures assigned Complexity Factor of 2			
Tracer	t_5 (hrs)	t_{50} (hrs)	t_{95} (hrs)	Maximum Release Rate (Bq/kg)
Re-186	280	900	12,000	2020
Ca-47	1000	3430	50,000	198
Cs-137	170,000	500,000	8,000,000	0.567
Ra-226	150,000	500,000	7,000,000	0.628
Tc-99	600,000	2,200,000	33,000,000	0.141
Am-241	1,600,000	5,000,000	80,000,000	0.0571

Table 4-9. Breakthrough statistics for Experiment C2 simulations assuming deterministic fracture complexity assignments as presented in the Task 6C report (mix of Complexity 2 and 3 features).

C2 Experiment: Mix of Complexity 2 and Complexity 3 structures			
Tracer	t_5 (hrs)	t_{50} (hrs)	t_{95} (hrs)	Maximum Release Rate (Bq/kg)
Re-186	290	1000	14,000	1780
Ca-47	1000	3900	50,000	174
Cs-137	170,000	600,000	9,000,000	0.493
Ra-226	150,000	500,000	8,000,000	0.549
Tc-99	600,000	2,500,000	36,000,000	0.124
Am-241	1,600,000	6,000,000	90,000,000	0.0499

4.5.3 The influence of background fracture network geometry

Size Distribution – Sensitivity Cases
Background Fractures
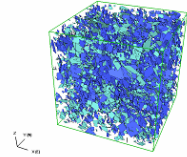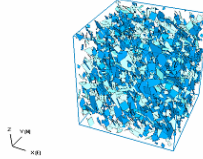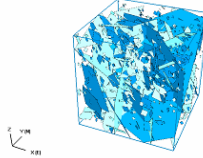
Lognormal Distribution Mean = 2m StDev= 2 m	
Lognormal Distribution Mean = 6 m StDev = 3 m	
Powerlaw Distribution D = 2.3 Min = 2 m	

Figure 4-10. *Background fracture size distributions used to evaluate the influence of background fracture network parameters on Experiment C2 results.*

Orientation Distribution – Sensitivity Cases
Background Fractures

		Fisher K	Truncated at 2m
SET #1: NNW Background Fractures Fisher Distribution Pole(211, 0.6)	Base Case	9.4	
	Case 1	2	
	Case 2	50	
SET #2: Shallow Background Fractures Fisher Distribution Pole(250, 54)	Base Case	3.8	
	Case 1	2	
	Case 2	50	

Figure 4-11. *Background fracture orientation distributions used to evaluate the influence of background fracture network parameters on Experiment C2 results. The orientation distribution parameters were taken from the Task 6C hydrostructural model report.*

Intensity – Sensitivity Cases

	Truncated at 0.5m	Truncated at 2m
NNW BG Fractures	• P32t = 0.0768 m²/m³ • Number of Fractures = 40782 • Mean fracture radius = 2.20m • Stdev fracture radius = 2.02m	• P32t = 0.0175 m²/m³ • Number of Fractures = 3111 • Mean fracture radius = 3.99m • Stdev fracture radius = 2.66m
Shallow BG Fractures	• P32t = 0.0573 m²/m³ • Number of Fractures = 32695 • Mean fracture radius = 2.20m • Stdev fracture radius = 2.05m	• P32t = 0.0148 m²/m³ • Number of Fractures = 2537 • Mean fracture radius = 3.95m • Stdev fracture radius = 2.94m

Figure 4-12. *Background fracture model intensity cases for Experiment C2 background fracture evaluation.*
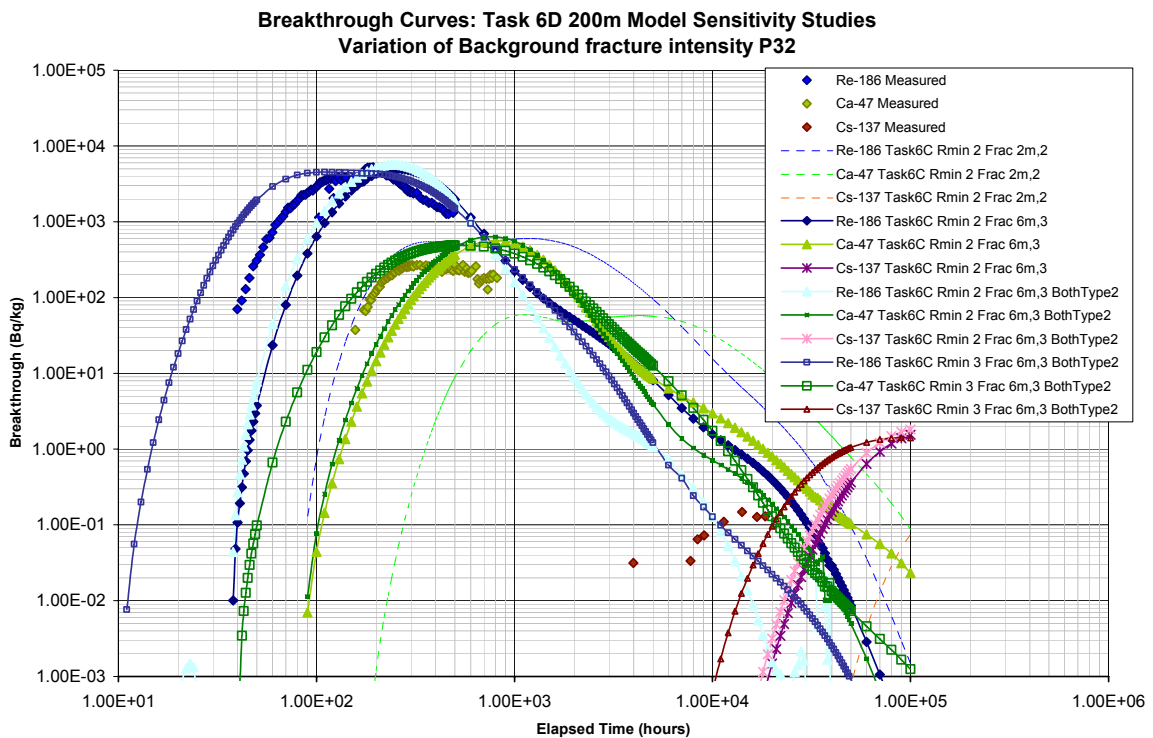
Figure 4-13. *Breakthrough curves from Task 6D background fracture network sensitivity study.*

49

Table 4-10. Breakthrough statistics for Task 6D background fracture network sensitivity study.

BGF Network: Radius Mean = 2 m, Std. Dev. = 2, Truncated @ 2 m.				
Tracer	t_5 (hrs)	t_{50} (hrs)	t_{95} (hrs)	Maximum Release Rate (Bq/kg)
Re-186	460	1400	8000	1210
Ca-47	1400	4800	26,000	139
Cs-137	100,000	N/R	N/R	0.00411

BGF Network: Radius Mean = 6 m, Std. Dev. = 2, Truncated @ 3 m.				
Tracer	t_5 (hrs)	t_{50} (hrs)	t_{95} (hrs)	Maximum Release Rate (Bq/kg)
Re-186	270	600	5000	2550
Ca-47	800	2100	17,000	285
Cs-137	100,000	N/R	N/R	0.234

BGF Network: Radius Mean = 2 m, Std. Dev. = 2, Truncated @ 2 m, All Type 2.				
Tracer	t_5 (hrs)	t_{50} (hrs)	t_{95} (hrs)	Maximum Release Rate (Bq/kg)
Re-186	240	500	2700	2960
Ca-47	700	1900	8000	322
Cs-137	100,000	N/R	N/R	0.376

BGF Network: Radius Mean = 6 m, Std. Dev. = 2, Truncated @ 3 m, All Type 2.				
Tracer	t_5 (hrs)	t_{50} (hrs)	t_{95} (hrs)	Maximum Release Rate (Bq/kg)
Re-186	80	260	1900	6350
Ca-47	300	1000	7000	601
Cs-137	50,000	N/R	N/R	1.67

4.6   Task 6D: JNC/Golder Results and Conclusions

The simulations of Task 6D through the use of DFN-CN models were carried out as forward models based on the Task 6C hydrostructural model, with its assignment of structural types and complexity, and the geometry of background fracturing. These forward models provided a surprisingly good match to in situ experiment results. This indicates the importance of the geological and geometrical site characterization which provided this information.

Sensitivity studies carried out indicate the following

- For experimental time frames, the presence of gouge and fracture infill minerals can significantly enhance retention. It is therefore important to have the geological type information available from site characterization.

- The increase flow wetted surface indicated by Complexity factors may also be important. However, the higher levels of complexity included in model sensitivity studies over predicted retention. This indicates a possibility that the simulations over-represented the increase in flow wetted surface area with increased complexity, at least for the radially converging flow field simulated.

- Fracture statistics of background fracture intensity, orientation, and size distributions also effect tracer breakthrough, but not to the same extent as complexity and structure type, at least for the range of simulations studied.

4.6.1   Main Conclusions

The main conclusions from simulations carried out by JNC/Golder for Task 6D include the following:

- Detailed site characterization data of background fracturing, fracture orientation, size, as well as geologic information constraining the microstructural model controlling transport is of significant value in constraining solute transport processes on experimental time scales.

- Discrete Fracture Network (DFN) modelling provides an approach to directly study the effect of site characterization information such as fracture geometry and geology on transport processes. This was much more difficult to do with equivalent continuum approaches such as MODFLOW.

- The Task 6D conceptual model provides a useful platform to continue to Task 6E for simulation of PA time scale solute transport.

4.6.2   Lessons learned and implications for Task 6 objectives

The following lessons have been learned from the Task 6D simulations:

- The DFN model which directly implemented the hydrostructural model was considerably more useful for studying the implications of site characterization data than the MODFLOW and GoldSim abstracted model.

- Increased attention should be paid to the effect of assumptions concerning microstructural models, and on site characterization to characterize fracture microstructure

- Experiments primarily constrain the more reactive, more porous immobile zones, such as gouge and cataclasite. These immobile zones may be less important for PA, since they are of limited extent

5 Task 6E – Performance Assessment Time Scale Simulations in a Rock Block

The goals of the JNC/Golder modelling team in the Task 6E effort were two-fold. First was to implement lessons learned from Task 6D to improve the level of detail of pore spaces and fracture complexity in the DFN/CN models. The second goal was to gauge the sensitivity of the immobile zone concept to various changes in material and network properties.

5.1 Modelling strategy

The JNC/Golder team utilized a forward modelling strategy; the Task 6C hydro-structural model was implemented directly. The model incorporated the flow geometry, boundary conditions, and material properties specified in the Task 6D and 6E specifications. As this was a forward model with a temporal dimension much larger than that of previous site characterization simulations, no formal calibration was attempted.

5.2 Model Implementation

5.2.1 Implementation of the Task 6C semi-synthetic hydrostructural model

The Task 6D specification requires that transport modelling be carried out within the 200-m scale "semi-synthetic" hydrostructural model developed within Task 6C (Dershowitz et al, 2002). The model combines:

- Deterministic structures directly identified in the Äspö TRUE Block Scale experiment;

- Semi-synthetic structures generated in Task 6C to provide connectivity and model detail in under-characterized areas of the TRUE Block Scale test area;

- Stochastic background fractures generated using the FracMan software package, based on analysis of Äspö data from the TRUE-BS block and other portions of the laboratory.

All 200 meter block structures and background fractures were modelled directly as specified in the Task 6C report using the FracMan software package. Structures extending outside the boundary of the 200 meter block were clipped. Figure 5-1 illustrates the 200 meter discrete fracture network used in Task 6E modelling. The model consists of 11 large-scale deterministic features, 19 large-scale semi-synthetic structures, and 5648 smaller-scale background fractures.

The initial DFN, based upon the Task 6C parameters, was then used through the PAWorks software package to decompose the three-dimensional discrete-feature network into a series of one-dimensional nodes linked by transport pipes. The resulting channel network is computationally more efficient than a network of polygonal finite elements, while still maintaining a three-dimensional problem space. The details of this transformation are described in Chapter 3.
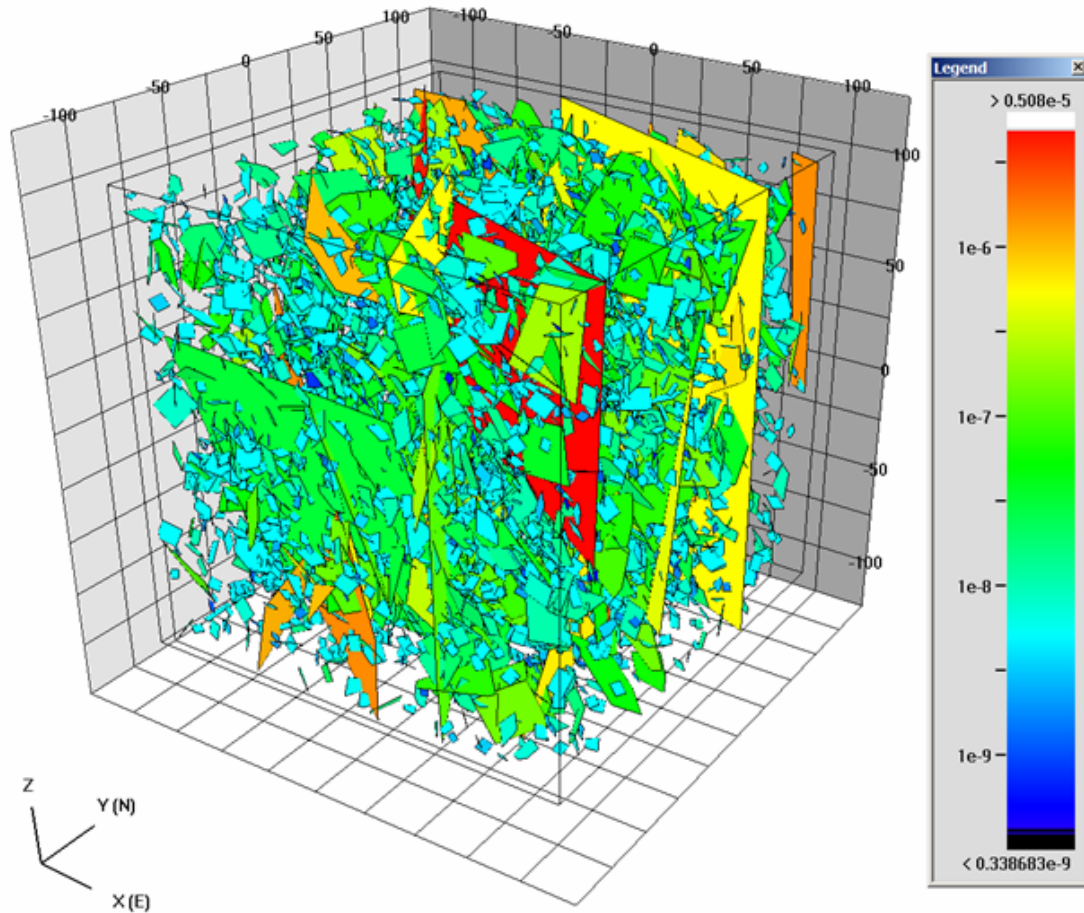
Figure 5-1. Deterministic, semi-synthetic, and background fractures used in the 200 meter block scale DFN model for the JNC/Golder team's Task 6E simulations. Fractures are colored by their transmissivity (m2/s).

The procedure for the DFN-CN model implementation was as follows.

1. The Task 6C hydrostructural model was implemented as a three-dimensional discrete feature network (DFN) model using the FracWorks XP software package. This model included all deterministic, semi-synthetic, and background structures.

2. The resulting DFN was converted into a one-dimensional pipe network model, using the PAWorks (Genpipe) software package. This pipe network was conditioned to match the connectivity of the DFN model, with pipe properties set to match the apertures and transmissivities of their host fractures. Pipes that did not connect to a head or flow boundary were removed from the system for computational efficiency

3. The specified steady state flow boundary conditions were applied to the boundaries of the model, and the new CN was run through the MAFIC software package to obtain a nodal head and flux field. The resulting flow solution assigned an advective transport velocity to all pipes.

4. The full channel network was converted into a smaller mesh of just the "downstream" network of pipes between the defined tracer injection source and sink. The new mesh was then exported this from PAWorks to the LTG solver. Immobile zone parameters are assigned to pipes based on set membership of their host fractures. Solute transport boundary conditions are also assigned at this stage.

5. Advective flow performance metrics (beta-factor and water residence time distributions) were obtained through particle tracking of 1,000 nuclides using the PAWorks software package and through the LTG simulation of a single tracer, neglecting all surface and matrix interactions.

6. β-values for the flow pathway that each particle took were calculated by dividing the travel time t_w in each pipe by the pipe aperture e, and summing the result over the length of the pipe.

7. Fracture complexity was simulated by altering the perimeters of pipes on a set-by-set basis in the LTG input files. Pipes belonging to fractures of complexity 2 had the pipe perimeter available to transport processes doubled, while pipes belonging to fractures of complexity 3 had their perimeters tripled. Flow perimeters, and therefore pipe velocities, were unchanged.

8. Solute transport was simulated using LTG in the pipe network. This program reported fluxes, concentrations, and cumulative releases at user-specified trace planes and at specified head / flux boundaries (the western edge of the 200-m TRUE block).

9. Additional performance measure statistics (breakthrough curves, t_5, t_{50}, t_{95}) were calculated from the LTG output files..

As specified in the Task 6E model requirements (Elert and Selroos, 2004b), performance metrics and tracer breakthrough statistics were computed for a series of north-south trending sampling traceplanes. The geometry of these traceplanes with respect to the tracer sources are presented in Figure 5-2.
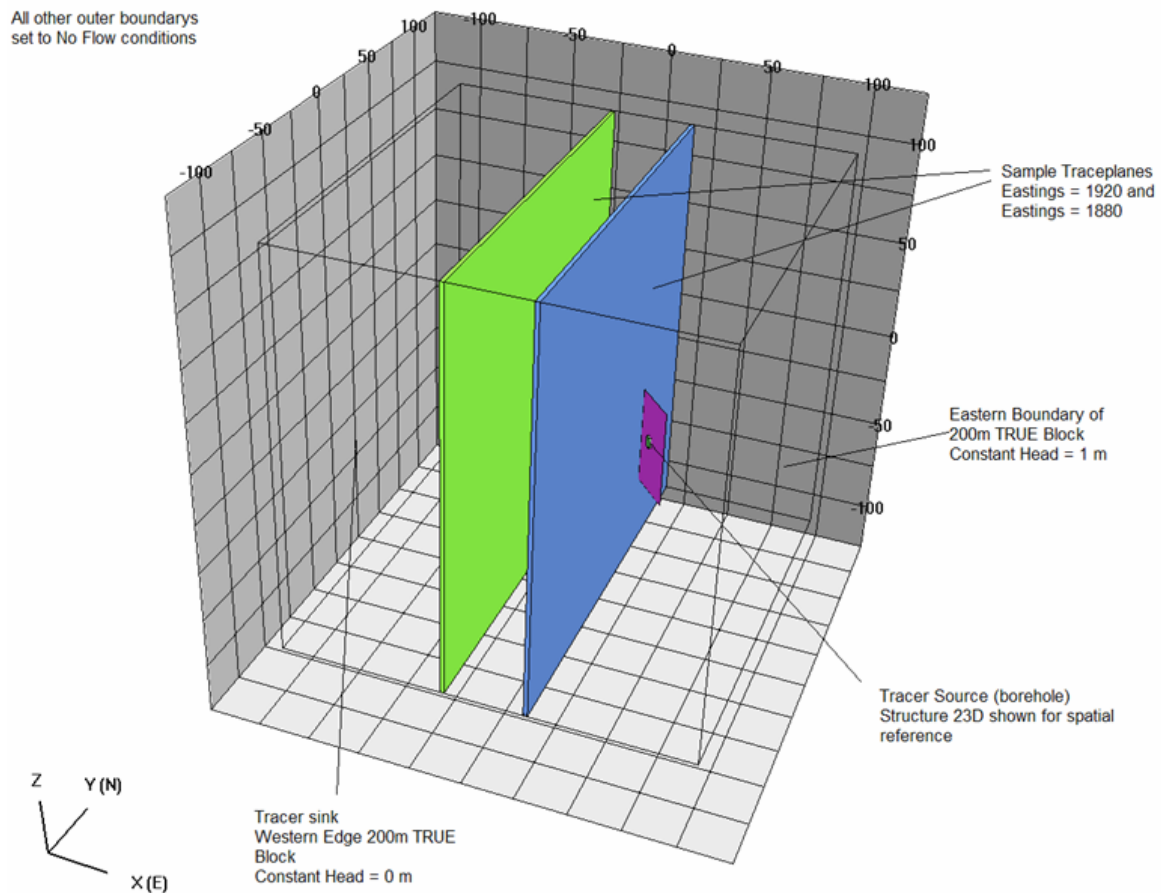
Figure 5-2. *Task 6E sampling traceplane locations and flow boundary conditions.*

5.2.2 Comparison to the Task 6D model implementation

Tasks 6D and 6E together represent the same rock block under site characterization and safety assessment boundary conditions respectively. Since an important goal of these tasks is to compare these safety assessment and PA modelling, the JNC/Golder team endeavoured to maintain the same model implementation between Task 6D and 6E. The changes to Task 6E were therefore primarily in the use of PA (natural gradient) boundary conditions and in the addition of immobile zones which only effect transport under long term transport boundary conditions. The immobile zones implemented for Task 6E represent full range of microstructural model. JNC/Golder implemented the model for Task 6D assuming only gouge and altered diorite immobile zones.

One additional change made between Task 6D and Task 6E was a revision to the method used to calculate the advective performance metrics. Task 6D results indicated that for the geometry and boundary conditioned modelled, particle tracking appear to better-represent transport processes occurring at the block scale than those computed using PAWorks graph-theory pathways. This is thought to be due to the forced gradient flow field used in Task 6D.

Task 6E modelling indicated that in areas with very small head or flux differences between connected and dead pathways (such as the region between the first sampling trace plane at Eastings 1920 meters and Structure 23), particle tracking may not be as suitable. The PAWorks graph theory pathways consistently found valid pathways between the sources and the sampling traceplanes, while a significant number of particles (approximately 50%) found themselves stuck down dead-end pathways. Therefore, for Task 6E the pathway metrics were based on graph theory pathway calculations.

5.2.3   Task 6E Flow Model

The JNC/Golder Task 6E simulation efforts utilized the FracMan/PAWorks and MAFIC approaches, as described in Chapter 3.1. The end result was a 1D channel network discretized from the Task 6C semi-synthetic hydrostructural DFN model.

5.2.3.1 Boundary Conditions

Task 6E models are designed to simulate radionuclide transport over long periods of time under natural groundwater conditions. The nuclide source repository is assumed to be closed, with all internal tunnels and access shafts sealed.

The western and eastern edges of the 200 meter TRUE Block cube are set as constant-head values, with an approximate 0.5% gradient across the test block. This corresponds to results presented by Walker and Gylling (1998) for the Äspö site. The other edges of the TRUE block are set to no flow boundary conditions.

5.2.3.2 Mathematical Description and Numerical Implementation

The mathematical description and numerical implementation of the 1D MAFIC solver are described in Chapter 3.1.

5.2.4   Task 6E Transport Model

Solute transport was simulated using the Laplace Transform Galerkin method, as implemented in the PAWorks / LTG software package (Dershowitz et. al., 2000). Radionuclide transport occurred within a three-dimensional channel network composed of one-dimensional pipe elements, with multiple immobile zones working in parallel to simulate rock and structural interactions.

5.2.4.1 Boundary Conditions

Tracers were introduced into a 3m long borehole section that penetrated Structure 23D near the middle of the TRUE Block volume. Tracers were allowed to dilute using natural gradients; there was no specified injection flux assigned to the model flow solution. The tracer source section was moved slightly laterally from the coordinates specified by SKB in order to fully penetrate Structure 23D.

Tracer concentrations were recorded along north-south trending traceplanes located at Eastings 1920 m (~10 meters from the source section), at Eastings 1880 m (~50 meters from the source section) and at Eastings 1800 (the western edge of the 200 meter TRUE block). Figure 5-2 illustrates the model boundary conditions and sampling locations.

Task 6E modelling requirements specifed a combination of tracers identical to those used in Task 6D simulations; the mix included both strongly and weakly sorbing radioactive tracers. The tracers used in the Task 6E transport simulations were ^{129}I$^-$, ^{47}Ca^{2+}, ^{137}Cs$^+$, ^{226}Ra, ^{99}Tc(IV) and ^{241}Am(III). Two separate injection profiles were used:

- Dirac pulse injection: 1 x 10^8 Becquerels injected in one hour (1.14 x 10^{-4} years). The same amount was injected for all tracers. The basic unit of time within the LTG solute transport code is years; time increments much smaller than hours tended to produce larger numerical errors in the transport solution.

- Extended pulse injection: 1 x 10^6 Becquerels per year injected for one thousand years.

5.2.4.2 Mathematical Description and Numerical Implementation

The mathematical descriptions and numerical implementations of the PAWorks and LTG packages are described in Chapter 3.2.

5.2.4.3 Parameters

Solute transport properties for Type I and Type II structures were provided in both the Task 6C final report and the Task 6D modelling specifications. The Task 6E simulations used the same chemical specifications.

Immobile zone parameters were assigned on a set-by-set basis, and were dependent largely on the geologic structure type. Table 4-2 and Table 4-3 specify basic parameters (porosity, thickness, and formation factor) relevant to solute transport for each geologic structure type. Table 4-4 and Table 4-5 present effective diffusivities (D_e) and volumetric sorption coefficients (K_d) for the specified tracers in contact with the different geological material types present in Type I and Type II features. K_d values are those provided for TRUE Block Scale groundwater in the Task 6D modelling specifications.

Table 5-1. Mineralogical breakdown and bulk density calculations for geologic materials used in Task 6E simulations (mineral fractions from the Task 6C report).

Mineral	Specific Gravity	Bulk Density (kg/m^3)	Fracture Coating		Fault Gouge		Cataclasite	
			%	Density Frac.	%	Density Frac.	%	Density Frac.
Smectite (assume montmorillonite)	2.5	2500	0	0	0.04	100.0	0	0
Illite	2.6	2600	0.025	65.0	0.12	312.0	0	0
Mixed layer clay	2.59	2590	0.025	64.75	0.08	207.2	0	0
Chlorite	2.95	2950	0.35	1032.5	0.25	737.5	0.06	177
Mica (50-50 mix musc and biotite)	2.84	2840	0	0.0	0.070	198.80	0	0
Epidote	3.4	3400	0.05	170.0	0.01	34.0	0.20	680
Plagioclase	2.69	2690		0.00	0.12	322.8	0.10	269.0
K-feldspar (orthoclase)	2.57	2570	0.10	257.0	0.06	154.2	0	0.0
Sulphides (est. average)	4.75	4750	0	0.0	0.01	47.5	0	0.0
Calcite	2.71	2710	0.350	948.5	0.080	216.80	0	0.0
Quartz	2.65	2650	0.080	212.0	0.160	424.00	0.140	371.0
Biotite	3	3000		0.0			0.03	90.0
Albite	2.62	2620		0.0			0.40	1048.0
Sericite	2.82	2820		0.0			0.04	112.8
Magnetite	5.18	5180		0.0			0.013	64.75
Hematite	5.26	5260	0.015	78.9			0.005	26.30
Titanite	3.48	3480		0.0			0.013	43.50
Apatite	3.175	3175		0.0			0.01	31.75
Pyrite	5.02	5020	0.005	25.10	0	0	0.0	0
Bulk Density			**2854**		**2755**		**2914**	
Bulk Density adj. for porosity			**2761**		**2404**		**2895**	

Mineral	Specific Gravity	Bulk Density (kg/m^3)	Altered Wall Rock		Intact Wall Rock	
			%	Density Frac.	%	Density Frac.
Smectite (assume montmorillonite)	2.5	2500	0	0.0	0	0.0
Illite	2.6	2600	0	0.0	0	0.0
Mixed layer clay	2.59	2590	0	0.0	0	0.0
Chlorite	2.95	2950	0.167	491.67	0	0.0
Mica (50-50 mix musc and biotite)	2.84	2840	0	0.0	0	0.0
Epidote	3.4	3400	0.167	566.67	0.05	170.0
Plagioclase	2.69	2690	0	0.0	0.47	1264.3
K-feldspar (orthoclase)	2.57	2570	0	0.0	0.10	257.0
Sulphides (est. average)	4.75	4750	0	0.0	0	0.0
Calcite	2.71	2710	0	0.0	0	0.0
Quartz	2.65	2650	0.167	441.67	0.14	371.0
Biotite	3	3000	0	0.00	0.18	540.0
Albite	2.62	2620	0.422	1106.22	0	0.00
Sericite	2.82	2820	0.022	62.67	0	0.00
Magnetite	5.18	5180	0.017	86.33	0.02	103.6
Hematite	5.26	5260	0.006	29.22	0	0.0
Titanite	3.48	3480	0.017	58.00	0.02	69.6
Apatite	3.175	3175	0.017	52.92	0.02	63.5
Pyrite	5.02	5020	0	0	0	2839.0
Bulk Density			**2895**		**2839**	
Bulk Density adj. for porosity			**2878**		**2830**	

A new addition is Table 5-1, which contains geologic material densities calculated using mineralogical breakdowns specified in the Task 6C hydrostructural report (Dershowitz et. al., 2002) and average chemical compositions of typical mineral end-members (Deer et. al., 1966). This allows for a more accurate estimation of the bulk densities of the geologic materials encountered along the Type I and Type II flow pathways for retardation calculations.

5.2.4.4 Immobile Zones

Seventeen immobile zones were neccesary to adequately characterize structural complexity within the 200 meter TRUE Block volume. These zones included:

- One immobile zone, representing intact Aspo granite / diorite, in contact with all fractures in the model. The perimters for pipes this zone were not adjusted for complexity

- Four altered diorite immobile zones for Type II (joint) structures: two for deterministic structures of complexity 2 and 3, and two for semi-synthetic structures of complexity 2 and 3.

- Four altered diorite immobile zones for Type I (fault) structures: two for deterministic structures of complexity 2 and 3, and two for semi-synthetic structures of complexity 2 and 3.

- Four fault gouge immobile zones for Type I structures: two for deterministic structures of complexity 2 and 3, and two for semi-synthetic structures of complexity 2 and 3.

- Four mylonite / cataclasite immobile zones for Type I (fault) structures: two for deterministic structures of complexity 2 and 3, and two for semi-synthetic structures of complexity 2 and 3.

5.3   Model Assumptions and Constraints

- Transport within smaller-scale background features was assumed to be minimal. As such, complexity (perimeter adjustment) was only applied to the deterministic and semi-synthetic block-scale structures.

- The tracer source was modeled as a borehole intersecting Structure #23D. The PAWorks package (Genpipes) discretized this condition to eight nodes in the plane of structure #23D. The use of an intersecting borehole rather than a line or point as a source for tracer injection results in a cleaner, better-connected pipe network.

- Water flow and radionuclide transport occurs within the fracture network. Transport within the rock matrix (outside of diffusion losses) was not modeled.

- Fracture mineral coatings are not a source of significant diffusion losses due to their relatively small volume with respect to the other elements of the microstructural model. The mineral coatings contribute to tracer retardation solely through surface sorption.

- Radioactive decay was not modeled.

- The LTG package models diffusion and sorption in immobile zones in parallel, rather than in series. PAWorks limits the user to two immobile zones; a non-flowing pore space and a matrix immobile zone. Additional immobile zones have to be added by hand to the output files. LTG supports up to five immobile zones per pipe (fracture) set.

5.4 Model calibration

As the JNC/Golder team's Task 6 modelling approach was one of forward modelling, no calibration was performed.

5.5 Task 6E Model Results

This section presents the results of the JNC/Golder Task 6E flow and transport simulations, expressed as the performance metrics requested by SKB (Elert and Selroos, 2004a). Model flow metrics are the results from an advection-only transport simulation using a single tracer with no matrix or surface interactions. The transport metrics are the result of the full JNC/Golder transport model implementation.

5.5.1 Flow

The results of the steady-state flow solution for Task 6E are presented below in Figures 1 and 2. The steady-state heads and pipe parameters are used to calculate transport velocities for input into the LTG solver.
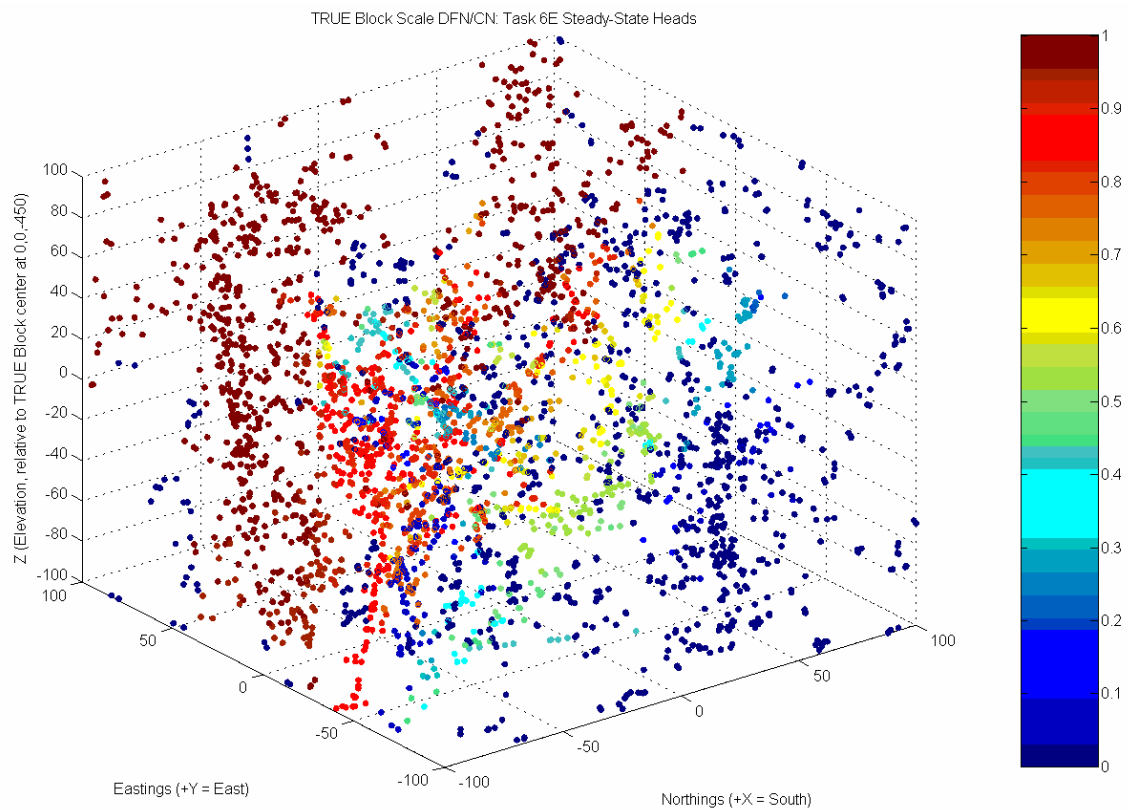
Figure 5-3. *Nodes that form the one-dimensional pipe network created by PAWorks from the three-dimensional polygonal fracture network. Node color corresponds to the steady-state head value at that position in meters.*
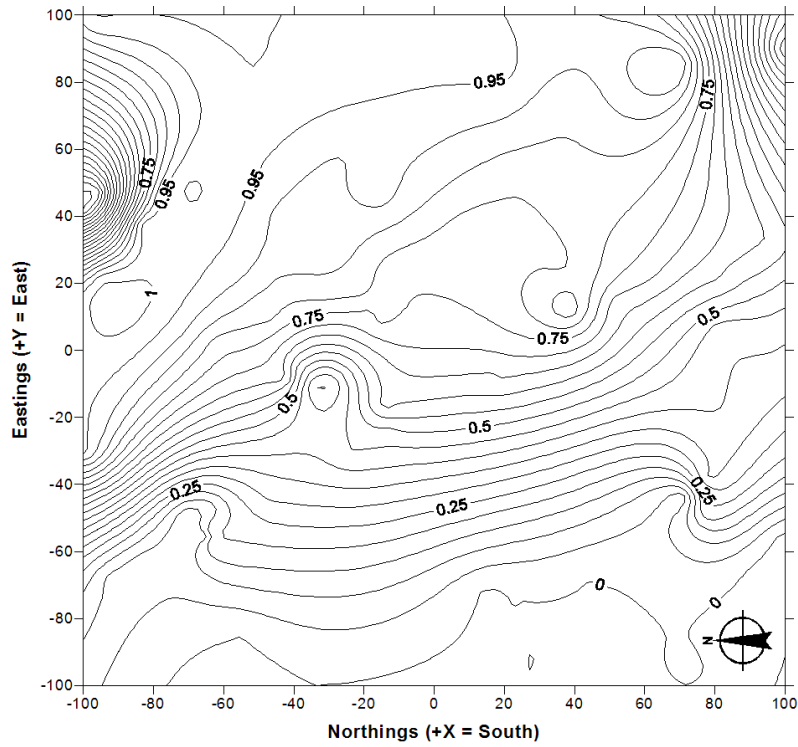
Figure 5-4. *Contour plot of Task 6E modelled heads on a horizontal trace plane through the center of the 200 meter TRUE Block. Contours are spaced in increments of 0.05 meters.*
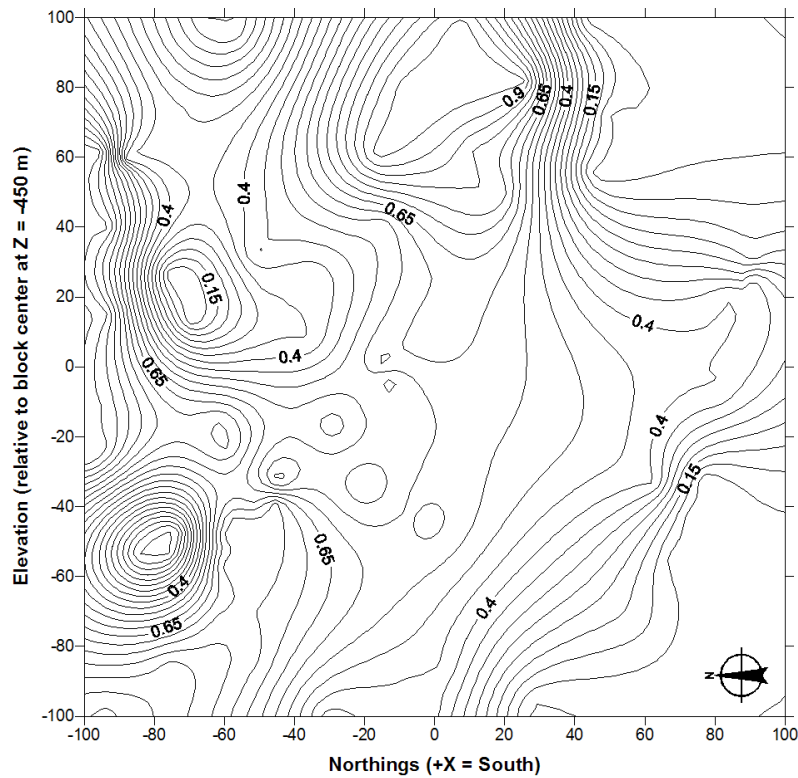
Figure 5-5. *Contour plot of Task 6E modelled heads at the second requested sampling trace place (Eastings = 1880 m). Contours are spaced in increments of 0.05 meters.*

5.5.1.1 Description of flow paths

Flow paths were evaluated in two stages:

1. PAWorks identification of significant pathways: The PAWorks software package uses a graph-theory search method to identify significant flow pathways between sources and sinks. The code can perform depth-first, breadth-first or parameter-weighted searches, based on user-specified parameters. The search results are used to construct representative pathways that characterize the flow system as a whole The drawback to the PAWorks method is that, by using a weighted search, transport pathways are limited to a subset of the total number of potential pathways. In addition, a PAWorks search may not necessarily identify all pathways in a system.

2. Particle tracking identification of pathways: Pathways identified through particle tracking represent transport through the complete network of pipes downstream of a given tracer source. The network of pathways is similar to that found by PAWorks using graph theory, but has the potential to capture the widest variety of significant pathways. Effectively, the particle-tracking is always flux-weighted, and will force transport along the highest-flux pathways. If model assumptions regarding network geometry and pathway connections are correct, particle tracking should produce the most consistent results.

5.5.1.2 PAWorks Graph Theory Paths

Transport pathways found using the PAWorks software package graph-theory search are presented below in Figure 5-6. The search was conducted using a breadth-first approach with pathways weighted towards those pipes that minimized the travel time between source and sink. Three vertical traceplane sinks were used: one at Eastings = 1920 meters (~10 meters from the tracer injection section), one at Eastings 1880 meters (~50 meters from the tracer injection section), and one at the western edge of the 200 meter TRUE Block scale volume. Table 5-2 contains basic pathway statistics derived from the graph-theory search results.

Table 5-2. Pathway statistics derived from PAWorks graph theory search of Task 6E DFN-CN model.

	Eastings 1920	Eastings 1880	West Edge TRUE Block
Pathway Length (m)			
Average	146.64	205.86	326.40
Std. Dev.	77.37	60.22	38.80
Maximum	336.12	347.40	482.81
Minimum	25.58	97.68	223.95
Travel Time (years)			
Average	52.28	14.77	50.62
Std. Dev.	134.81	10.11	199.71
Maximum	947.02	55.80	1967.80
Minimum	1.53	3.96	5.33
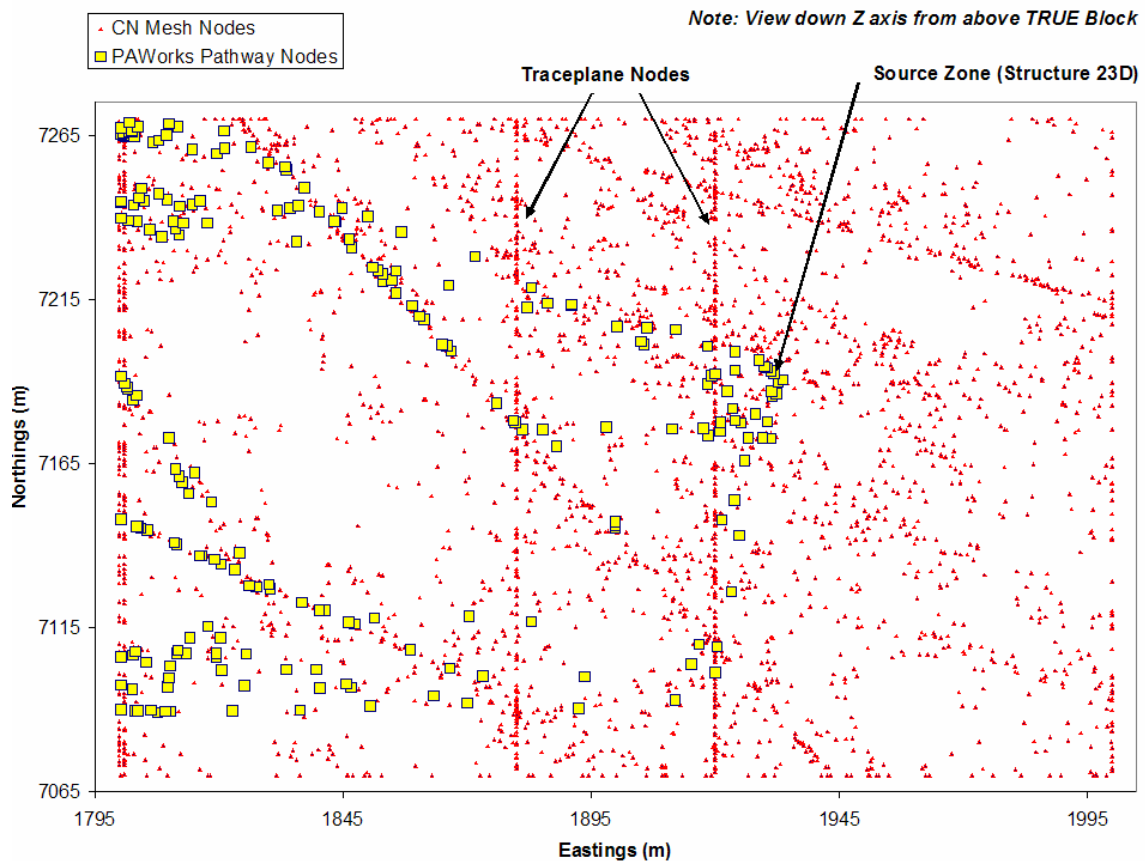
Figure 5-6. Locations of nodes (ends of flow pipes) defined in CN model, overlain with nodes identified as components of significant pathways by PAWorks graph theory search. View is down Z-axis from above TRUE block; center of block is at (1900, 7170).

5.5.1.3 Particle Tracking Pathways

Transport pathways found using the particle tracking facilities built into the PAWorks software package are presented below in Figure 5-7. 1000 particles were released into the steady-state flow system. Due to software limitations, the only pathways identified were those between the source section in Structure 23D and the model sink (west edge of the 200-meter TRUE Block volume). Table 5-3 contains basic pathway statistics derived from the particle tracking results.

Table 5-3. Pathway statistics derived from particle tracking in Task 6E DFN-CN model.

Particle Tracks (West Edge of 200m TRUE Block Scale volume as sink)					
Distance Traveled (m)		Travel Time (years)		Beta Factor (yr/m)	
Average	391.27	Average	25.77	Average	1.63E+05
Std. Dev.	68.58	Std. Dev.	21.12	Std. Dev.	1.17E+05
Maximum	663.87	Maximum	251.00	Maximum	1.11E+06
Minimum	252.42	Minimum	7.06	Minimum	5.60E+04
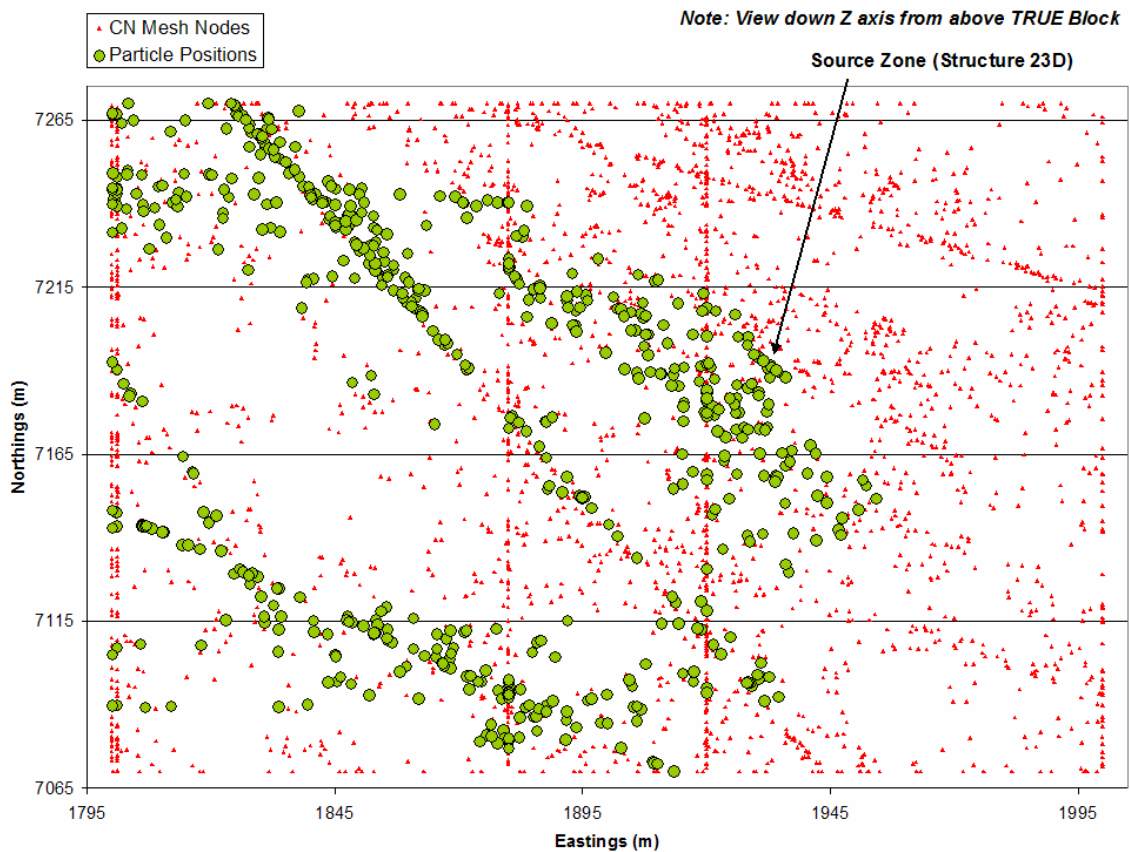
Figure 5-7. *Locations of nodes (ends of flow pipes) defined in CN model, overlain with nodes identified as components of significant pathways through particle tracking. View is down Z-axis from above TRUE block; center of block is at (1900, 7170).*

5.5.1.4 Water Residence Time Distribution

The water residence time distribution was estimated by calculating the breakthrough for a single conservative tracer assuming advection only (no surface or matrix interactions). A 'mass' of $1x10^8$ Becquerels was released into the DFN-CN model over a period of one hour (on PA time scales, a one-hour injection is effectively a Dirac pulse injection); this release profile mirrors that of the formal tracer tests described below in the Transport section. Attempts to use time steps smaller than one hour resulted in excessive numerical instabilities that manifested as concentration fluctuations before actual tracer breakthrough.

Note the relatively wide time distribution for pathways leading to (and through) the first sampling traceplane at Eastings = 1920 meters. The relatively long late-time points are due to pathways that migrating across and back through the boundary. Since the traceplane is not considered a sink region by the PAWorks code, pathways are free to migrate through the traceplane several times. This effect is only significant for areas where the source (Structure 23D) is relatively close to the sink, and there is no strongly-defined sink region.

The water residence time distribution is summarized below in Figure 5-8; formal time-series data was submitted as a Microsoft Excel® spreadsheet.

66
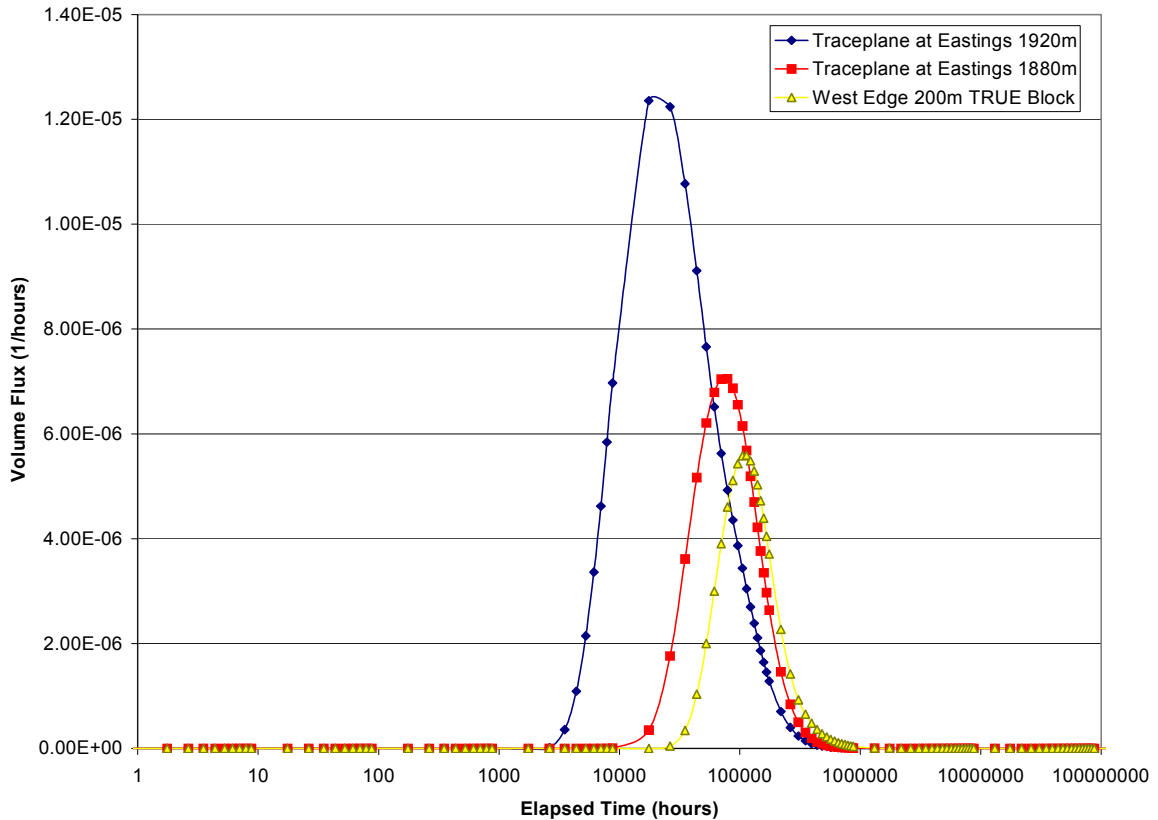
Figure 5-8. *Water residence time distribution calculated for advection-only Dirac-pulse input into the JNC/Golder Task 6E DFN/CN model.*

5.5.1.5 β-factor – ratio of flow wetted surface to water flow

Task 6D models calculated β-factor by using flow pathways defined using PAWorks graph-theory searches. The β-factor for each identified pathway was calculated by dividing the average channel cross-sectional area by the channel flux rate.

The current JNC/Golder Task 6E model computed the β-factor using two methods:

1. Through PAWorks particle tracking trajectories. A β-factor was calculated for each pipe in a track by dividing the particle travel time for that segment by the fracture half-aperture. The b-values were then summed along the total particle track to provide an accurate count for the complete pathway.

2. Through PAWorks pathways identified using a weighted graph theory algorithm. For each pipe in a given pathway (200 total theoretical pathways), the flow wetted surface length was divided by the product of the pipe area and the pipe velocity. All calculations assumed a parallel-plate approximation for the network rather than a stream tube.

Only the pathways between the source borehole and the ultimate sink (the western edge of the TRUE block) were used in the β-factor calculations; current software limitations prevent the use of traceplane elements as particle sinks.

67

β-factors calculated for the JNC/Golder Task 6E channel network models generally match those produced by other modelling teams. However, the model did produce flow pathways that were generally longer and slower than the other modelling teams. This is most likely due to model assumptions as to how pipe flow and transport widths are calculated from the base DFN.

Particle tracking results suggest general transport pathway lengths in the range of 300 to 500 meters. This suggests that the channel network possesses significant internal longitudinal dispersion, as the Cartesian distance between the source borehole and the model boundary is approximately 270 meters. Our models suggest a power-law relationship between travel time and β-factor, rather than a straight linear one; however, there is significant scatter (see Figure 5-9) in the particle tracking data points.
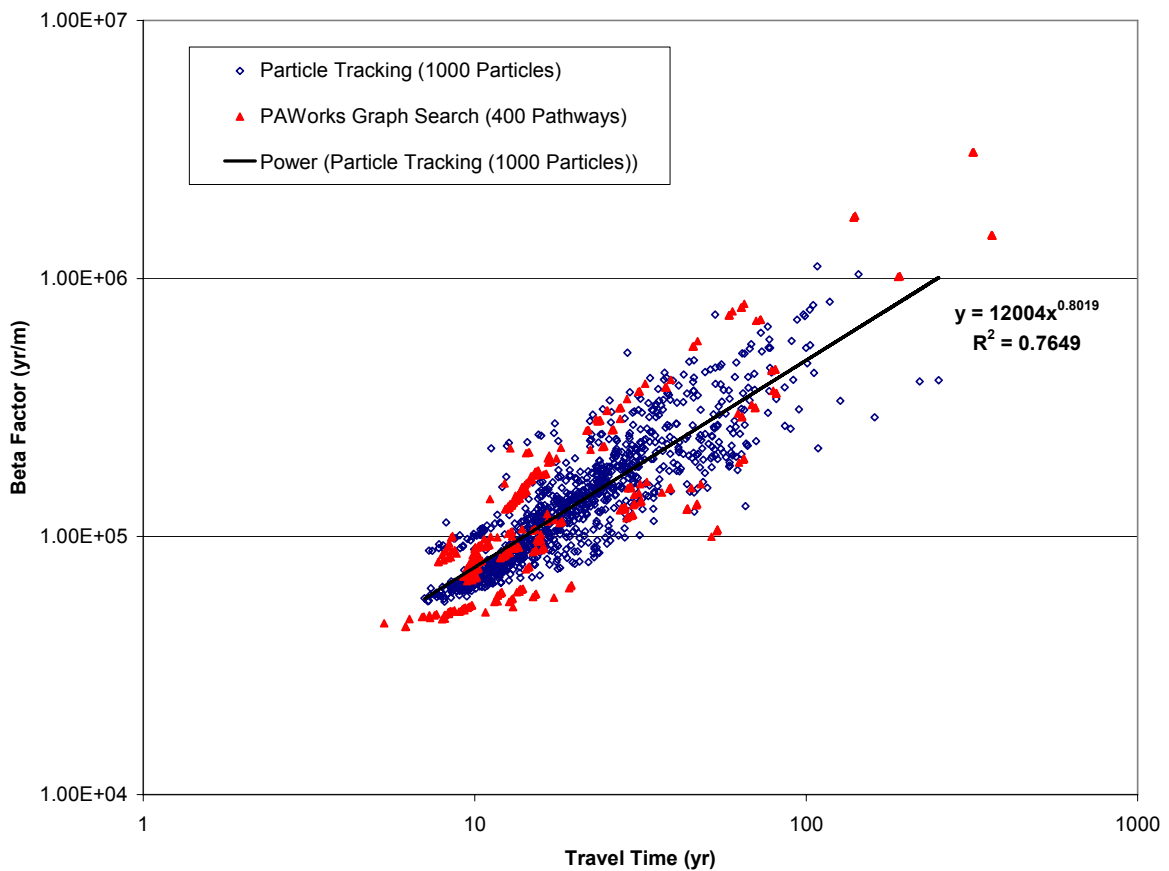
Figure 5-9. *τ (travel time in years) – β (years / meter) distribution for JNC/Golder Task 6E model. β-factor derived using PAWorks particle tracking.*
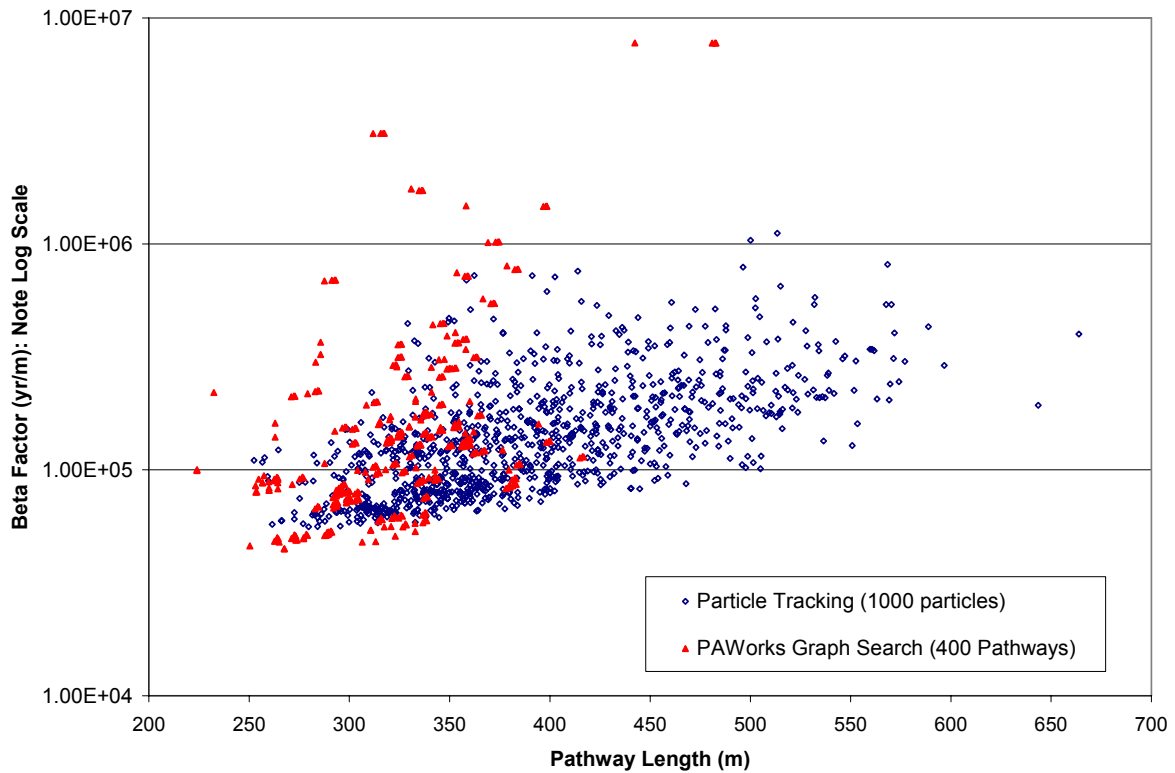
Figure 5-10. *β-factor as a function of pathway length between source and ultimate sink (western edge of the 250-meter scale TRUE Block). β-factor derived using PAWorks particle tracking.*

5.5.2   Transport

5.5.2.1 Breakthrough Curves

Tracer breakthrough curves, presented below in Figure 5-11 through Figure 5-18, are plotted based on normalized activity flux rates (1/years). Output from the LTG software package consists of cumulative release amounts for each tracer at each time step (Becquerels) and an activity flux rate at each sink (Becquerels per year). Normalized activity flux values are plotted by dividing the activity flux rate by the injected activity; due to rounding errors, this may result in cumulative recoveries higher than 100% of injected mass.
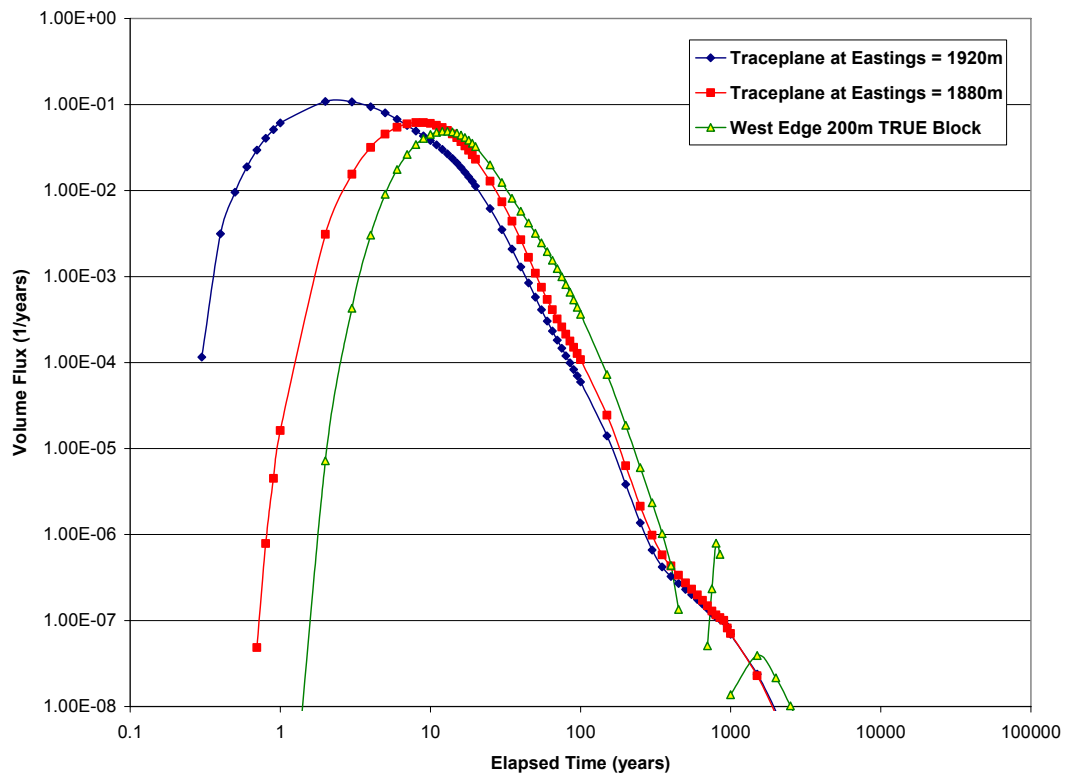
Figure 5-11. *Breakthrough curves for Dirac pulse injection, assuming only advective transport (no sorption or diffusion). A total activity of 1.0×10^8 Bq was injected in one hour.*
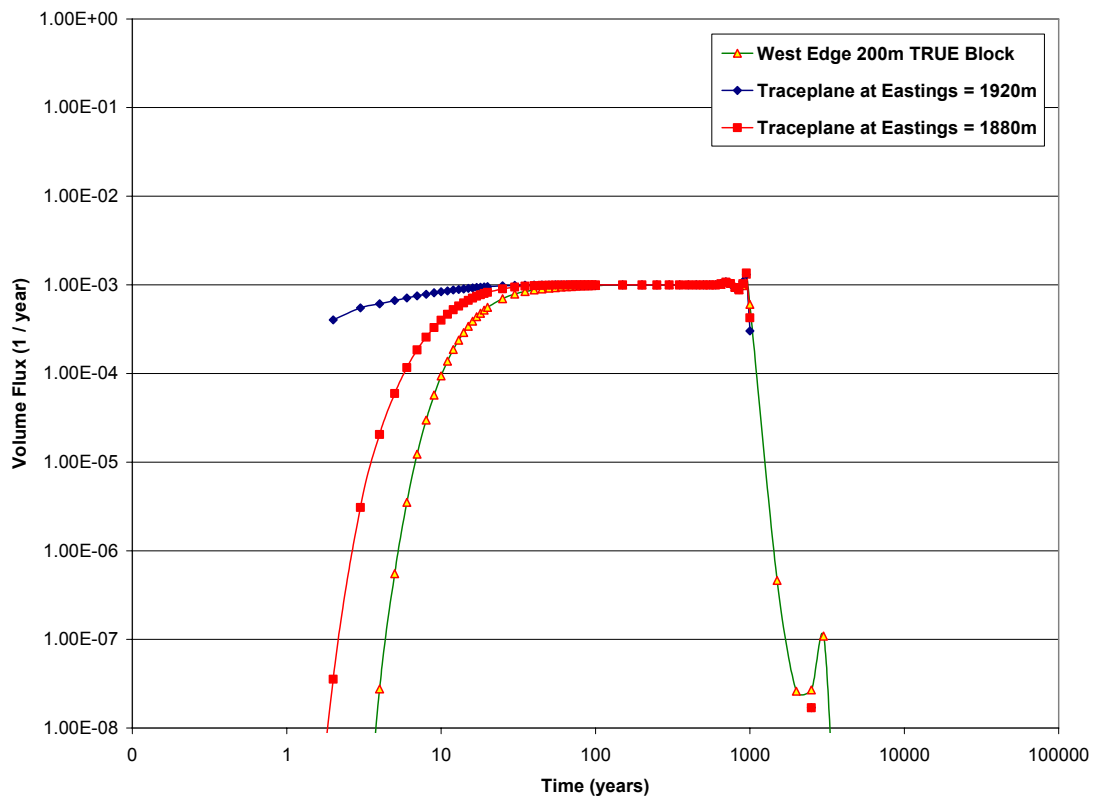
Figure 5-12. *Breakthrough curves for extended pulse injection, assuming only advective transport (no sorption or diffusion). Tracer was injected at a rate of 1.0×10^6 Bq per year for 1000 years.*
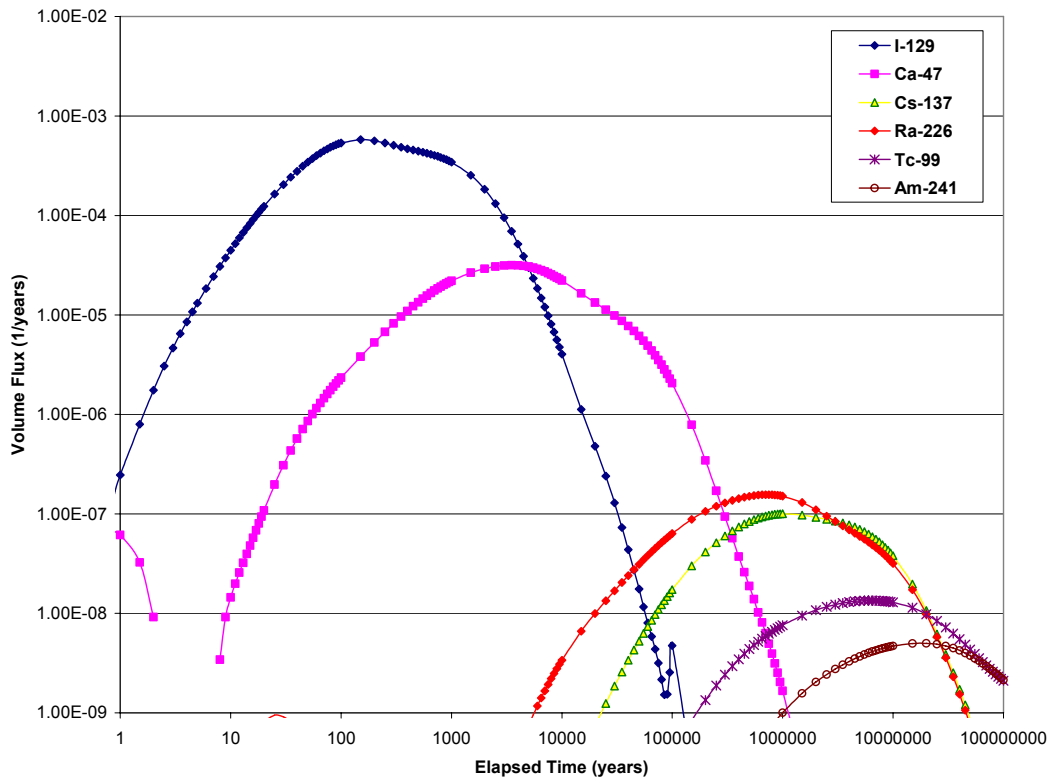
Figure 5-13. *Breakthrough curves for Dirac pulse injections, with a total activity of 1.0 x 10^8 Bq injected in one hour. Concentrations measured at a sampling traceplane at* Eastings = 1920 m.
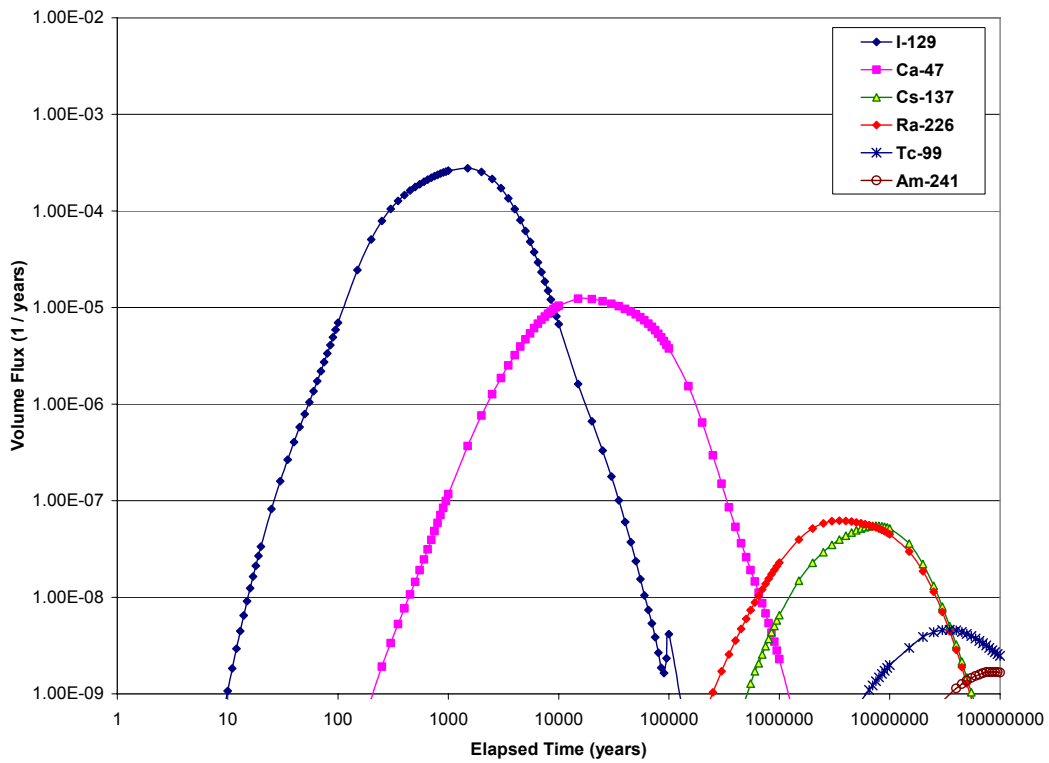
Figure 5-14. *Breakthrough curves for Dirac pulse injections, with a total activity of 1.0 x 10^8 Bq injected in one hour. Concentrations measured at a sampling traceplane at Eastings = 1880 m.*
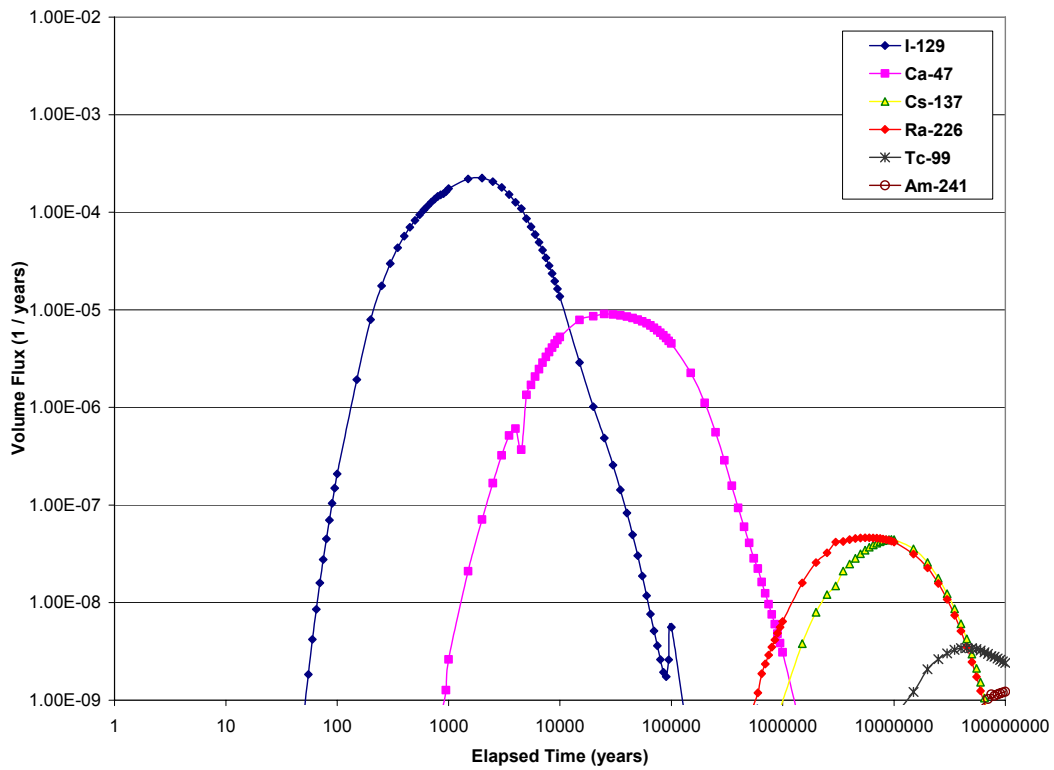
Figure 5-15. *Breakthrough curves for Dirac pulse injections, with a total activity of 1.0 x 10⁸ Bq injected in one hour. Concentrations measured at the western edge of the 200m TRUE Block Scale volume.*
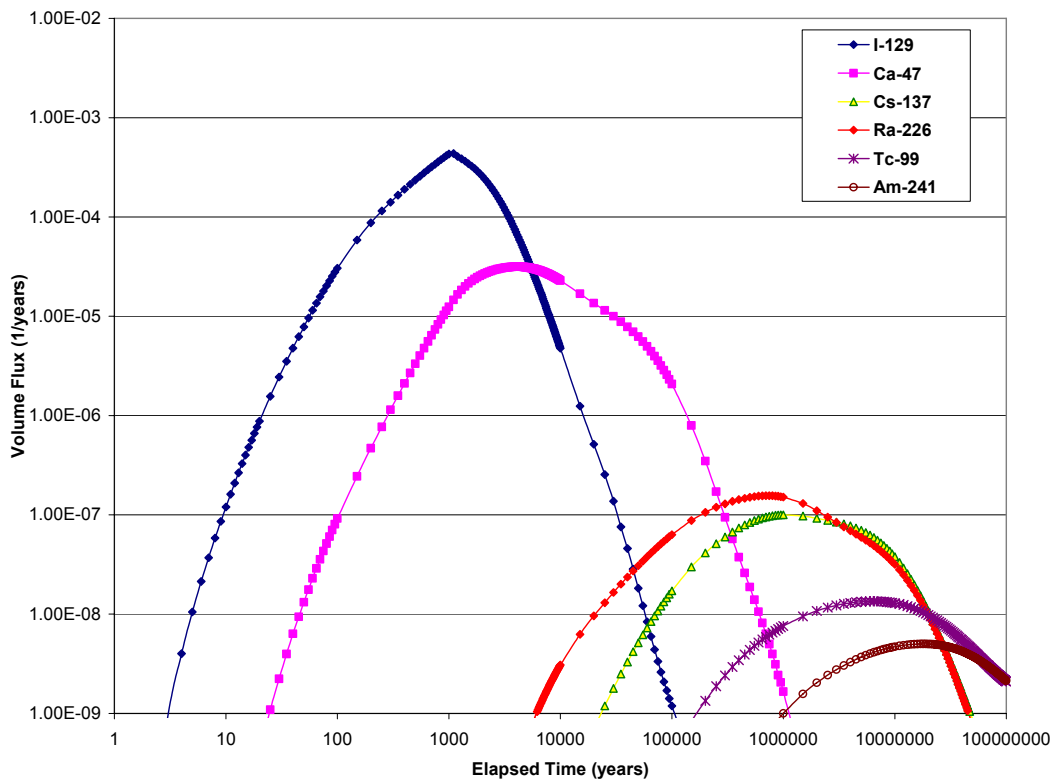
Figure 5-16. *Breakthrough curves for extended pulse injections (activity flux of 1.0 x 10⁶ Bq per year for 1000 years). Concentrations measured at a sampling traceplane at Eastings = 1920 m.*

Figure 5-17. *Breakthrough curves for extended pulse injections (activity flux of 1.0 x 10^6 Bqs per year for 1000 years). Concentrations measured at a sampling traceplane at Eastings = 1880 m.*
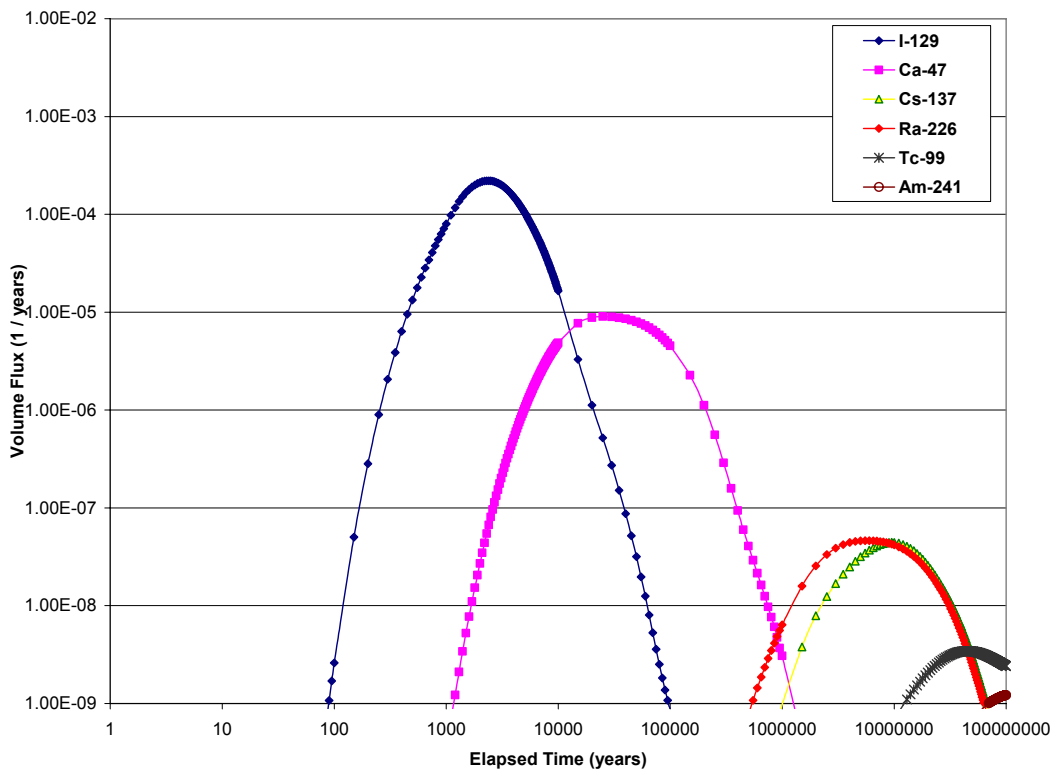
Figure 5-18. *Breakthrough curves for extended pulse injections (activity flux of 1.0 x 10^6 Bq per year for 1000 years). Concentrations measured at the western edge of the 200m TRUE Block Scale volume.*

5.5.2.2 Tracer Test Statistics

Results of the JNC/Golder Task 6E tracer test statistics are presented below in Table 5-4 through Table 5-7.

Table 5-4. Tracer breakthrough statistics for Task 6E Dirac pulse injection simulations.

Breakthrough Times at West Edge of 200m TRUE Block			
Tracer	t_5 (yr)	t_{50} (yr)	t_{95} (yr)	Max. Release Rate (1/yr)
I-129	800	3000	10,000	2.24E-04
Ca-47	10,000.00	70,000	250,000	9.06E-06
Cs-137	4,000,000.00	15,000,000	50,000,000	4.44E-08
Ra-226	3,000,000.00	10,000,000	45,000,000	4.62E-08
Tc-99	30,000,000.00	Not Reached	Not Reached	3.44E-09
Am-241	85,000,000.00	Not Reached	Not Reached	1.22E-09

Breakthrough Times: Traceplane at Eastings = 1920			
Tracer	t_5 (yr)	t_{50} (yr)	t_{95} (yr)	Max. Release Rate (1/yr)
I-129	100	1000	5500	5.78E-04
Ca-47	2000	25,000	100,000	3.16E-05
Cs-137	750,000	6,000,000	25,000,000	1.00E-07
Ra-226	450,000	5,000,000	25,000,000	1.56E-07
Tc-99	4,500,000	70,000,000	Not Reached	1.35E-08
Am-241	10,000,000	Not Reached	Not Reached	5.01E-09

Breakthrough Times: Traceplane at Eastings = 1880			
Tracer	t_5 (yr)	t_{50} (yr)	t_{95} (yr)	Max. Release Rate (1/yr)
I-129	550	2000	7500	2.77E-04
Ca-47	10,000	50,000	200,000	1.23E-05
Cs-137	3,000,000	10,000,000	35,000,000	5.51E-08
Ra-226	2,000,000	10,000,000	35,000,000	6.20E-08
Tc-99	20,000,000	Not Reached	Not Reached	4.61E-09
Am-241	60,000,000	Not Reached	Not Reached	1.69E-09

Table 5-5. Tracer breakthrough statistics for Task 6E extended pulse injection simulations.

		Breakthrough Times at West Edge of 200m TRUE Block		
Tracer	t_5 (yr)	t_{50} (yr)	t_{95} (yr)	Max. Release Rate (1/yr)
I-129	1200	3500	10,000	2.21E-04
Ca-47	15,000.00	70,000	250,000	9.05E-06
Cs-137	4,000,000.00	15,000,000	52,000,000	4.44E-08
Ra-226	2,500,000.00	13,000,000	48,000,000	4.62E-08
Tc-99	32,000,000.00	Not Reached	Not Reached	3.44E-09
Am-241	88,000,000.00	Not Reached	Not Reached	1.22E-09

		Breakthrough Times: Traceplane at Eastings = 1920		
Tracer	t_5 (yr)	t_{50} (yr)	t_{95} (yr)	Max. Release Rate (1/yr)
I-129	450	1700	6200	4.36E-04
Ca-47	2800	25,000	100,000	3.15E-05
Cs-137	750,000	6,000,000	29,000,000	1.00E-07
Ra-226	450,000	5,000,000	27,000,000	1.56E-07
Tc-99	4,500,000	70,000,000	Not Reached	1.35E-08
Am-241	13,000,000	Not Reached	Not Reached	5.01E-09

		Breakthrough Times: Traceplane at Eastings = 1880		
Tracer	t_5 (yr)	t_{50} (yr)	t_{95} (yr)	Max. Release Rate (1/yr)
I-129	950	2800	8300	2.71E-04
Ca-47	10,000	50,000	200,000	1.23E-05
Cs-137	3,000,000	12,000,000	38,000,000	5.51E-08
Ra-226	2,000,000	11,000,000	36,000,000	5.78E-08
Tc-99	22,000,000	Not Reached	Not Reached	4.61E-09
Am-241	61,000,000	Not Reached	Not Reached	1.68E-09

Table 5-6. Tracer transport statistics for Dirac pulse injections, advection only.

	Breakthrough Times		
Performance Metric	Eastings 1920m	Eastings 1880m	West Edge TRUE Block
t5 (yr)	1 (2%)	4 (3%)	7 (4%)
t50 (yr)	6 (48%)	12 (48%)	17 (48%)
t95 (yr)	25	35 (94%)	60 (94%)
Max Release Rate (1/yr)	1.08E-01	6.18E-02	4.90E-02

Table 5-7. Tracer transport statistics for extended pulse injections, advection only.

	Breakthrough Times		
Performance Metric	**Eastings 1920m**	**Eastings 1880m**	**West Edge TRUE Block**
t5 (yr)	55	65	75
t50 (yr)	500 *(49.4%)*	500 *(48.6%)*	550 *(52.5%)*
t95 (yr)	950	950	975
Max Release Rate (1/yr)	1.31E-03	1.36E-03	1.32E-03

5.5.3   Sensitivity Studies

A limited parameter analysis was performed on the JNC/Golder Task 6E channel network to determine where the model is most sensitive to changes. A single non-sorbing tracer (I-129) and a single moderately sorbing tracer (Tc-99) were used to evaluate the effects of mesh generation options, geologic feature type, and structural complexity.

5.5.3.1   JNC/Golder Task 6E Model Sensitivity to Pipe Network Generation Options

The PAWorks software package converts three-dimensional planar fractures into one-dimensional pipes by connecting nodes located at the midpoints of fracture intersections. The pipe width, which is used to simulate an equivalent parallel-plate fracture feature, is calculated by multiplying the 3D intersection trace lengths by user-specified parameters (see Figure 3-1). The resulting pipe area is then multiplied by an area correlation factor W_{af} (Dershowitz et. al., 2000). A correlation factor of one results in equivalence between total pipe area and fracture area.

Figure 5-19. *JNC/Golder Task 6E DFN-CN model sensitivity to changes in fracture-pipe area correlation factor. Tracer concentrations were measured at the west edge of the 200-meter TRUE Block volume.*

The pipe width, in combination with the fracture aperture, affects pathway velocities, which, in turn, affect tracer travel times. Figure 5-19 illustrates the effects of varying the area correlation factor. Note that, on PA timescales, the pipe width effect appears to be fairly minimal. Fracture aperture and pipe length may be more significant parameters.

5.5.3.2 JNC/Golder Task 6E Model Sensitivity to Geologic Feature Type

In both the JNC/Golder channel network model and the Task 6C hydrostructural model, the choice of geologic feature type between Type 1 (fault) or Type II (joints) has a large affect on tracer transport. Type I features have significantly more surface area available for surface retardation and diffusion, due to the way these processes are implemented in the PAWorks/LTG toolchain. In addition, Type 1 features contain geologic materials (clay minerals, brecciated surfaces) that are significantly more reactive than Type II features, which are typically surfaced in unaltered to slightly altered granitic rock.

Results of this sensitivity study are presented as breakthrough curves in Figure 5-20. The effects of changing geologic structure type are fairly predictable. If all transport pathways behave as Type II structures (joints), initial tracer breakthroughs occur sooner (by a factor of 2 – 5 times) while the tracer tail is relatively unaffected. If all transport pathways behave as Type I structures (faults), tracer initial breakthroughs are retarded by almost an order of magnitude, but again with relatively little effect on the tracer tails.

Figure 5-20. *JNC/Golder Task 6E model sensitivity to changes in geological structure type. Tracer concentrations were measured at the west edge of the 200-meter TRUE Block volume.*

5.5.3.3 JNC/Golder Task 6E Model Sensitivity to Complexity Factor

In the JNC/Golder Task 6E channel network model, structural complexity was implemented solely in the transport code; the basic pipe network and advective flow field was not affected. Complexity was simulated by changing the pipe perimeter surface available to diffusion and sorption. By multiplying the pipe perimeter by a constant equal to the structural complexity, LTG approximated the effects of multiple transport pipes on a feature.

The pipe perimeter available to transport processes was determined on an immobile zone basis; it was possible to have differing complexity factors for the different geological material types (fault gouge, cataclasite, fracture mineralization, etc.). However, the sensitivity study addressed only the effects of changing the complexity factor of all immobile zones simultaneously. Results, in the form of tracer breakthrough curves, are presented below in .

As implemented in the Task 6 CN models, feature complexity had a much larger influence on tracer breakthrough times than the pipe width generation algorithm or the geological structure type. This was largely due to the massive increase in surface area available for sorption. The effect was especially notable when the complexity of the background fracture network is increased.
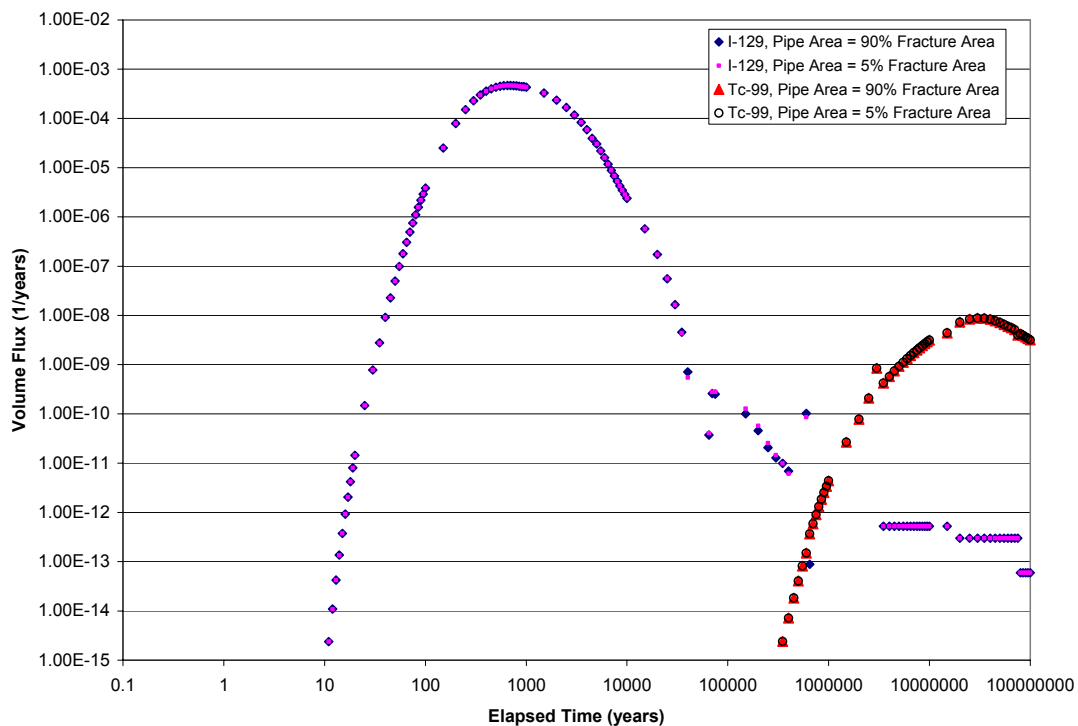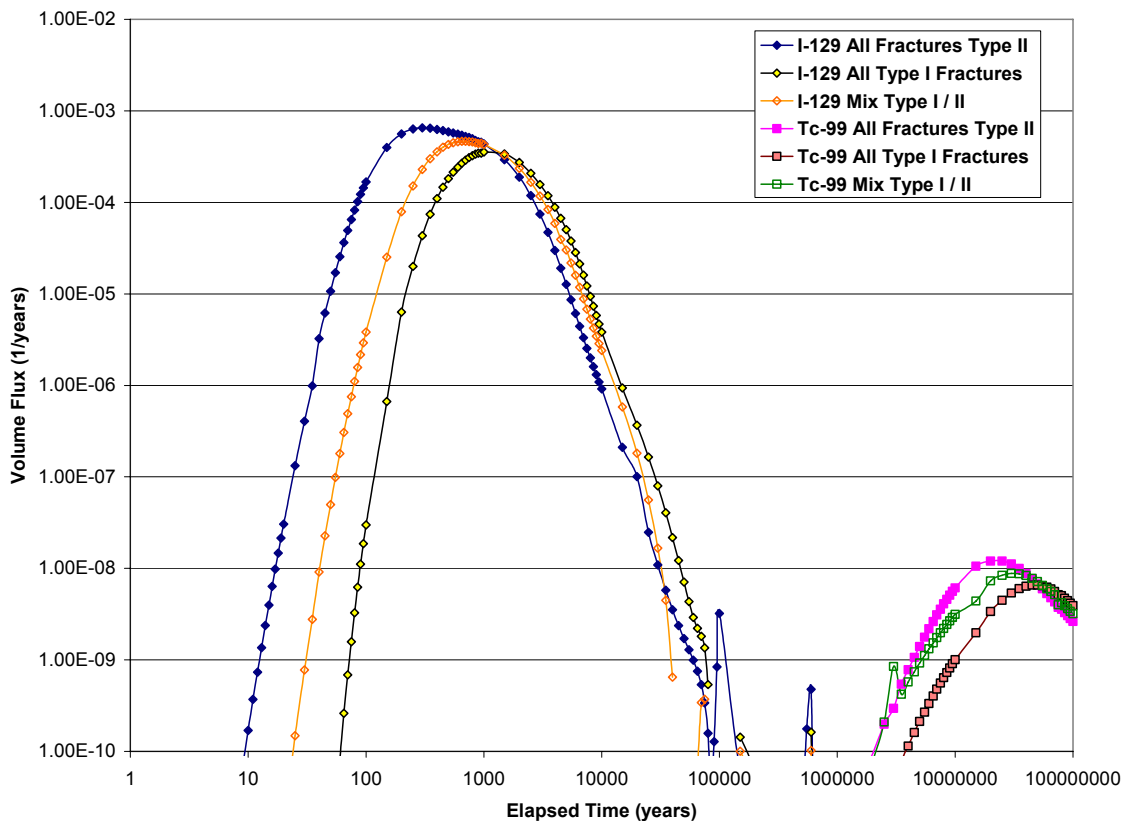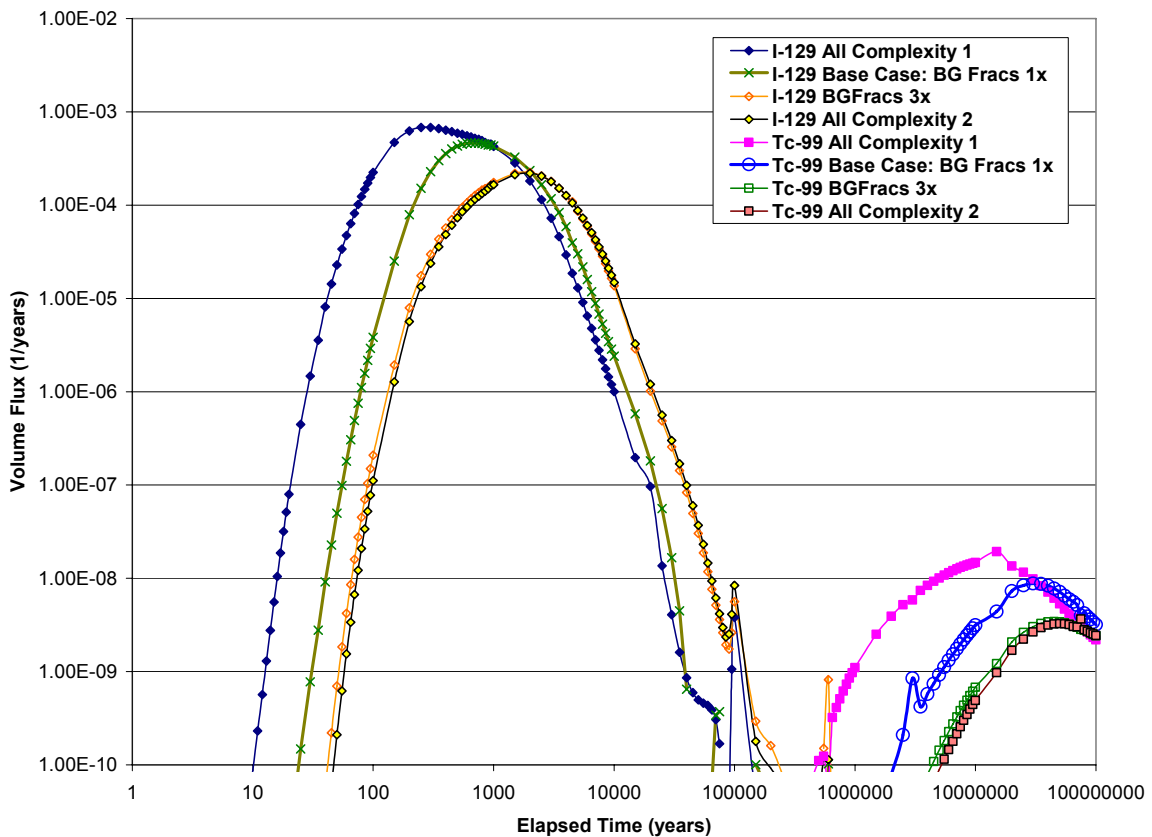

Figure 5-21. *JNC/Golder Task 6E CN model sensitivity to changes in fracture complexity. Tracer concentrations were measured at the west edge of the 200-meter TRUE Block volume.*

5.6 Task 6E Conclusions

5.6.1 Discussion of Results

The Task 6E DFN/CN simulations represent a forward modelling approach to simulating tracer transport on performance-assessment (PA) timescales of decades to millennia. As it is a forward model, true calibration is impossible given the timescales involved. However, the basic modelling methodology stems from the JNC/Golder Task 6D simulations, which demonstrated relatively good matches to shorter-timescale tracer test experiments.

One disappointing aspect was the poor performance of the channel network model when the sampling traceplane was located extremely close (~10 meters) to the tracer source section. We believe that this is due largely to the sampling mechanism (a geometric 'flow window') is partially to blame; as it is not a true sink, pathways and particles are free to migrate through and across it as many times as necessary before reaching an ultimate sink or dead end.

5.6.2 Conclusions

The JNC/Golder Task 6E simulations and corresponding sensitivity studies suggest the following:

1. In both experimental and performance-assessment timescales, feature complexity and structure type were important parameters with respect to solute retention. In particular, the large surface areas available for sorption through either multiple pathways or along gouged or brecciated surfaces appeared to be especially critical.

2. In general, variations in pipe geometry generation parameters appeared to have minimal effects on tracer retention. The only significant exception was fracture aperture, which directly influences pathway velocities (and therefore tracer travel times).

3. The effect of damaged zones (mylonite/cataclasite, fault gouge, brecciation) along transport pathways was significant. These zones have the potential to increase retardations by an order of magnitude in some cases.

4. On performance-assessment timescales, accurate microstructural modelling appears to be more critical in predicting the transport of non-reactive species. Significant retardation for moderately- to strongly-sorbing tracers was noted in all simulation cases.

6 Task 6F – Network Transport Benchmark

The goal of the JNC/Golder team for Task 6F was to facilitate inter-comparison between the transport models used by the different Task Force modelling groups. To do this, it was necessary to create an approximation of the Task 6C semi-synthetic hydrostructural model on a spatial and temporal scale that was accessible to other modelling teams not using DFN models. The ability to combine a simpler DFN network (transport along the plane of a single feature) with the PAWorks/LTG channel-network approach allowed the JNC/Golder team to simplify the number of variables that affected tracer breakthrough; this made model analysis and sensitivity analysis much easier.

6.1 Modelling strategy

The JNC/Golder team again utilized a forward modelling strategy in the completion of Task 6F. The target structures (1S, 4S) for the Task 6F modelling effort were two stochastic 500-m scale fractures created during the benchmark DFN modelling of Task 6C (Dershowitz et al., 2002). The JNC/Golder team utilized both the existing Task 6D/6E TRUE Block scale deterministic structure model and the Task 6C parameterized background fracture network to populate new model subdomains around the target Task 6F structures. As this was a forward model with a temporal dimension much larger than that of previous site characterization simulations, no formal calibration was attempted. A flowchart graphically describing the modelling process is presented below as Figure 6-1.
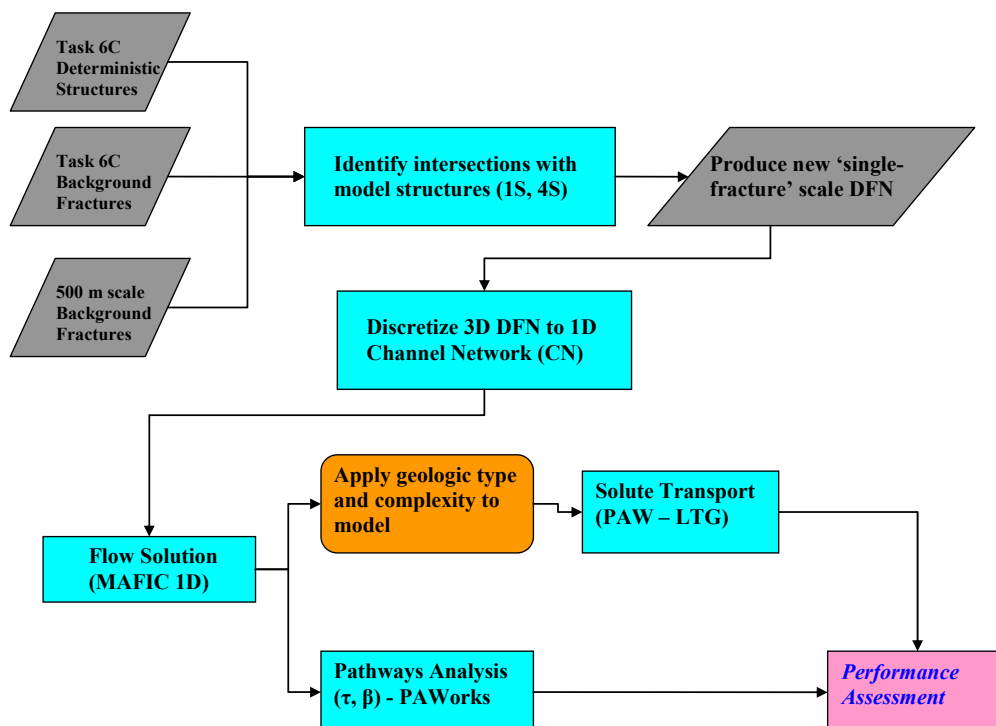
Figure 6-1. *Task 6F modelling workflow for JNC/Golder DFN-CN conceptual model. This general model is also applicable to Tasks 6D and 6E.*

6.2   Model Implementation

6.2.1   Implementing the Task 6F DFN-CN Model

The Task 6F modelling specification calls for a simplifed fracture network, consisting of either a single Type I structure (synthetic feature 1S from the Task 6C report) or a single Type II structure (synthetic feature 4S from the Task 6C report). These features are documented in Figure 6-2.
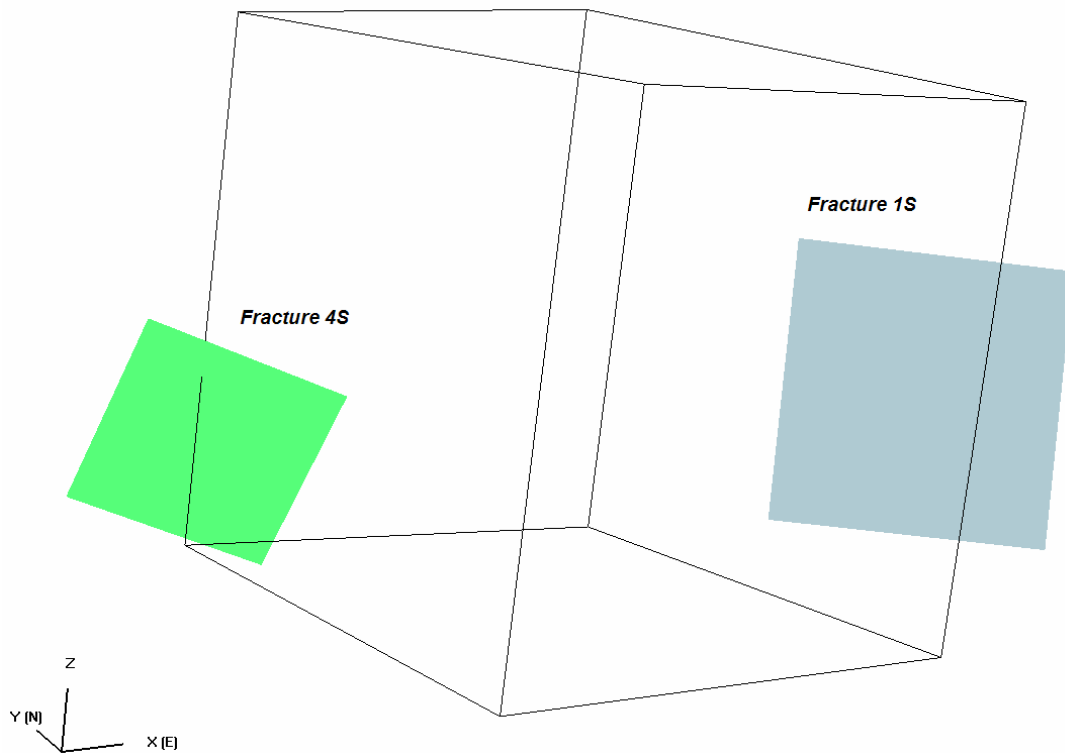
Figure 6-2. *Task 6F target structures. Structure 1S is the larger yellow fracture on the right. The 200m scale TRUE Block volume (black wireframe) is included for spatial reference and for scale.*

The goal of the task was to limit tracer transport to within a single fracture; however, this is incompatible with the conceptual model behind the JNC/Golder CN approach. Even for a single-plane problem, a network of background fractures is required to obtain sufficient connectivity; pipes are created in the plane of the target structure by intersections with other features (Dershowitz et al., 2000).

As such, the JNC/Golder team adapted the Task 6F model specifications slightly to meet our requirements. Specifically, the JNC/Golder team utilized both the 200m scale background fracture network and the deterministic structure network for the TRUE Block Volume, as presented in the Task 6C report (Dershowitz et al., 2002), to design a local-scale DFN around each targeted structure. The DFN modelling workflow consisted of:

1. Computed the intersections of the existing TRUE Block deterministic structures, the semi-stochastic fracture network, and the 2000m large-scale semi-stochastic fracture network with Structures 1S and 4S. The fractures used to compute the intersections in the model region are presented as Figure 6-3 through Figure 6-5. Fracture properties assigned to Structures 1S and 4S were supplied in Elert and Selroos (2004c), and are summarized in Table 6-2.

2. A new fracture generation region around each of the target structures was assigned for the generation of a 'local' background fracture network. These bounding boxes were generally 40 m thick, and were slightly larger than the target fractures so as to minimize edge effects.

3. The existing existing Task 6C-derived DFN fractures (Step 1) were clipped to the model bounding boxes defined in Step 2.

4. New sets of '500-m scale' background fractures were generated within the local model bounding boxes (Figure 6-6). These sets were generated using the two background fracture sets identified in the Task 6C report; the set properties are summarized in Table 6-1.
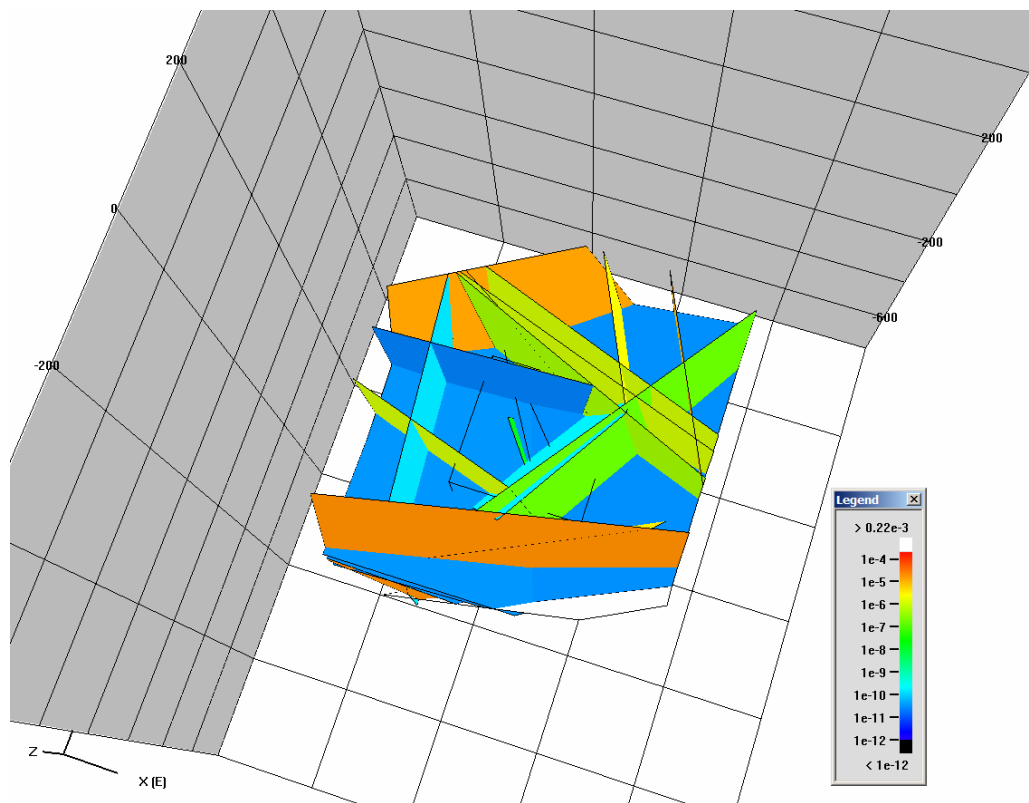
Figure 6-3. *Task 6C deterministic structures used to provide intersections in the Task 6F DFN-CN model. Fractures are colored by log10 of their transmissivity.*
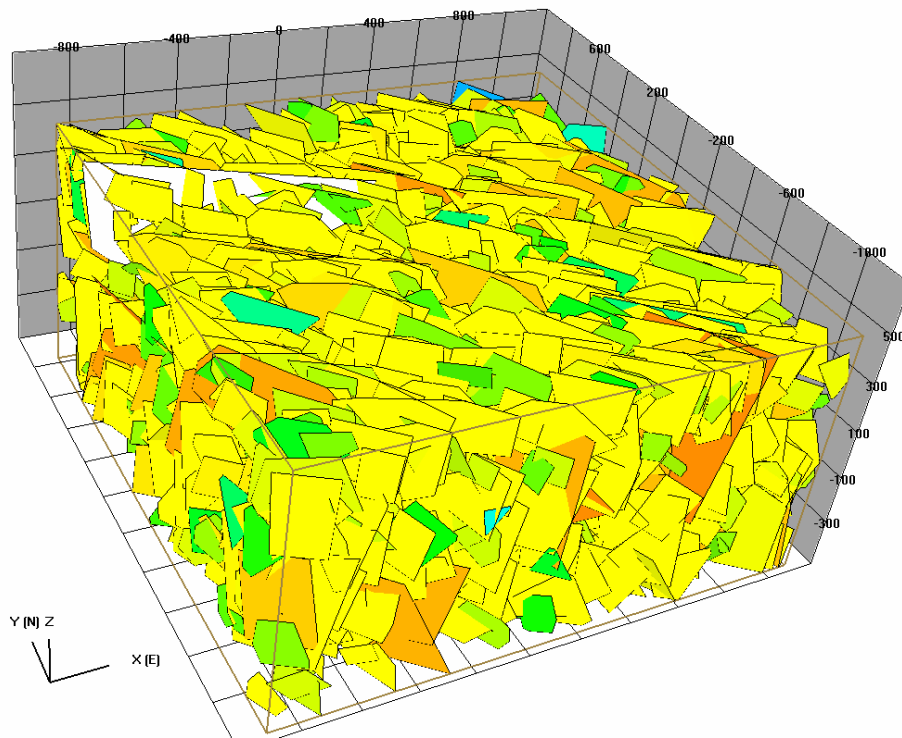
Figure 6-4. *Task 6C 2000m-scale 'lognormal' semi-stochastic fractures used to provide intersections in the Task 6F DFN-CN model. Fractures are colored by log10 of their transmissivity.*
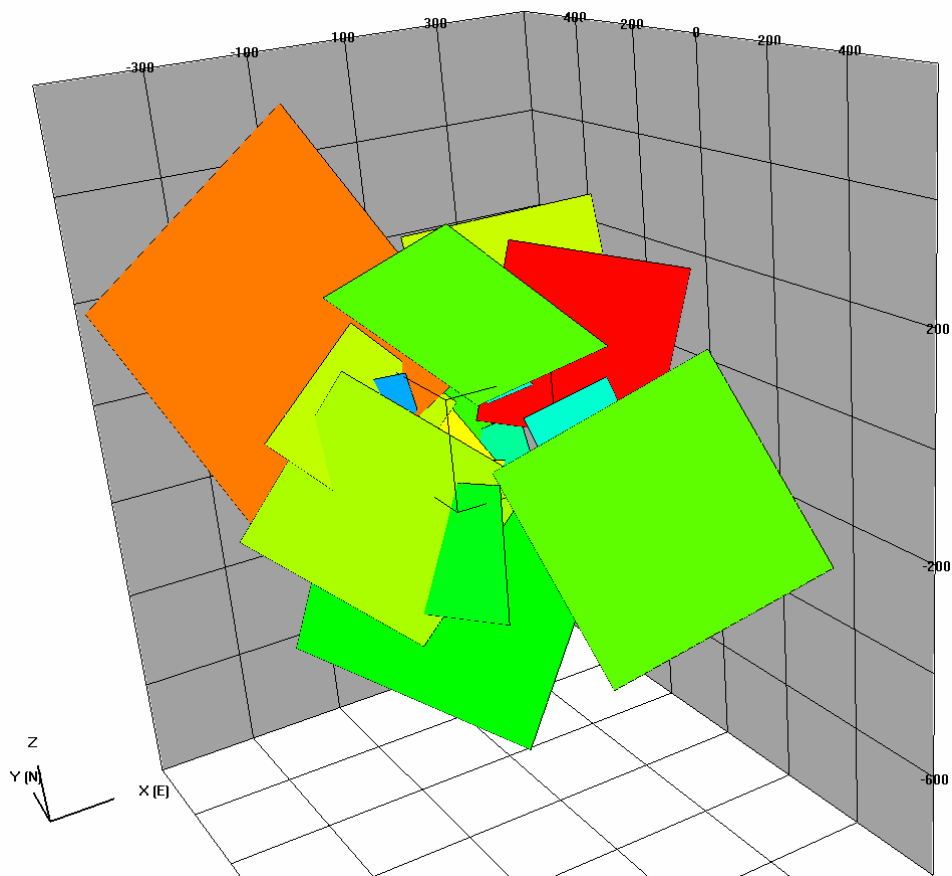
Figure 6-5. *Task 6C 200 m-scale semi-stochastic fractures used to provide intersections in the Task 6F DFN-CN model.*

Table 6-1. Parameters for background fracture networks surrounding each Task 6F target structure (from Task 6F report).

Property	Background Fracture Set #1	Background Fracture Set #2
Orientation Distribution	Univariate Fisher, Mean Pole of (211, 0.6), with a Fisher dispersion K = 9.4	Univariate Fisher, Mean Pole of (250, 54), with a Fisher dispersion K = 3.8
Intensity (P_{32})	0.16 m^2/m^3	0.13 m^2/m^3
Size Model	Log-normally distributed, Mean equivalent radius of 2 m, standard deviation of 1m, truncated at 2 m (lower) and 50 m (upper)	
Geologic Stucture Type	20% Type I features (fault-like), 80% Type II features (joint-like)	
Structural Complexity	Assigned via length-type relationship (Section 4.4.1, Task 6C report) $P[\text{Type 1}] = 1\text{-}e^{-0.7\ S/So}$	
Hydraulic Parameters	*Storativity* (1 x 10-6 ; not used in steady-state flow models) *Transmissivity*: $T(L,r) = 5 \times 10^{-10} \times L^{(1.386\ +0.3r)}$; Eq. 4-3, Task 6C Report *Hydraulic Aperture*: $e_h = a_h\ T^{bh}$ (a_h = 0.46, b_h = 0.5; Eq. 4-5, Task 6C Report) *Transport Aperture*: e_t = *Hydraulic Aperture* e_h	
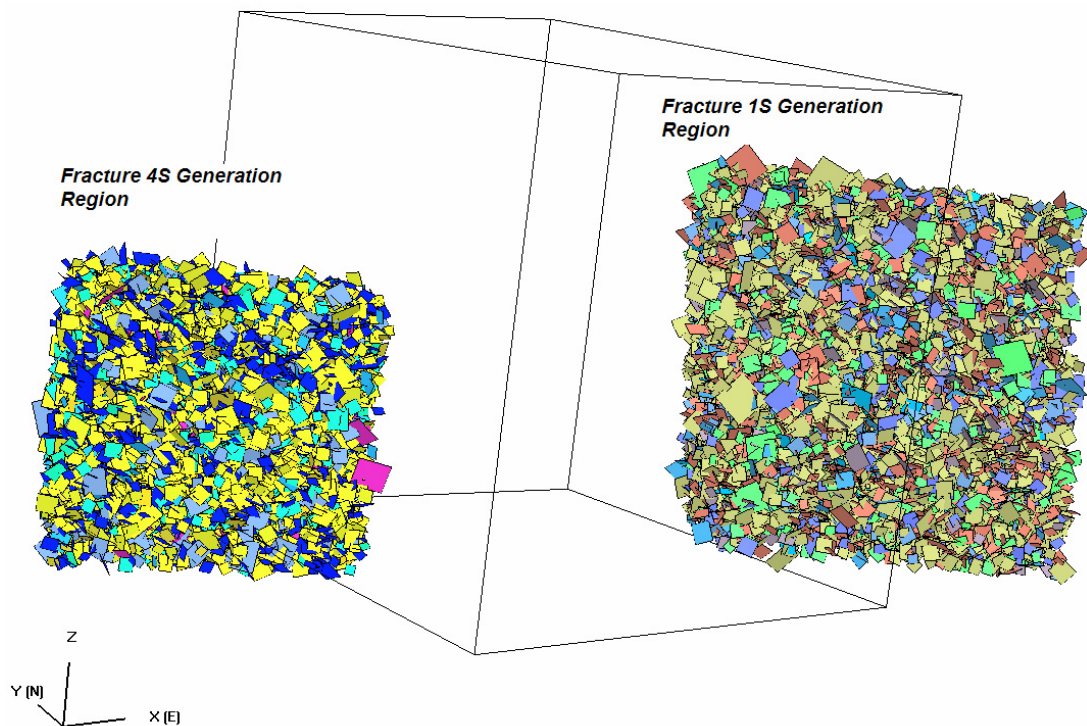
Figure 6-6. *Task 6F background fracture networks surrounding target structures 1S and 4S.*

The resulting new DFNs are a composite model; they utilize the deterministic and large-scale (2000-m scale stochastic log-normal and 500-m semi-stochastic) fractures directly from the Task 6C, while implementing a local version of the Task 6C background fracture model. The resulting local networks are illustrated in Figure 6-7 and Figure 6-8.
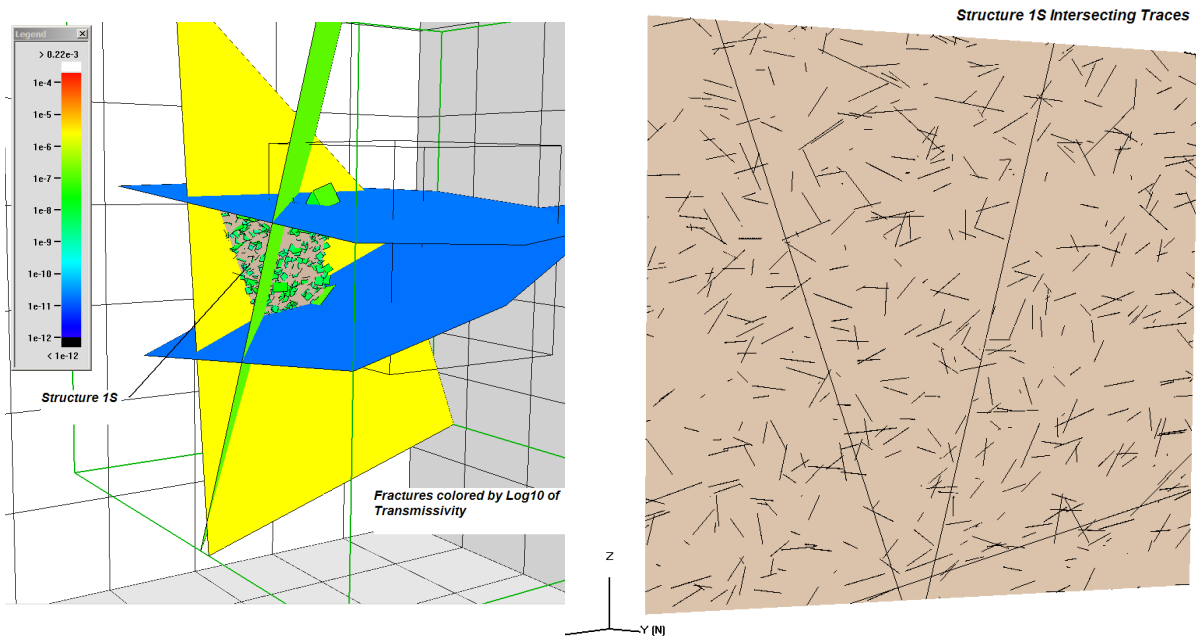
Figure 6-7. *Task 6F Structure 1S DFN model. The figure on the right shows the fracture trace intersections with Structure 1S. Note the two long traces that cut across the entire fractures; these represent the intersection of major TRUE Block Scale deterministic structures.*
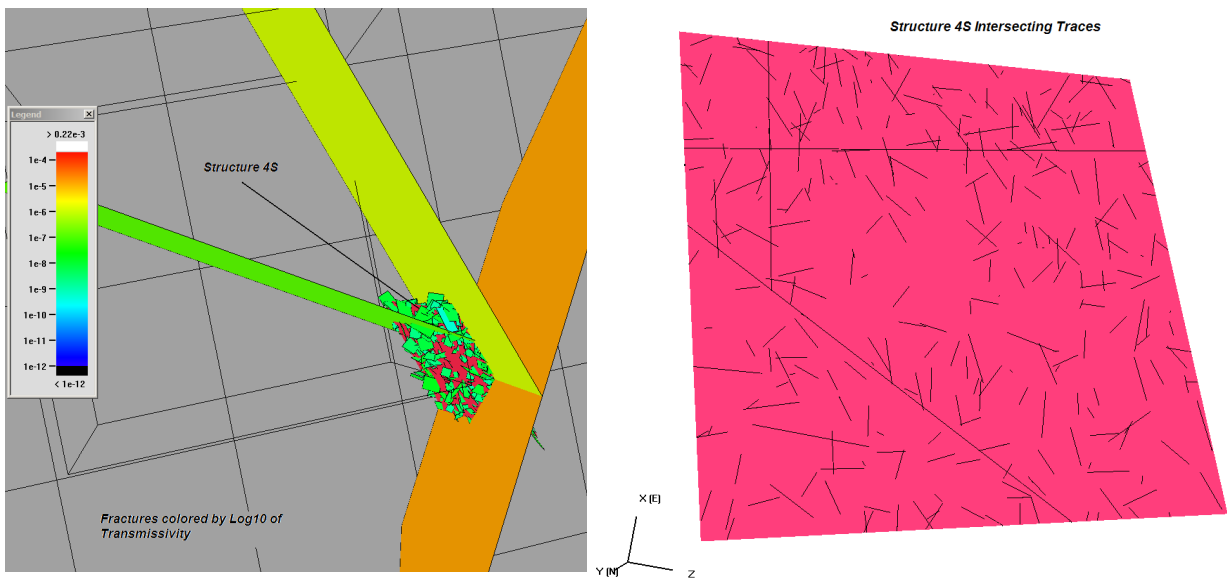
Figure 6-8. *Task 6F Structure 4S DFN model. The figure on the right shows the fracture trace intersections with Structure 4S. Note the two long traces that cut across the entire fractures; these represent the intersection of major TRUE Block Scale deterministic structures.*

Table 6-2. Task 6F property assignments for deterministic structures 1S and 4S (from Elert and Selroos, 2004c).

Structure Name	Width & Length	Structure Type	Complexity Factor	Transmissivity (m2/s)	Hydraulic Aperture (m)
1S	112.44	1	2*	3.14×10^{-7}	2.58×10^{-4}
4S	80.55	2	2*	1.90×10^{-7}	2.01×10^{-4}

* Note: Structural complexity was NOT simulated in Task 6F

6.2.2   Task 6F Flow Model

The JNC/Golder Task 6F simulations utilized the FracMan/PAWorks and MAFIC approaches, as described in Chapter 3.1. The end result was a 1D channel network discretized from the modified DFN described in Section 6.2.1.

The Task 6F hydraulic boundary conditions were constrained by Elert and Selroos (2004c) in the modelling task specification. Model hydraulic boundary conditions consisted of one-dimensional flow across the plane of the target structures (1S, 4S), with no-flow boundaries on all other interfaces. The model geometry is illustrated in Figure 6-9. A series of specified constant-head boundary conditions were provided; these boundary conditions were set so as to produce estimated groundwater advective travel times of 0.1, 1, and 10 years respectively. The specified heads are presented below as Table 6-3.

Table 6-3. Task 6F model boundary condition cases (from Elert and Selroos, 2004c).

Model Case	Advective Travel Time (years)	Head difference (m)	
		1S	4S
A	0.1	0.584	0.539
B	1	0.0584	0.0539
C	10	0.00584	0.00539
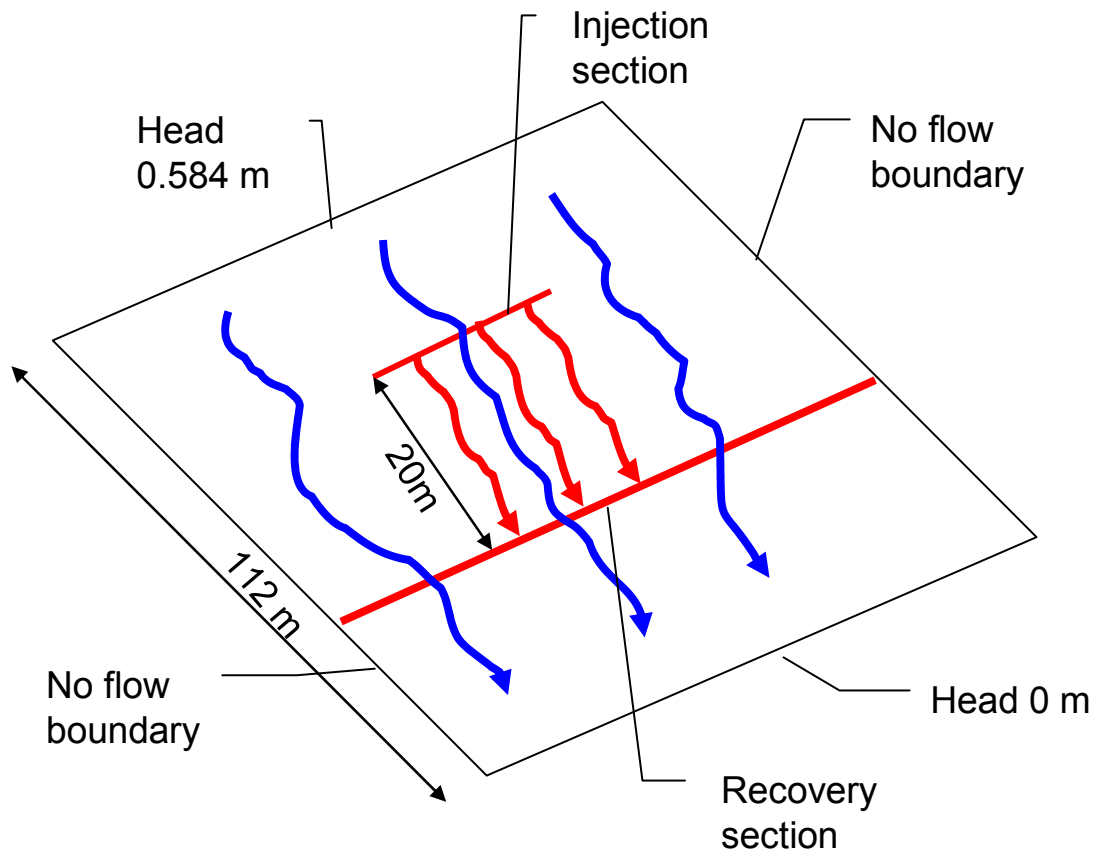
Figure 6-9. *Task 6F specified model geometry and example boundary condition for Structure 1S, Case A (Elert and Selroos, 2004c).*

The constant head boundary edges of the model (Figure 6-9) were implemented as a series of vertical interconnected boreholes. This was neccesary to allow for sufficient connectivity within the model, and to allow for a wider variety of potential transport pathways to be identified within the channel network.

Figure 6-10 and Figure 6-11 illustrate the 1D channel network models developed for Structures 1S and 4S from the above-described 3D discrete-fracture networks. The CN was created using PAWorks crossing pipes' alogirthm with pipe width assigned based on the projected trace lengths of the intersecting fractures. Pipe width assignment was weighted towards the smaller of the two projected trace lengths.
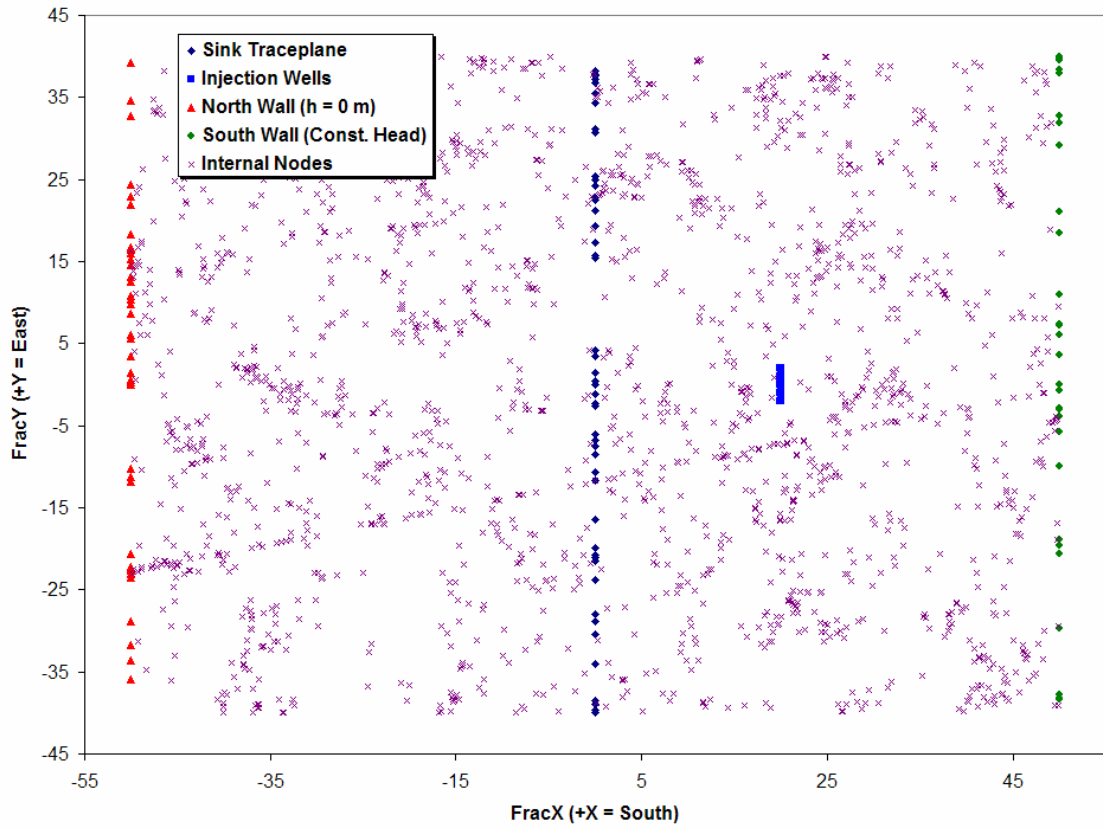
Figure 6-10. *View of Task 6F CN model of Structure 1S. This view is looking down the +Z axis at the plane of the fracture. 'X's mark the locations of model nodes.*
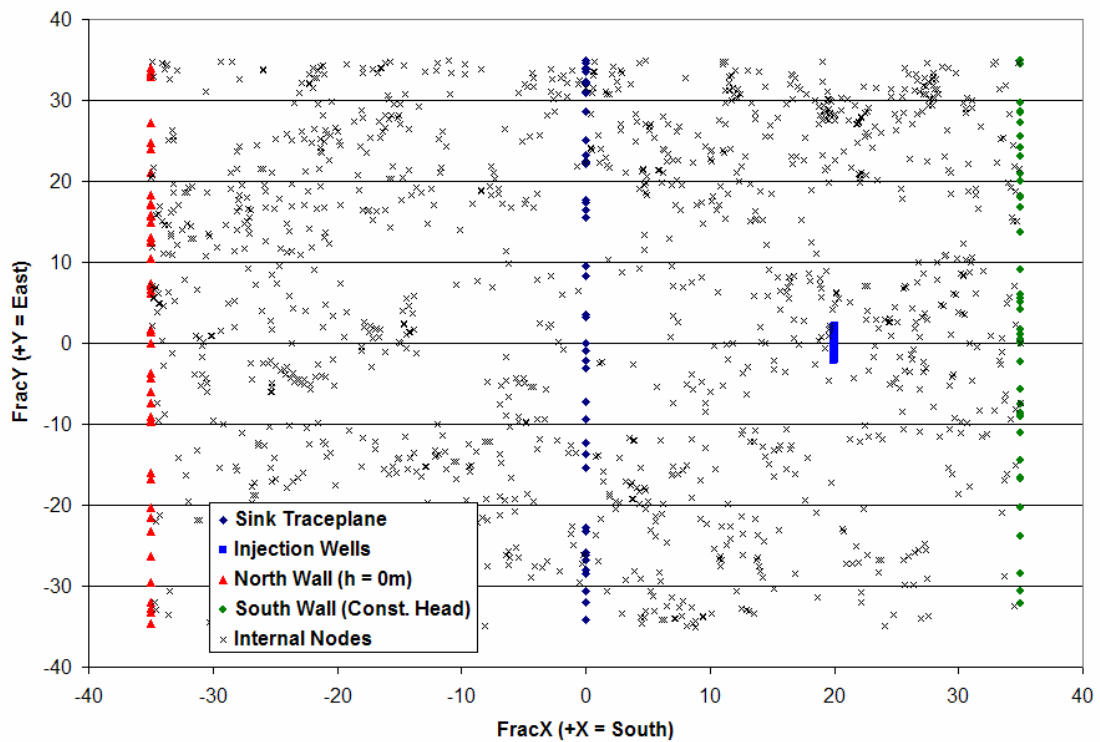
Figure 6-11. *View of Task 6F CN model of Structure 4S. This view is looking down the +Z axis at the plane of the fracture. 'X's mark the locations of model nodes.*

6.2.3 Task 6F Transport Model

Solute transport was simulated using the Laplace Transform Galerkin method, as implemented in the PAWorks / LTG software package (Dershowitz et. al., 2000) and described in Chapter 3.2. Radionuclide transport occurred within a three-dimensional channel network composed of one-dimensional pipe elements, with multiple immobile zones working in parallel to simulate rock and structural interactions.

6.2.3.1 Boundary Conditions

The Task 6F conceptual model assumes that tracer is released from a fracture intersection with the target structure (1S or 4S) with an approximate trace length of three meters. The choice of source definition (line source or a series of point sources) was left to the individual modelling teams.

The JNC/Golder team elected to simulate tracer release from five (5) individual point sources; we utilized five small borehole sections, spaced evenly along a five-meter long strip near the center of the target fracture. The boreholes were assigned a group flux boundary condition of zero, effectively making them transparent in the hyraulic model. Tracer was released from these boreholes as a Dirac pulse using an activity flux boundary condition; 1×10^8 Becquerels of tracer was released into the CN model over a one-minute period. A very small (10^{-10} m^3/s) constant flux boundary condition was used at the source boreholes to ensure tracer dilution.

The Task 6F specification requested that all performance metrics be based on arrival times at an additional intersecting fracture located approximately 20 meters in the plane of the fracture from the tracer source. The JNC/Golder team implemented this as model-cutting traceplane window; all performance metrics utilize concentrations and arrival times at this window. However, the zero-head boundary (composed of 10 overlapping boreholes) was used as the ultimate sink for all PAWorks and LTG modelling (a traceplane itself cannot be a designated sink). Figure 6-12 illustrates the model geometry and borehole locations used in the JNC/Golder Task 6F modelling efforts.

Figure 6-12. *Task 6F CN Tracer Boundary Conditions. Note that all fracture sets are translated and rotated so that the model is centered at (0, 0, 0) in local coordinates.*

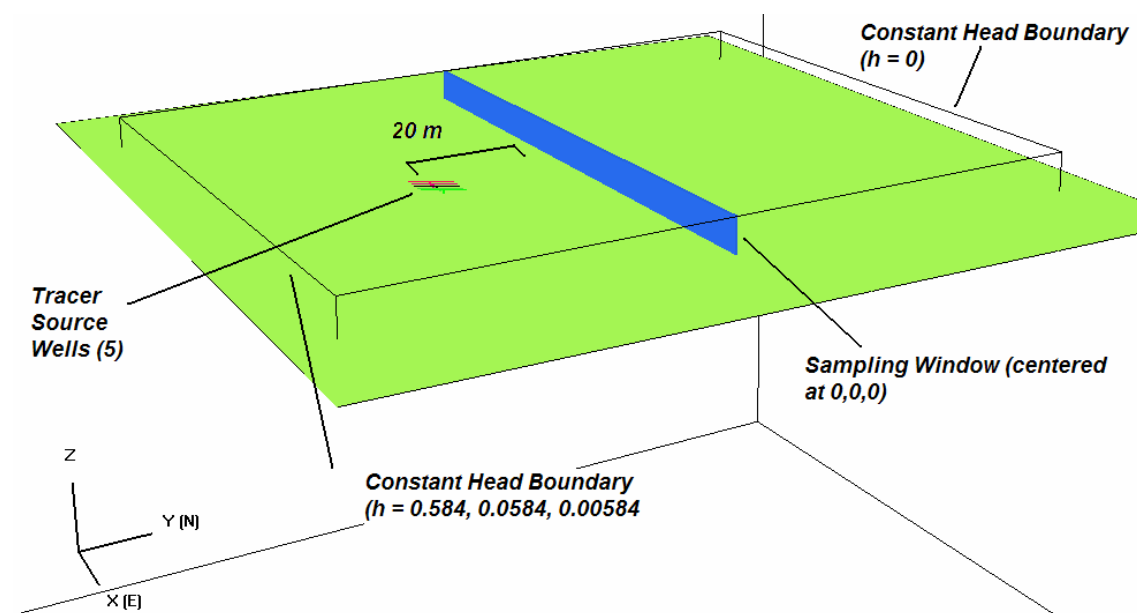The Task 6F modelling specification called for the simulation of the behavior of three tracers ($^{129}I^-$, $^{137}Cs^+$, and ^{241}Am); all three tracers were used in previous in-situ experiments or modelling cases and are specifically relevant at performance-assessment (PA) scales. All three tracers featured the same boundary conditions.

6.2.3.2 Mathematical Description and Numerical Implementation

The mathematical descriptions and numerical implementations of the PAWorks and LTG packages are described in Chapter 3.2.

6.2.3.3 Parameters

The JNC/Golder DFN-CN implementation of the Task 6F model specification was virtually identical to that of the models in Task 6D and 6E. The single major exception was that, as per the modelling specification, fracture complexity is NOT simulated. The transport model parameter breakdowns for Type I and Type II structures were the same as in Task 6D (Table 4-2 and Table 4-3, respectively). Bulk densities for all geologic materials were the same as in Task 6E (Table 5-1). Tracer-specific distribution coefficients (K_d) are presented below as Table 6-4, while free-water diffusivities are presented as Table 6-5. Effective diffusivity was calculated in an identical manner as in Task 6D (see Chapter 4.2.3.2).

Table 6-4. Distribution coefficients (K_d) for Task 6F tracers. Values are taken from the Task 6C hydrostructural model report, Chapter 2.2.7, Table 2-4 (Dershowitz et al, 2002).

Tracer	Fracture Coating (m^3/kg)	Fault Gouge (m^3/kg)	Cataclasite (m^3/kg)	Altered Wall Rock (m^3/kg)	Intact Wall Rock (m^3/kg)
$^{129}I^-$	0	0	0	0	0
$^{137}Cs^+$	5.2×10^{-2}	1.6×10^{-1}	1.5×10^{-2}	2.00×10^{-2}	1.0×10^{-2}
^{241}Am	0.5	0.5	0.5	0.5	0.5

Table 6-5. Free-water diffusivities for Task 6F tracers. Values are taken from the Task 6C hydrostructural model report, Chapter 2.2.6, Table 2-6 (Dershowitz et al, 2002).

Tracer	Free-Water (m^2/s)	Fracture Coating (m^2/s)	Fault Gouge (m^2/s)	Cataclasite (m2/s)	Altered Wall Rock (m^2/s)	Intact Wall Rock (m^2/s)
$^{129}I^-$	2.0×10^{-9}	1.2×10^{-11}	1.1×10^{-10}	9.8×10^{-13}	4.4×10^{-13}	1.5×10^{-13}
$^{137}Cs^+$	2.07×10^{-9}	1.3×10^{-11}	1.2×10^{-10}	1.0×10^{-12}	4.5×10^{-13}	1.5×10^{-13}
^{241}Am	5.95×10^{-10}	3.7×10^{-12}	3.3×10^{-11}	2.9×10^{-13}	1.3×10^{-13}	4.4×10^{-13}

6.2.3.4 Task 6F Immobile Zones

Seven immobile zones were necessary to completely accommodate the geologic conceptual model for the Task 6F simulations. These immobile zones consisted of:

- Four immobile zones describing the behaviour of the cataclasite, fault gouge, mineral coatings, and altered wall rock surrounding a Type I (fault) geologic structure. This immobile zone was only applied to Type I fractures (Sets 1, 3, 5, 7, 9, 11, 12, 13, 15, and 16)

- Two immobile zones describing the behaviour of the mineral coatings and the altered wall rock layer that surround a Type II (joint) structure. This immobile zone was only applied to Type II fractures (Sets 2, 4, 6, 8, 10, 14, 17, and 18).

- A single immobile zone applied to every fracture set that described the behaviour of the unaltered wall rock (Äspö Diorite).

6.3   Model Assumptions and Constraints

- Fracture complexity was NOT simulated, as per the Task 6F modelling specifications (Elert and Selroos, 2004c).

- TRUE Block Scale groundwater chemistry was assumed for all tracers.

- The decay of radioactive tracers was not simulated.

- All simulations were carried out to a maximum duration of 1×10^8 years.

- The LTG package models diffusion and sorption in immobile zones in parallel, rather than in series. PAWorks limits the user to two immobile zones; a non-flowing pore space and a matrix immobile zone. Additional immobile zones have to be added by hand to the output files. LTG supports up to five immobile zones per pipe (fracture) set.

- Water flow and radionuclide transport occurs within the fracture network. Transport within the rock matrix (outside of diffusion losses) was not modeled.

6.4   Model Calibration

As in other Task 6 simulations, all JNC/Golder Task 6F simulations were conducted as forward models. No calibration was carried out.

6.5   Task 6F Model Results

Model deliverables for Task 6F were similar to those requested for Task 6D and 6E. The suite of additional performance metrics of Elert and Selroos (2004a), which included a detailed description of the JNC/Golder model conceptualization of pore space, matrix parameter groups, water residence time distributions, and β-factor distributions, were computed for all model cases. These additional performance metrics were shipped as Microsoft Excel® spreadsheets to SKB through the GMS website; the water residence time and β-factor distributions are reproduced below. Breakthrough curve data was shipped as normalized time-series; the full breakthrough curves and statistics are presented below.

6.5.1   Flow

The results of the steady-state flow solution for Task 6F are presented below in Figure 6-13 through Figure 6-18. The steady-state heads and pipe parameters are used to calculate transport velocities for input into the LTG solver.
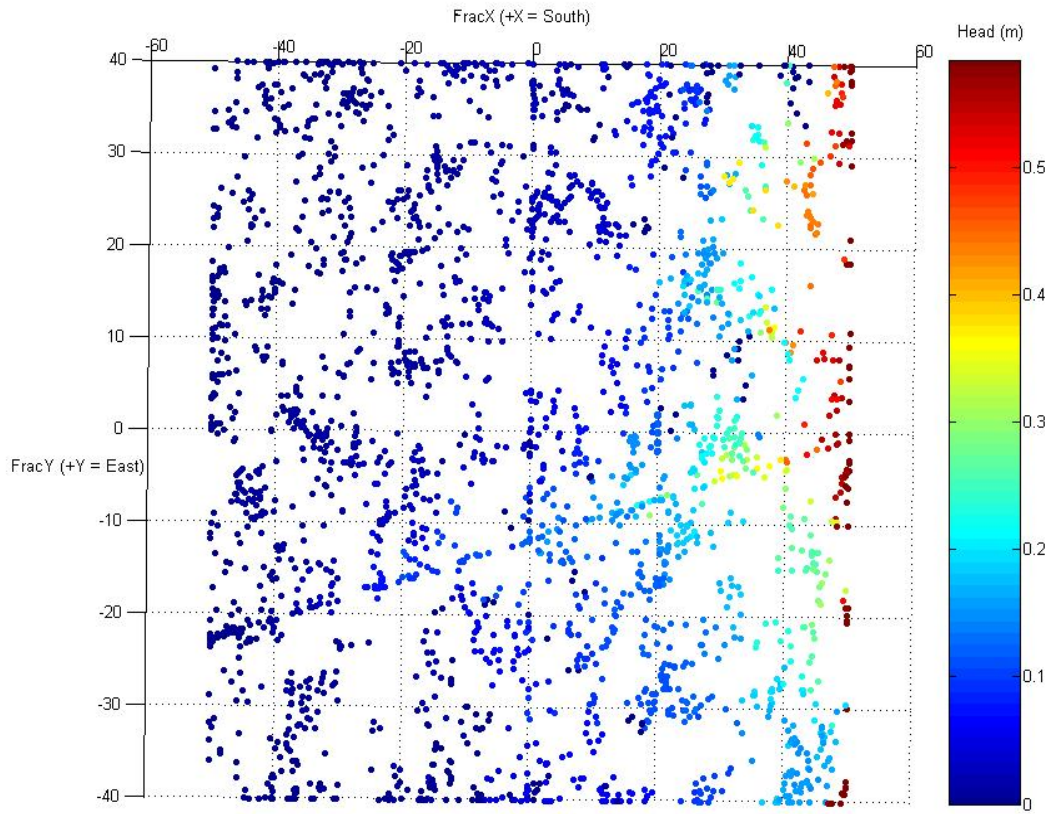
Figure 6-13. *Heads within Structure 1S, Model Case A1.*
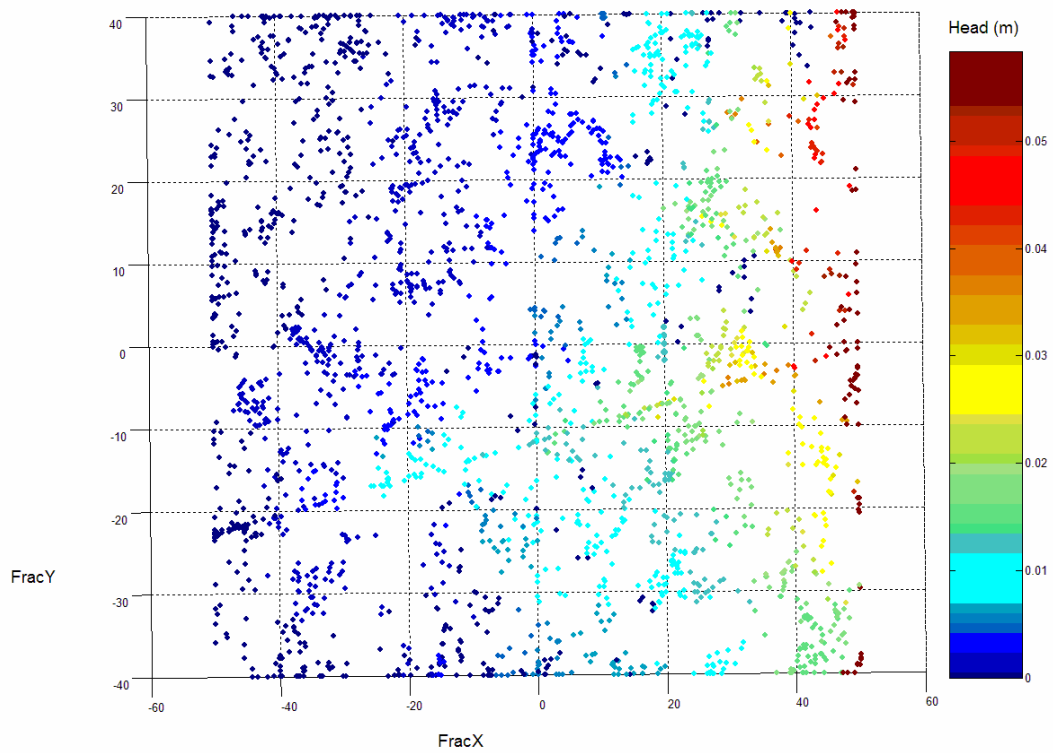
Figure 6-14. *Heads within Structure 1S, Model Case B1.*
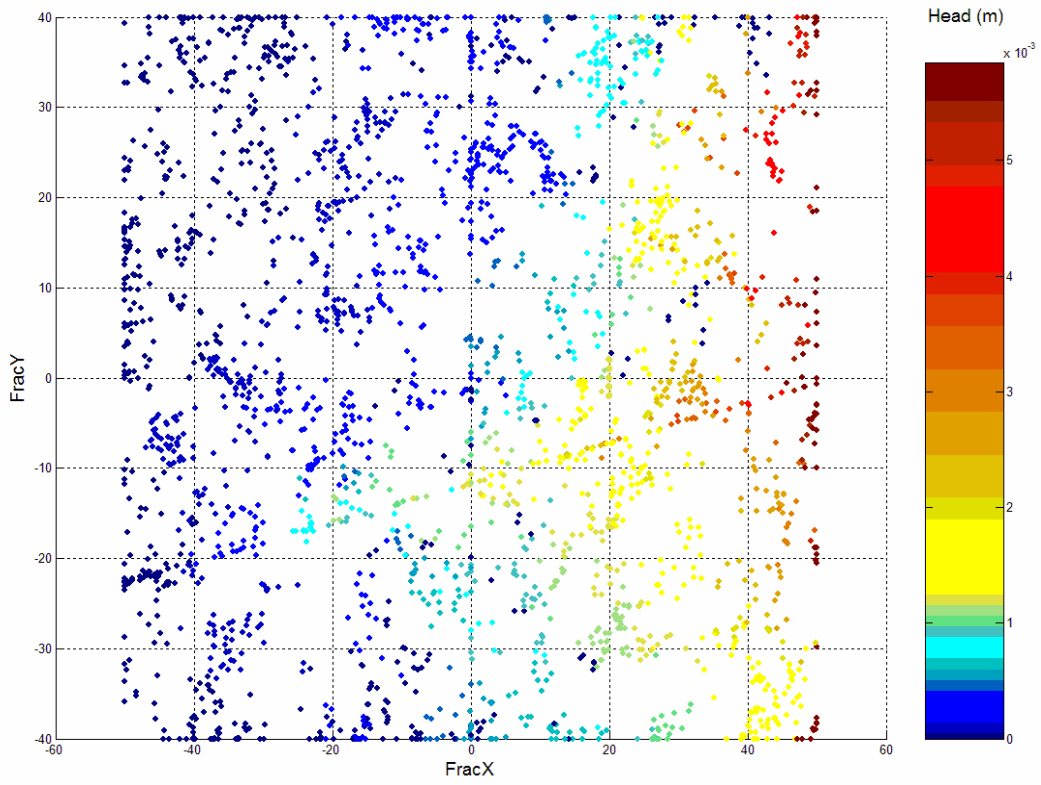
Figure 6-15. *Heads within Structure 1S, Model Case C1.*
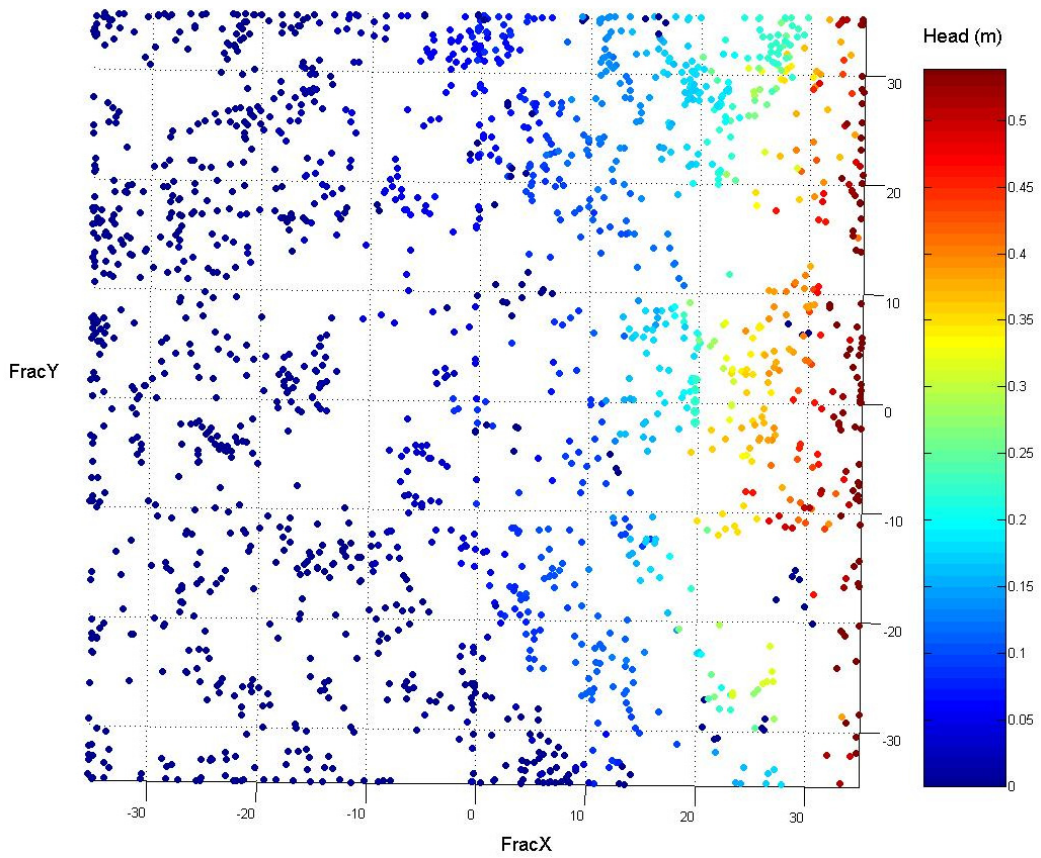
Figure 6-16. *Heads within Structure 4S, Model Case A2.*

94
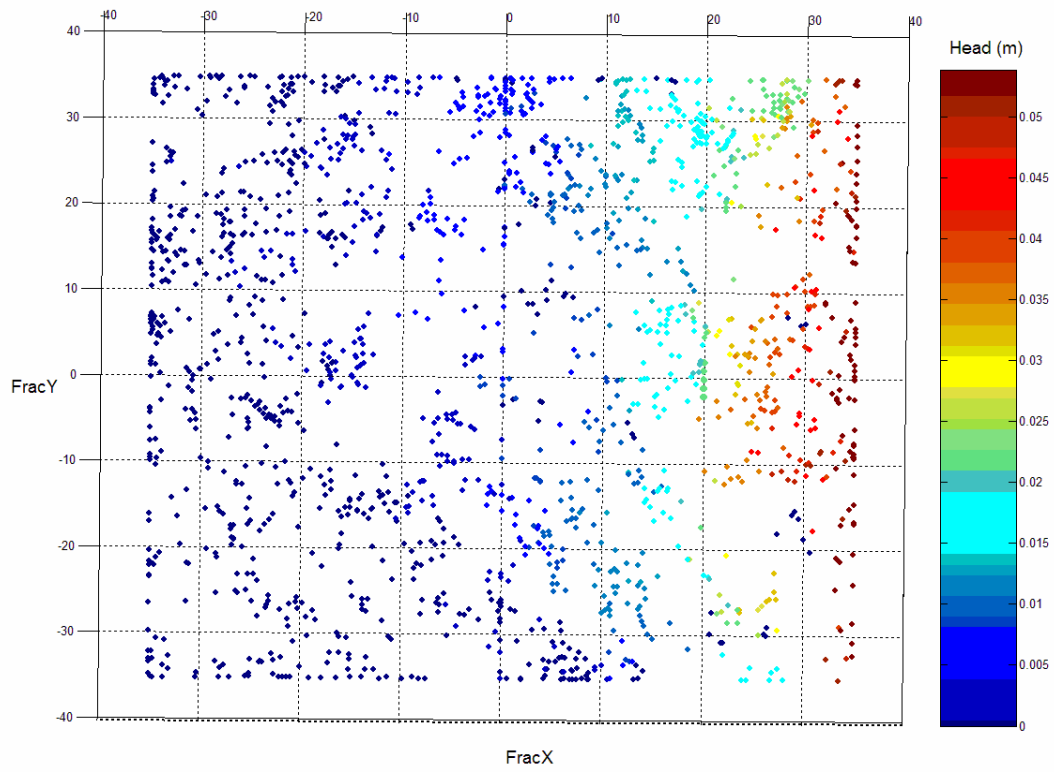
Figure 6-17. *Heads within Structure 4S, Model Case B2.*
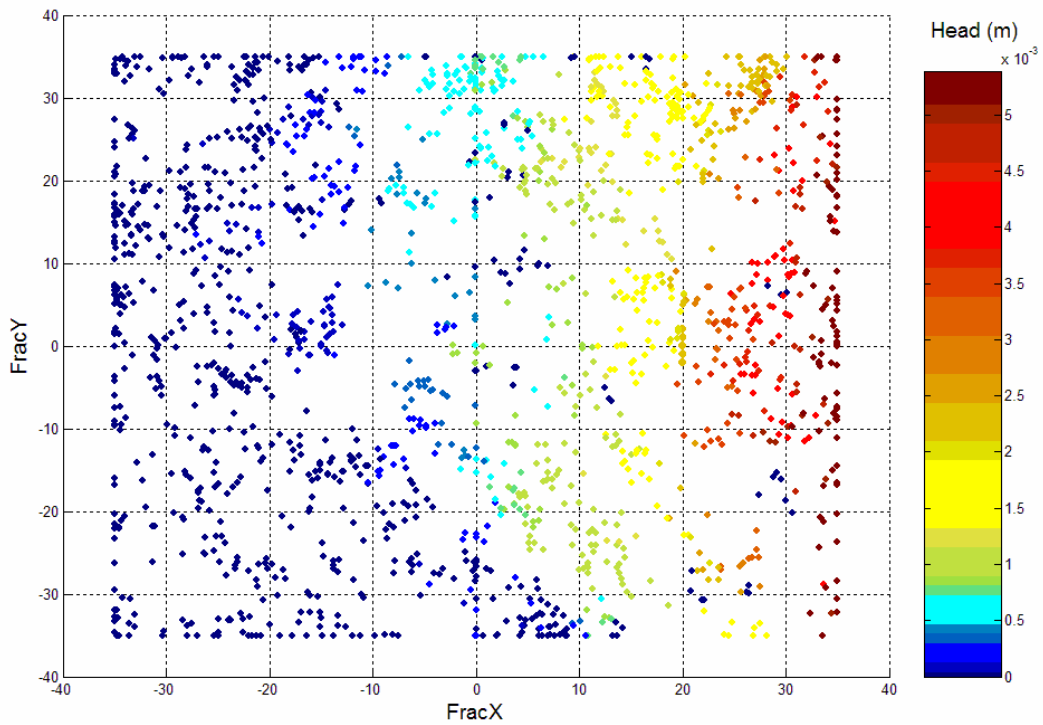
Figure 6-18. *Heads within Structure 4S, Model Case C2.*

6.5.1.1 Description of Flow Paths

Due to time constraints, flow path modelling was only performed explicitly for Model Cases A1 and A2. The assumption was that, given an unchanging channel network, changes in the magnitude of the applied gradient would not drastically affect the flow paths. Flow paths were evaluated both through advection-only particle tracking and through a PAWorks graph-theory pathway search. Illustrations of model flow paths are presented as Figure 6-19 through Figure 6-22.
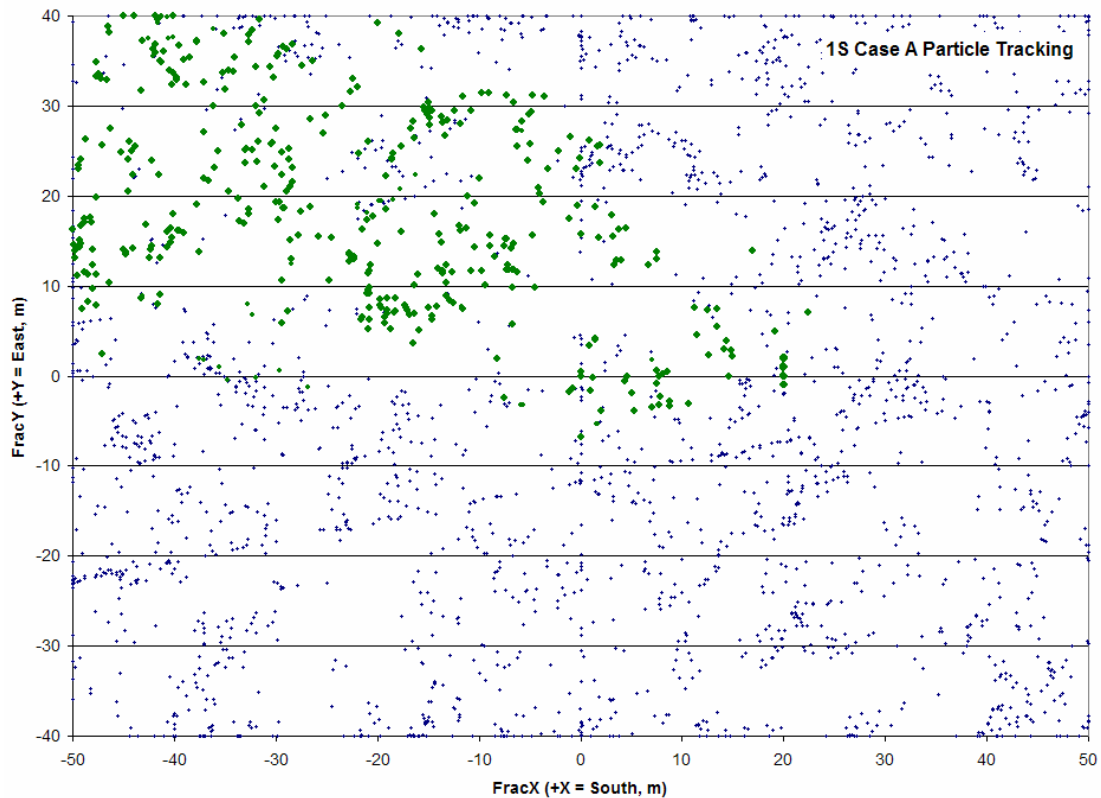
Figure 6-19. *Particle tracking results for Case A1 in Structure 1S.*
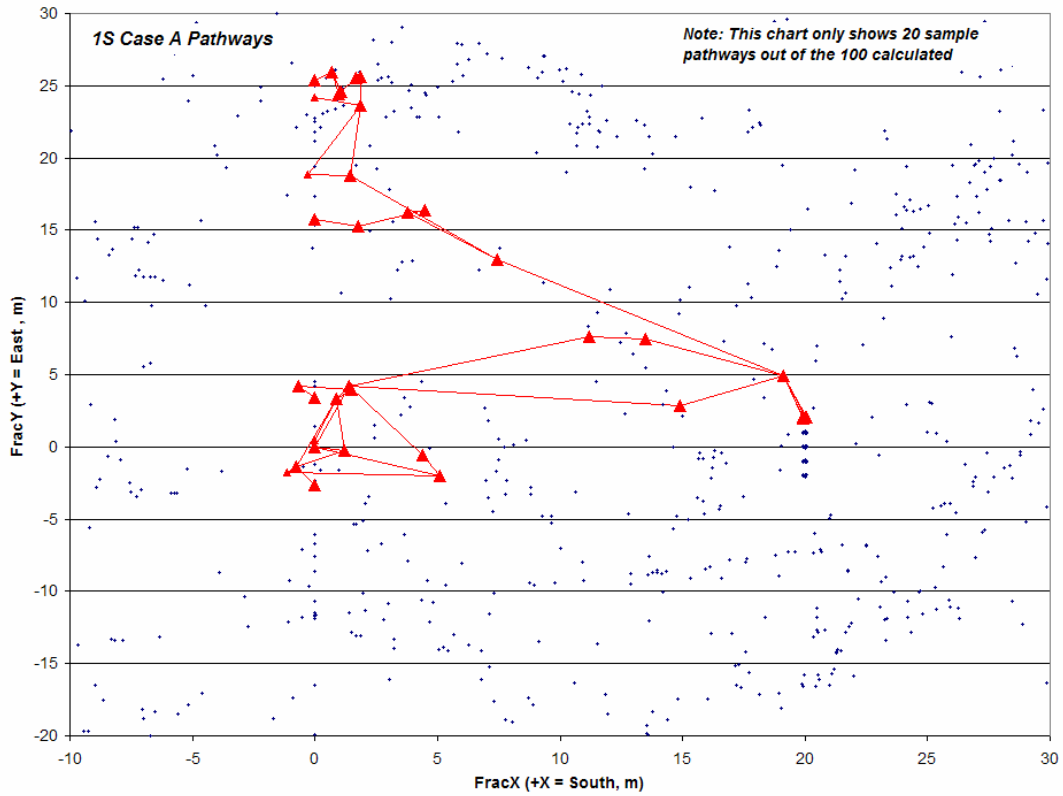
Figure 6-20. *Potential transport pathways through Structure 1S channel network (Case A1). Pathways were identified using a breadth-first graph-theory search within PAWorks, with a bias towards minimizing the advective travel time.*
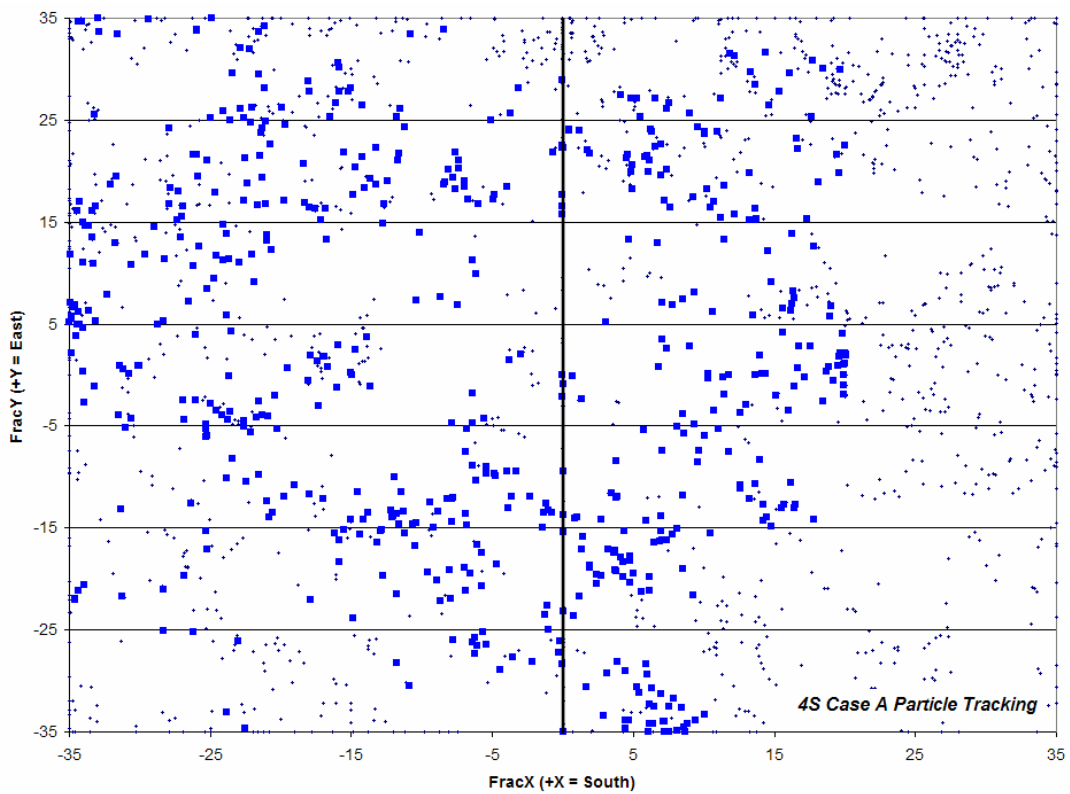
Figure 6-21. *Particle tracking results for Case A2 in Structure 4S.*

97
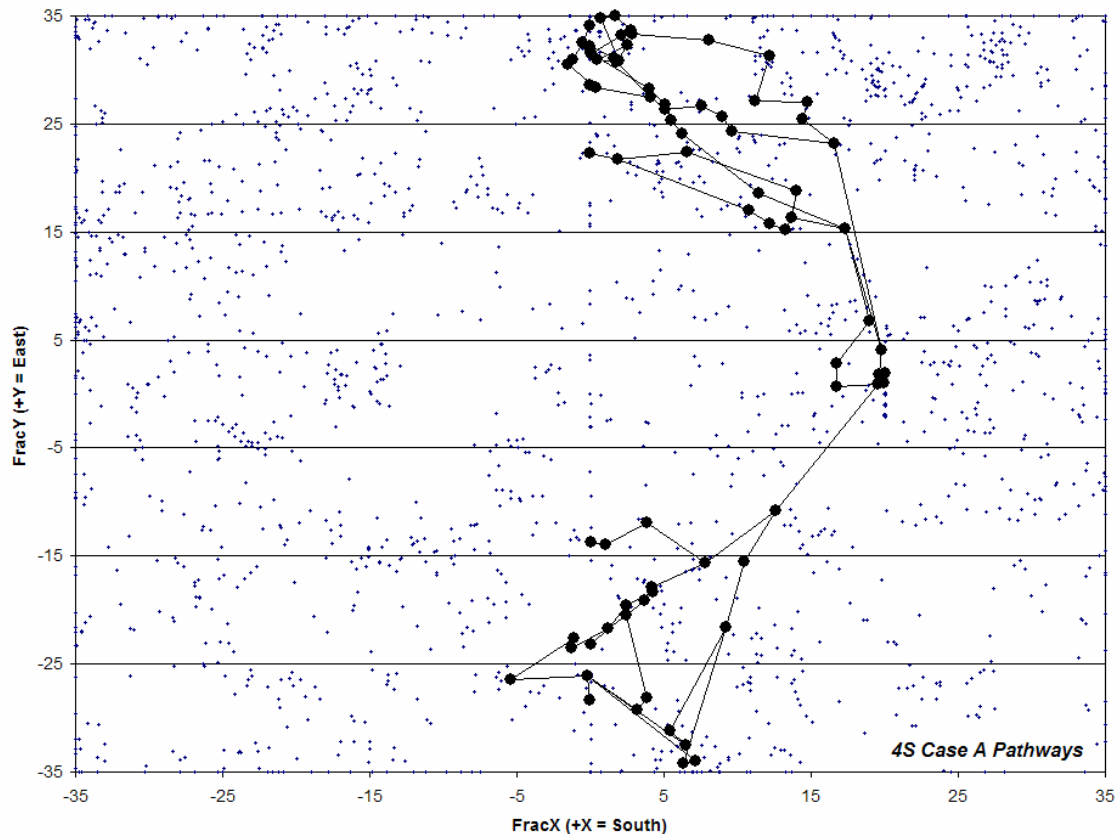
Figure 6-22. *Potential transport pathways through Structure 4S channel network (Case A2). Pathways were identified using a breadth-first graph-theory search within PAWorks, with a bias towards minimizing the advective travel time.*

Note the wide dispersion for particles released in Fracture 4S; we believe that this stems from the intersection of a Task 6C deterministic structure that cuts across the entire model, from one head boundary to another (Figure 6-19). This feature produced unusually large gradients near the center of the model, which resulted in the migration of particles down pathways with locally steep gradients into hydraulically 'dead' zone along the sides of the model. This effect would be minimal in a true 3D network, with the model boundaries further away (such as in the TRUE Block Scale experiments).

6.5.1.2 Water Residence Time Distributions

The water residence time distributions were estimated by calculating the breakthrough for a single conservative tracer assuming advection only (no surface or matrix interactions). A 'mass' of 1×10^8 Becquerels was released into the DFN-CN model over a period of one minute. Note, however, that for pure advective flow, one-minute time steps for a Dirac pulse injection produced some numerical instability in the final steps of the LTG transport solution.

The water residence time distributions for each model case are summarized below in Figure 6-23 and Figure 6-24; formal time-series data were submitted as a Microsoft Excel® spreadsheet.
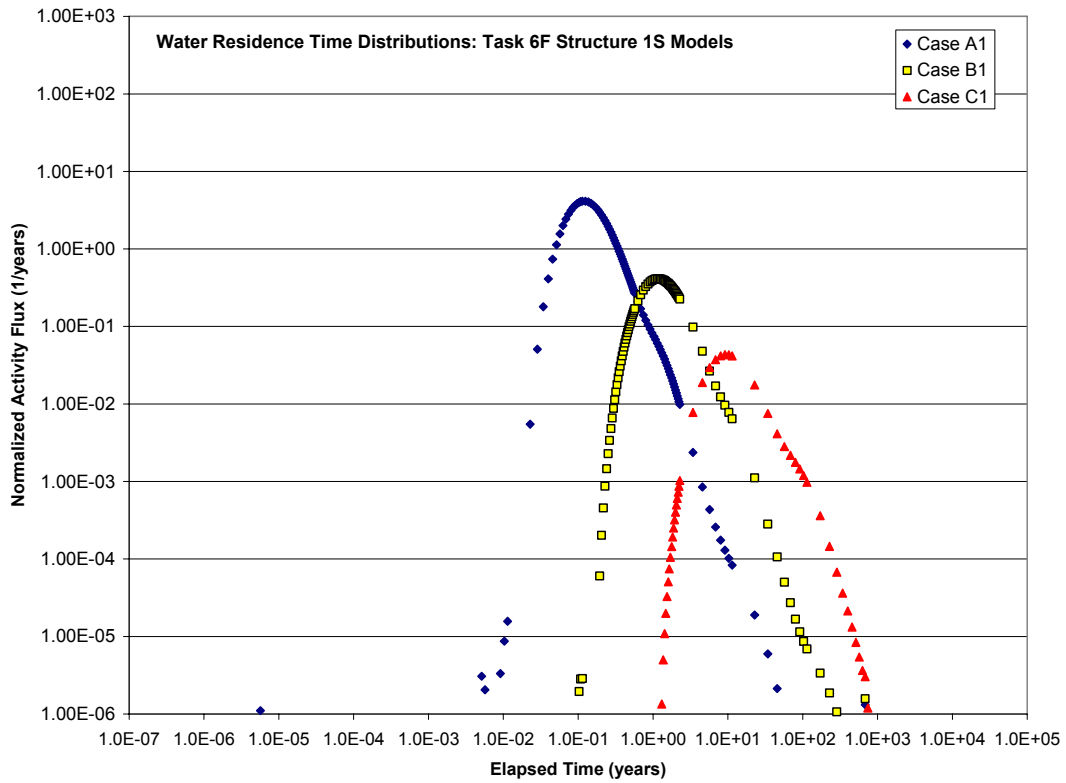
Figure 6-23. *Water residence time distribution for all Task 6F model cases utilizing Structure 1S.*
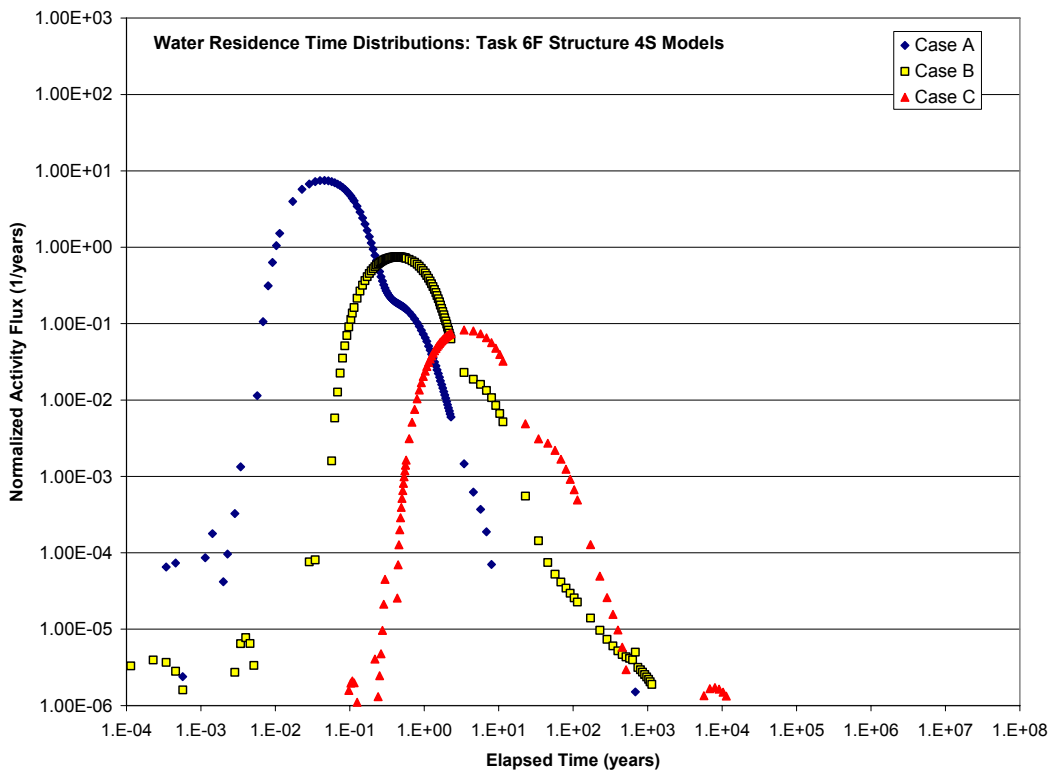
Figure 6-24. *Water residence time distribution for all Task 6F model cases utilizing Structure 4S.*

6.5.1.3 β-factor – ratio of flow wetted surface to water flow

Task 6F models calculated β-factor by using flow pathways defined through PAWorks breadth-first graph-theory searches (see Chapter 6.5.2). To compute the β-factor for each identified pathway, the flow-wetted surface length of the pathway was divided by the product of the pipe area and the pipe velocity. All calculations assumed a parallel-plate approximation for the network rather than a stream tube. PAWorks was instructed to cease the pathway search after the identification of 100 different potential pathways through the channel network.

The relationship between pathway β-factors and pathway travel times (τ) are presented below in Figure 6-25 and Figure 6-27. Note that each modelling case (A, B, C) appear similar; since the only difference between the model cases is the head gradient, the pathway geometries remain the same from case to case. Only the pathway velocities (and therefore travel times) change. Pathway statistics are presented in Table 6-6 and Table 6-7.

Table 6-6. τ-β statistics, Structure 1S pathways.

Statistic	Case A (Δh=0.584)		Case B (Δh=0.0584)		Case C (Δh=0.00584)	
	Travel Time (yrs)	Beta (yrs / m)	Travel Time (yrs)	Beta (yrs / m)	Travel Time (yrs)	Beta (yrs / m)
Mean	2.47	31.44	52.13	2.41E+05	391.29	4.99E+06
Std. Dev.	4.66	4.22	82.75	2.62E+05	829.29	6.65E+06
5%	0.23	25.62	2.29	8.87E+03	20.14	7.81E+04
50%	1.08	31.28	11.01	1.44E+05	192.76	2.08E+06
95%	7.56	39.05	148.54	7.46E+05	1024.98	2.19E+07

Regression calculations on subsets (Figure 6-26 and Figure 6-28) of the τ-β data suggest a power-law relationship; this was also observed during the Task 6D, 6E, and BS2B TRUE Block simulations.

Figure 6-25. *τ-β relationship for Task 6F model cases within Structure 1S.*

Figure 6-26. *Regression fits to τ-β data for Model Case A, Structure 1S.*
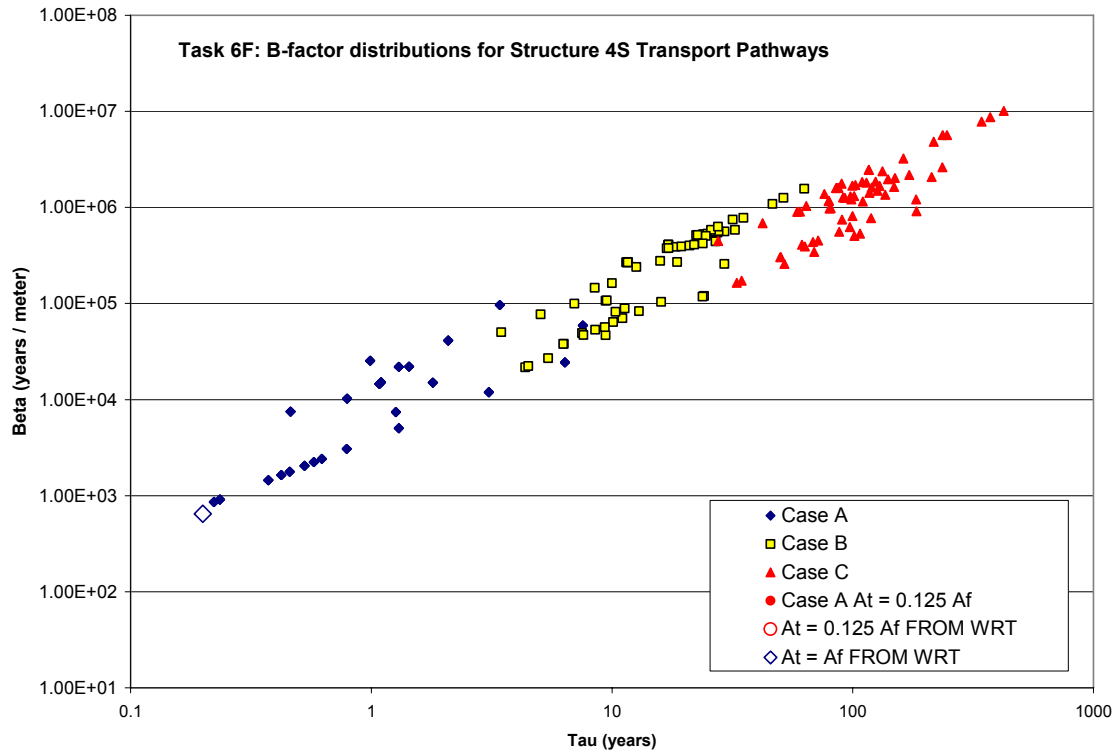
Figure 6-27. *τ-β relationship for Task 6F model cases within Structure 4S.*
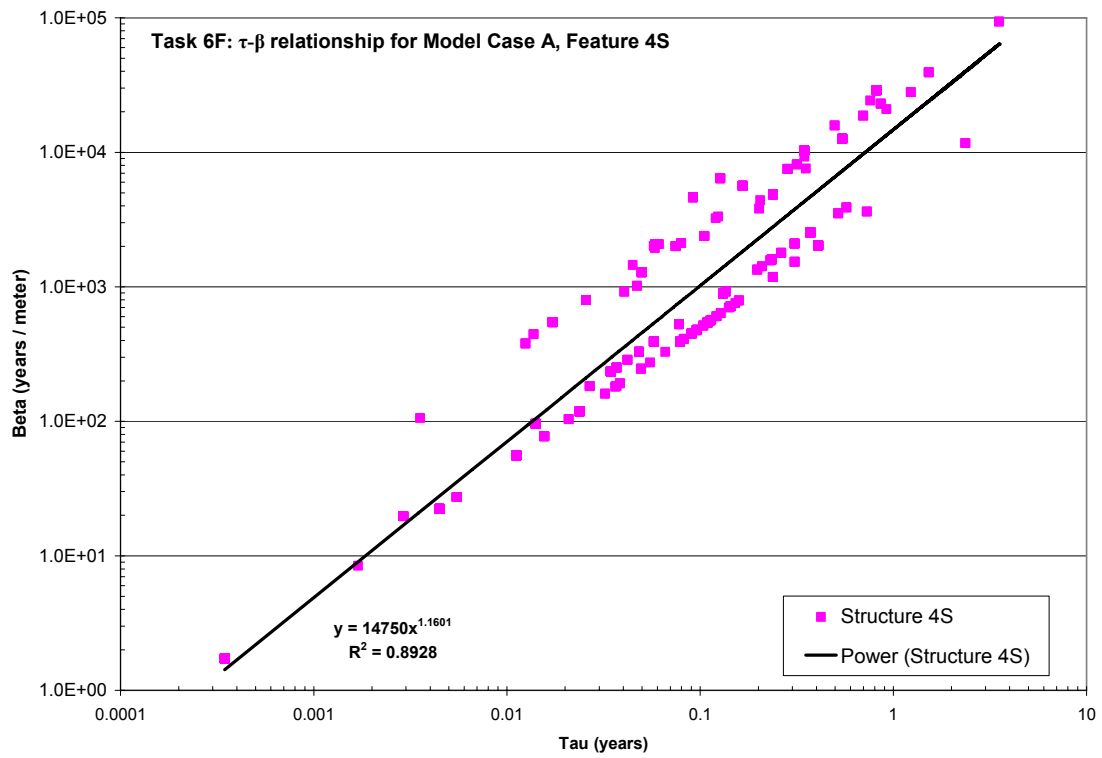
Figure 6-28. *Regression fits to τ-β data for Model Case A, Structure 4S.*

Table 6-7. τ-β statistics, Structure 4S pathways.

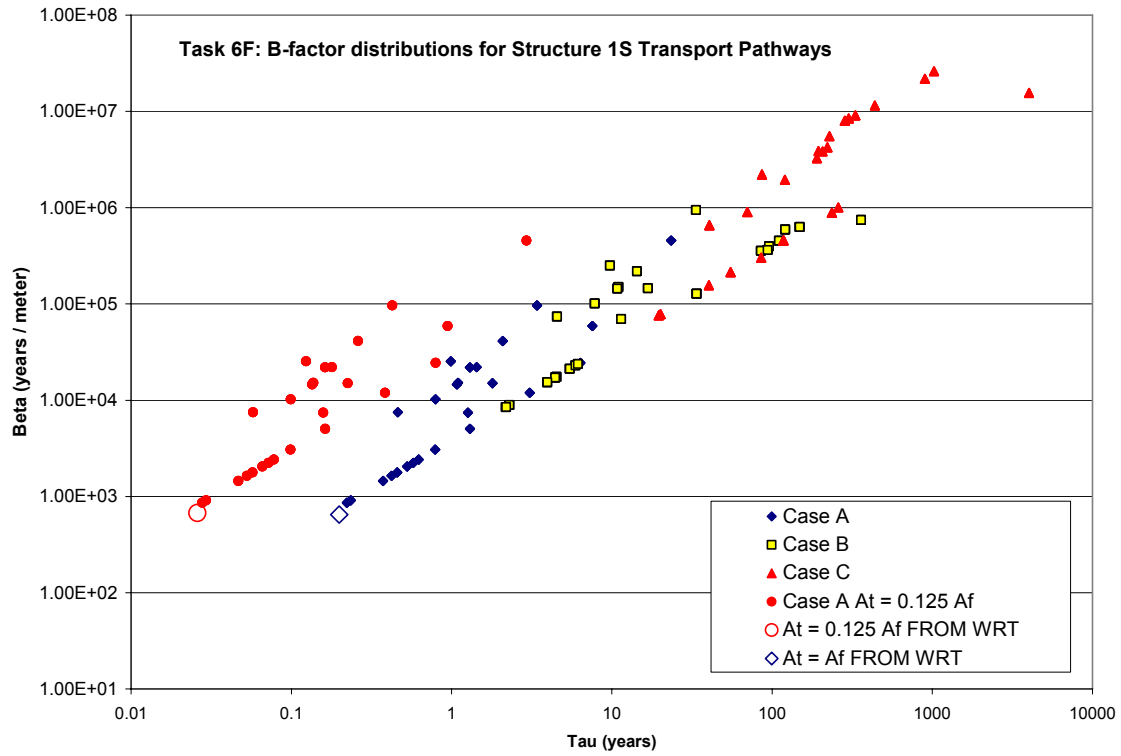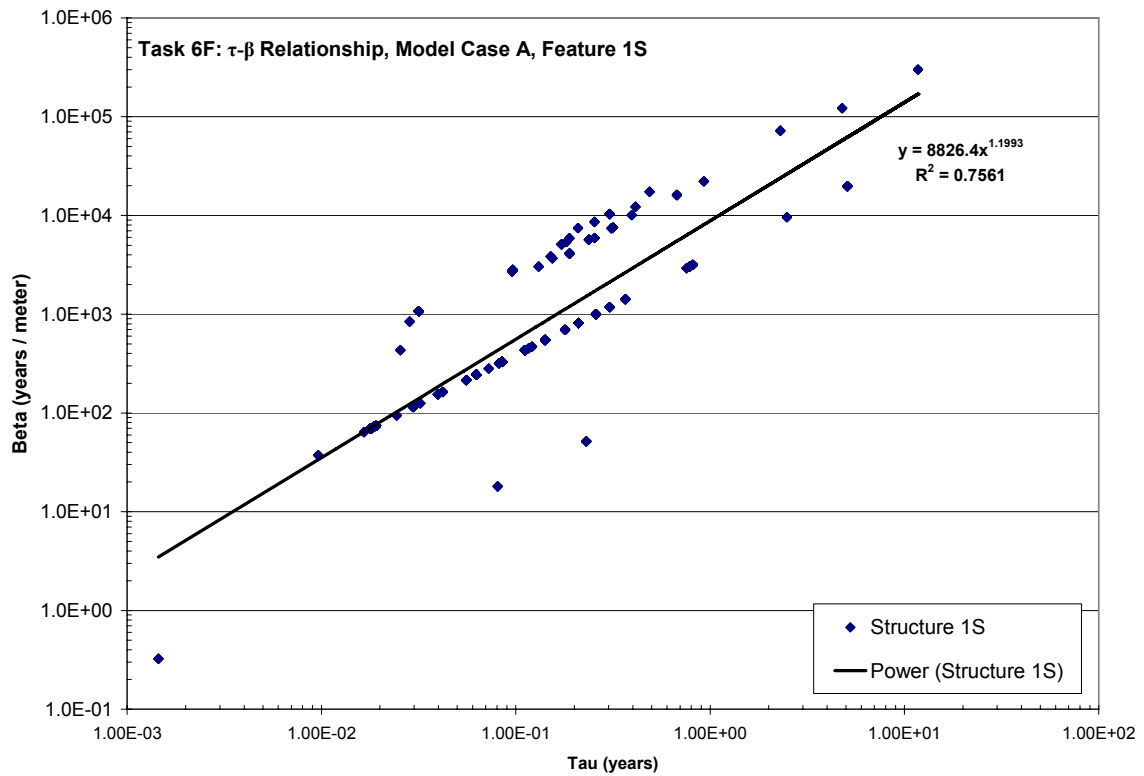| Statistic	Case A (Δh = 0.539)		Case B (Δh = 0.0539)		Case C (Δh = 0.00539)	
	Travel Time (yrs)	Beta (yrs / m)	Travel Time (yrs)	Beta (yrs / m)	Travel Time (yrs)	Beta (yrs / m)
Mean	2.47	31.44	18.45	3.39E+05	79.91	1.19E+06
Std. Dev.	4.66	4.22	11.56	3.05E+05	83.33	1.76E+06
5%	0.23	25.62	5.09	3.80E+04	0.00	0.00E+00
50%	1.08	31.28	17.11	2.69E+05	79.60	7.61E+05
95%	7.56	39.05	34.86	7.75E+05	235.68	4.86E+06

6.5.2 Transport

6.5.2.1 Tracer breakthrough curves

Tracer breakthrough curves, presented below in Figure 5 11 through Figure 5 18, are plotted based on normalized activity flux rates (1/years). Output from the LTG software package consists of cumulative release amounts for each tracer at each time step (Becquerels) and an activity flux rate at each sink (Becquerels per year). Normalized activity flux values are plotted by dividing the activity flux rate by the injected activity; due to rounding errors, this may result in cumulative recoveries higher than 100% of injected mass.

In addition, breakthrough time statistics (Table 6-8 through Table 6-13) were also computed, as per the Task 6F modelling specifications. Both these statistics and the tracer breakthrough time-series data were shipped to SKB as Microsoft Excel® spreadsheets.

Table 6-8. Tracer breakthrough statistics for Model Case A, Structure 1S.

Tracer	t_5 (years)	t_{50} (years)	t_{95} (years)	Max. Rel. Rate (1/years)	Recovery %
$^{129}I^-$	0.627	1.88	11.4	4.09E-01	100%
$^{137}Cs^+$	513	1140	34200	3.90E-04	99%
^{241}Am	4560	11400	68400	5.32E-05	99%

Table 6-9. Tracer breakthrough statistics for Model Case B, Structure 1S.

Tracer	t_5 (years)	t_{50} (years)	t_{95} (years)	Max. Rel. Rate (1/years)	Recovery %
$^{129}I^-$	6.84	11.4	228	3.42E-02	100%
$^{137}Cs^+$	7990	68400	N/R	1.61E-05	90%
^{241}Am	57000	250000	N/R	3.25E-06	80%

Table 6-10. Tracer breakthrough statistics for Model Case C, Structure 1S.

Tracer	t_5 (years)	t_{50} (years)	t_{95} (years)	Max. Rel. Rate (1/years)	Recovery %
$^{129}I^-$	57	228	3420	2.97E-03	100%
$^{137}Cs^+$	150000	N/R	N/R	5.50E-07	40%
^{241}Am	850000	N/R	N/R	1.14E-07	7%

Table 6-11. Tracer breakthrough statistics for Model Case A, Structure 4S.

Tracer	t_5 (years)	t_{50} (years)	t_{95} (years)	Max. Rel. Rate (1/years)	Recovery %
$^{129}I^-$	0.0285	0.125	4.56	5.29E+00	100%
$^{137}Cs^+$	34.2	228	22800	3.20E-03	100%
^{241}Am	342	1140	91300	3.83E-04	100%
Note: Incomplete tracer recovery due to dead ends along side of model					

Table 6-12. Tracer breakthrough statistics for Model Case B, Structure 4S.

Tracer	t_5 (years)	t_{50} (years)	t_{95} (years)	Max. Rel. Rate (1/years)	Recovery %
$^{129}I^-$	0.308	1.48	114	4.70E-01	100%
$^{137}Cs^+$	513	4560	900000	1.89E-04	95%
^{241}Am	3420	22800	N/R	2.88E-05	90%
* Note: Incomplete tracer recovery due to dead ends along side of model					

Table 6-13. Tracer breakthrough statistics for Model Case C, Structure 4S.

Tracer	t_5 (years)	t_{50} (years)	t_{95} (years)	Max. Rel. Rate (1/years)	Recovery %
129I-	2.28	22.8	3420	3.57E-02	100%
137Cs+	10300	350000	N/R	6.51E-06	61%
241Am	57000	N/R	N/R	1.45E-06	48%
Note: Incomplete tracer recovery due to dead ends along side of model					

Simulations of transport within Structure 4S did not reach complete tracer recovery. We believe that this was due to dead-end pathways along the southern edge of the model, as discussed in Chapter 6.5.1.1. Local gradients are steep enough to allow for tracer migration to a model boundary, but not for it to migrate back up gradient towards the sink wells.

The noise in the early-time history is a result of the Dirac pulse injection term; the LTG package occasionally has difficulty reaching a quality solution with very large concentration, very short time release boundary conditions.

Figure 6-29. *Task 6F normalized breakthrough curve, Structure 1S, Model Case A.*
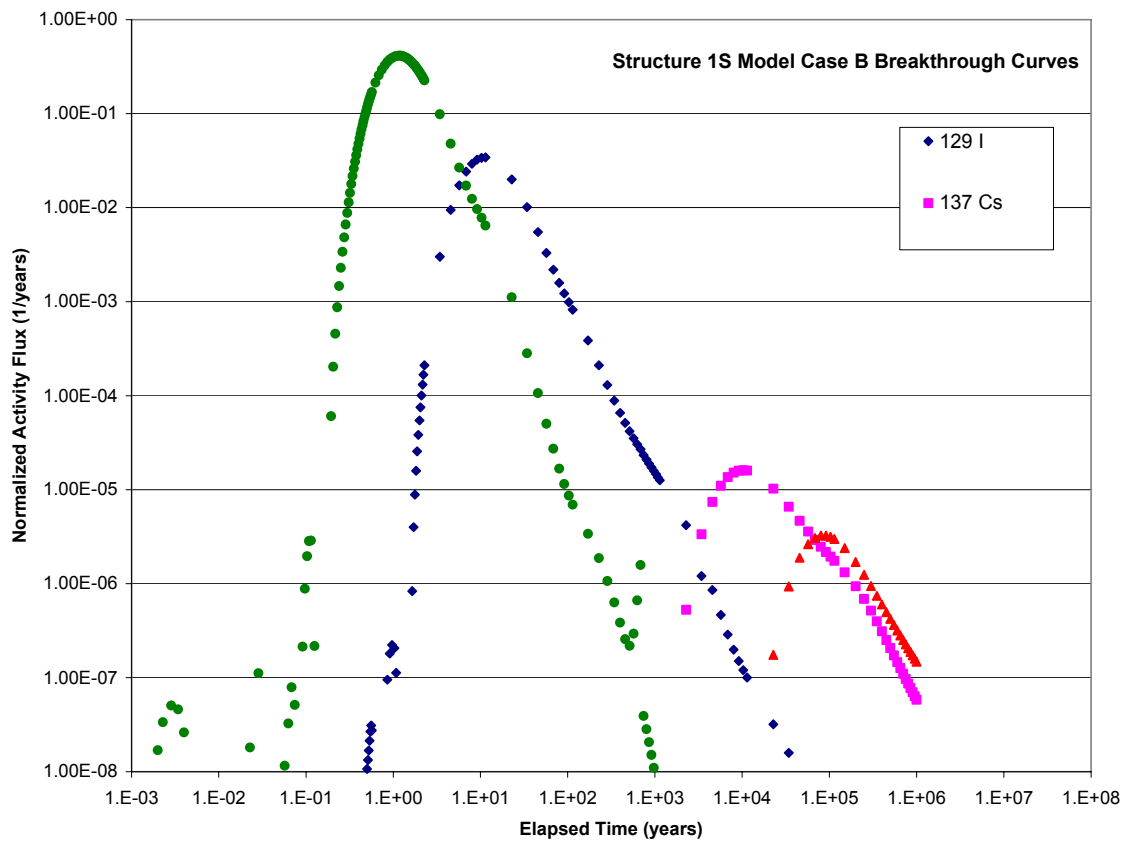
Figure 6-30. *Task 6F normalized breakthrough curve, Structure 1S, Model Case B.*

105
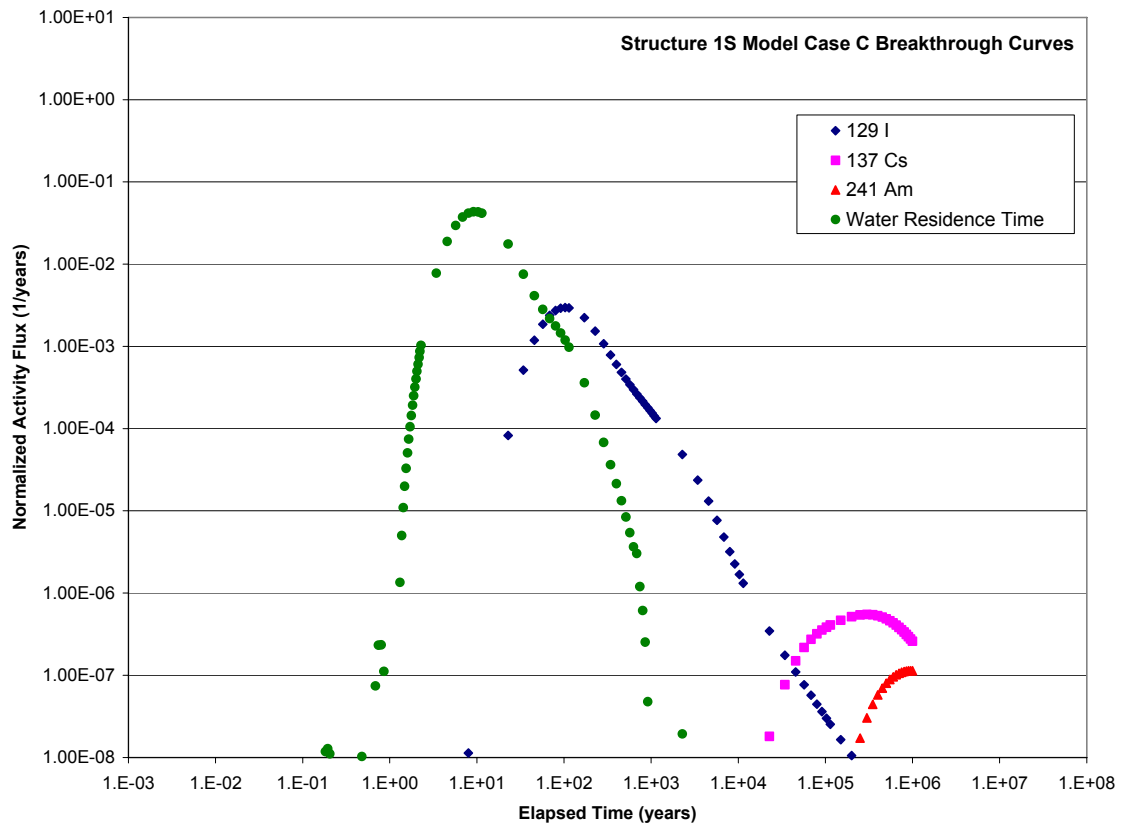
Figure 6-31. *Task 6F normalized breakthrough curve, Structure 1S, Model Case C.*
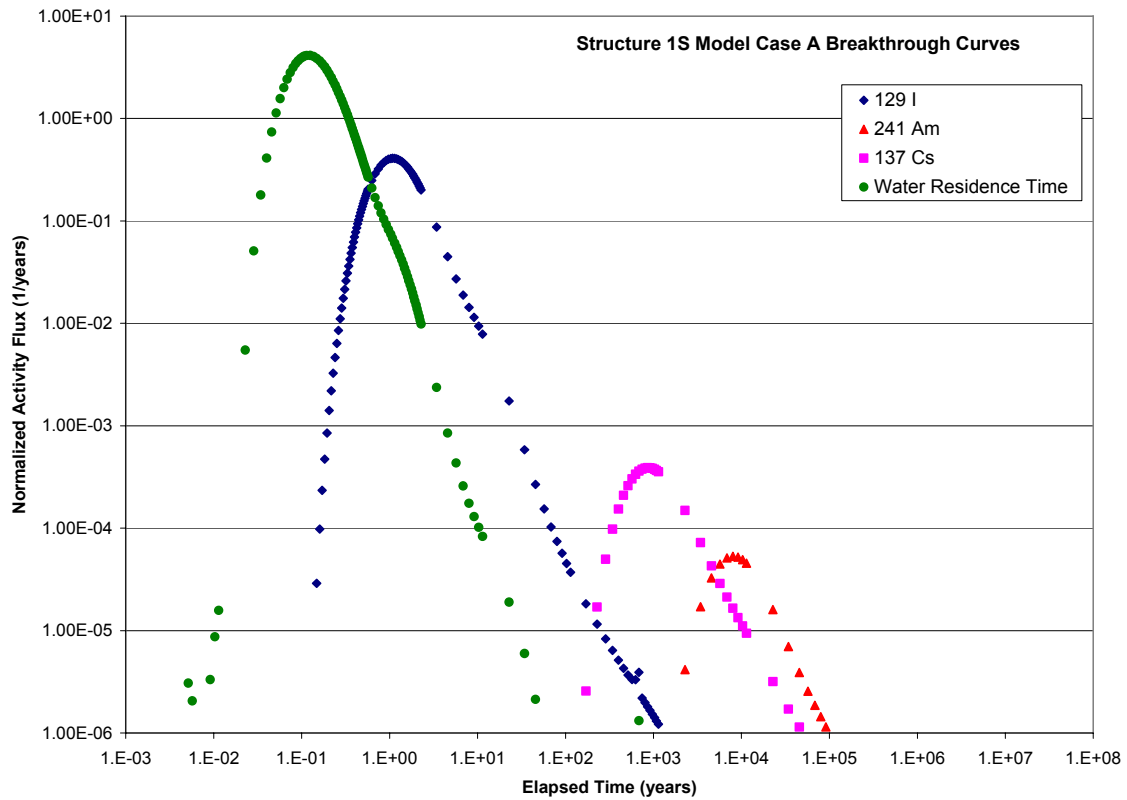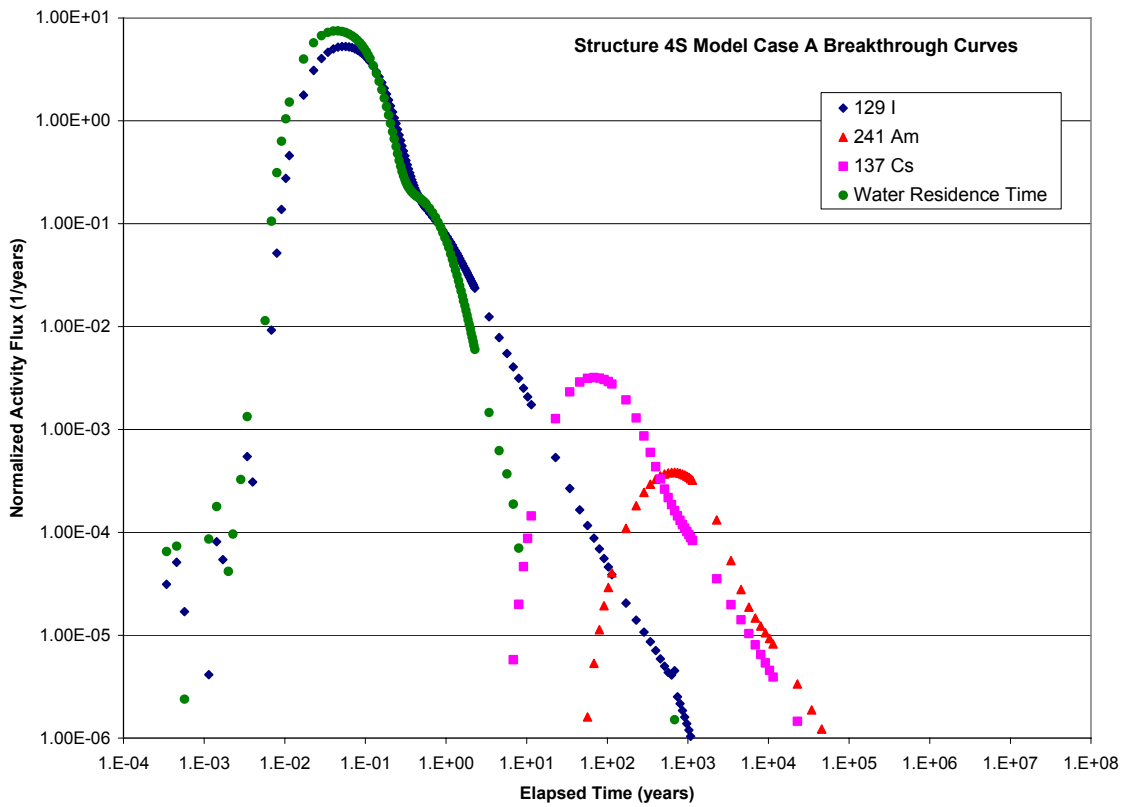

Figure 6-32. *Task 6F normalized breakthrough curve, Structure 4S, Model Case A.*
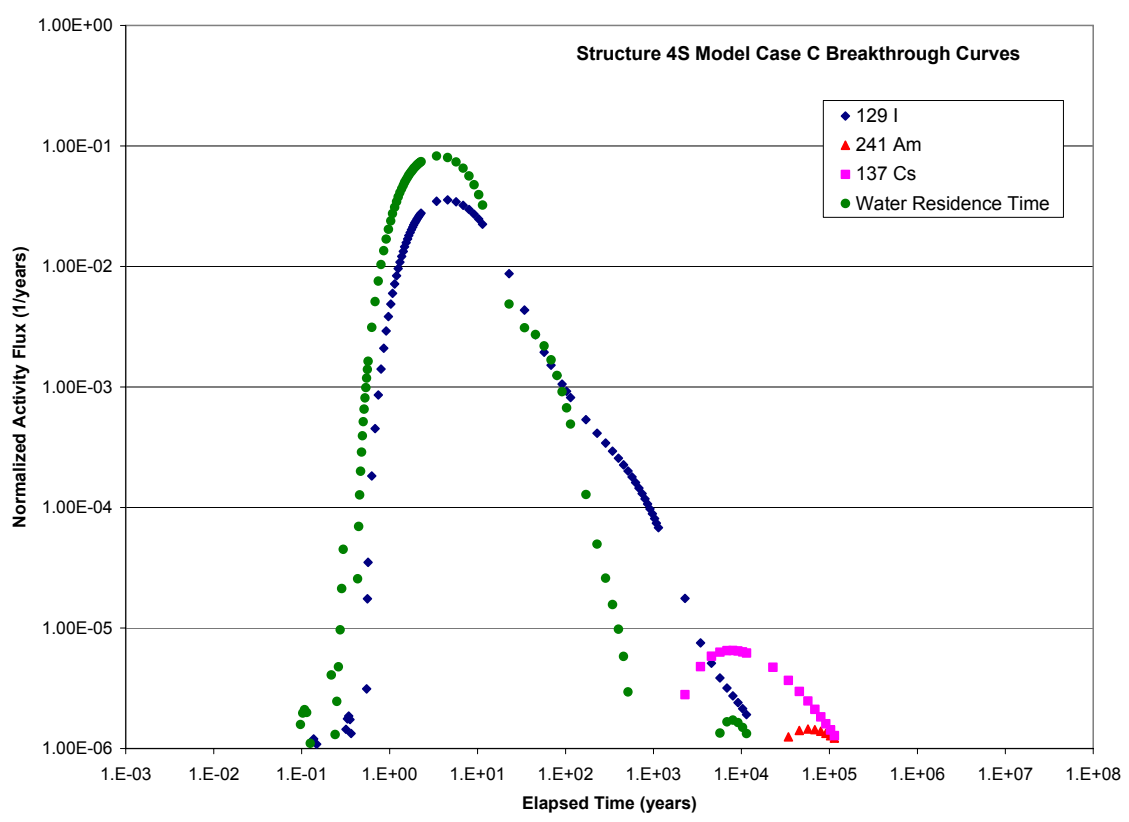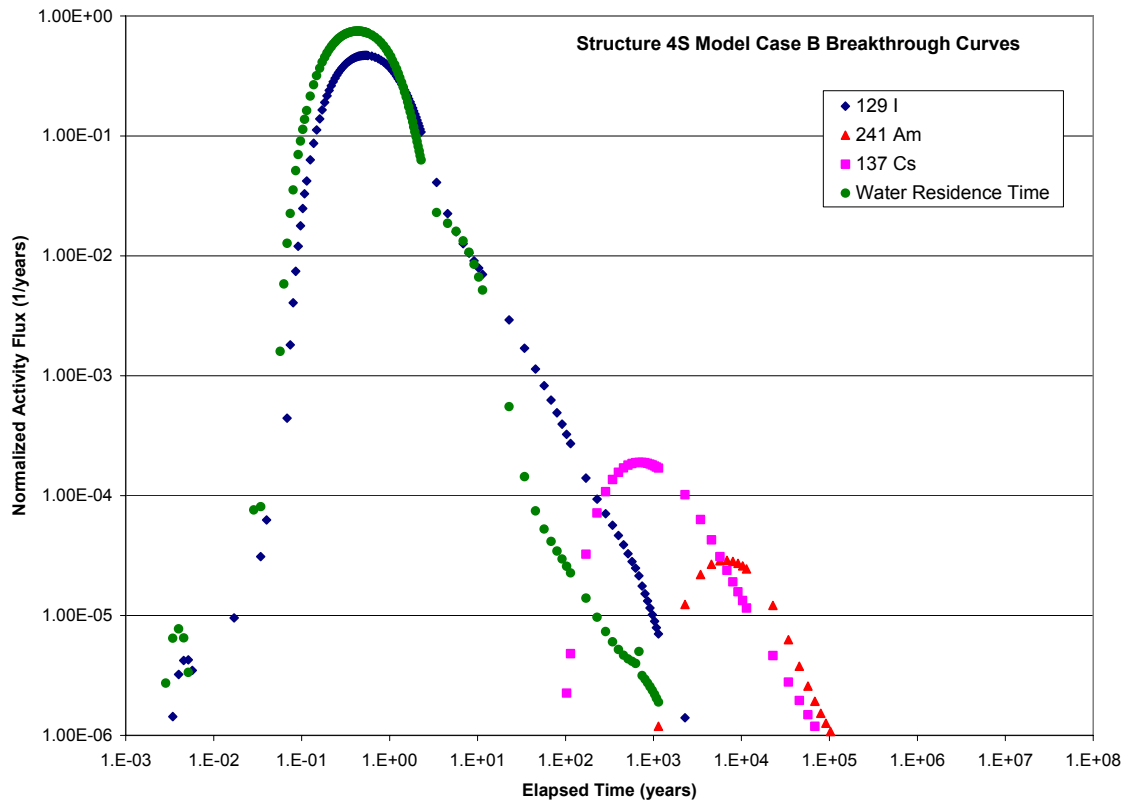
Figure 6-33. *Task 6F normalized breakthrough curve, Structure 4S, Model Case B.*
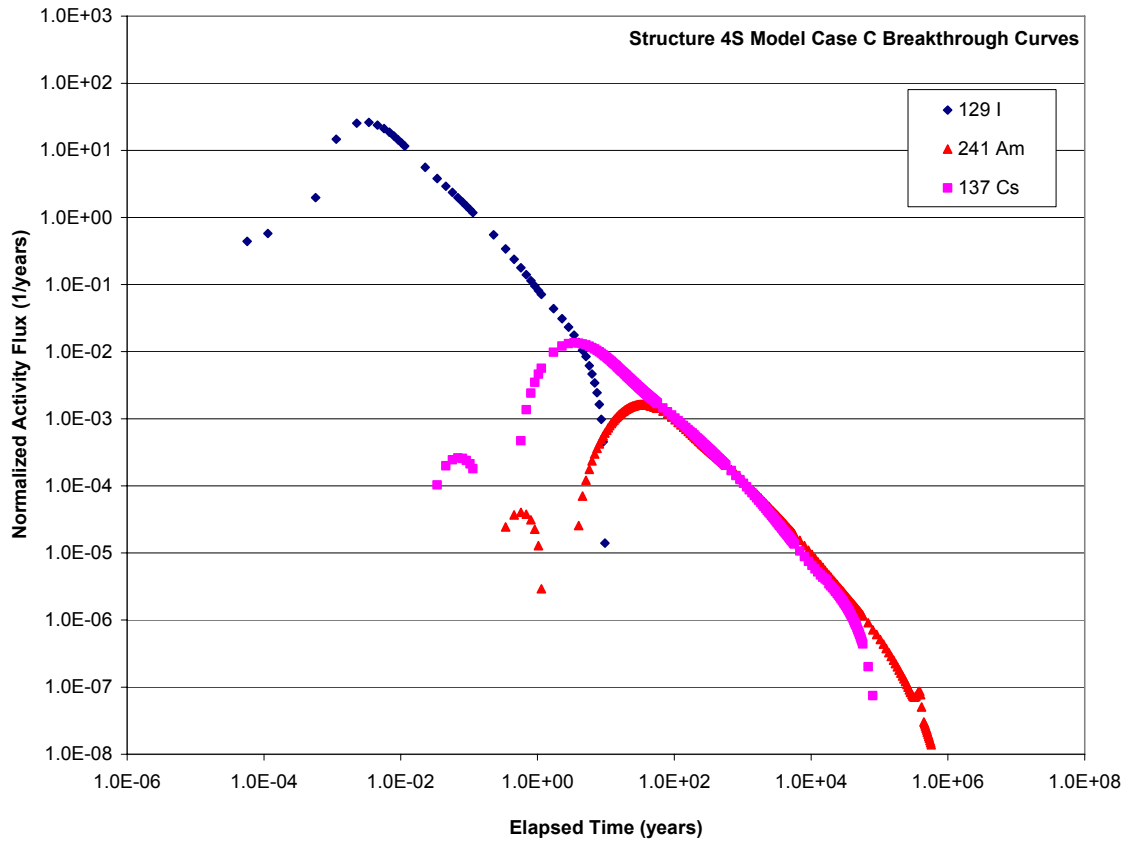
Figure 6-34. *Task 6F normalized breakthrough curve, Structure 4S, Model Case C.*

6.6 Task 6F2: Single-Fracture Sensitivity Studies

For the Task 6F2 sensitivity studies, the JNC/Golder team elected to study the effect of the channel network geometry on the flow and transport results. Specifically, we focused on the discretization of the three-dimensional discrete fracture network into a one-dimensional network of nodes and pipes.

6.6.1 Model Hypotheses

The JNC/Golder team addressed two specific questions during the Task 6F2 sensitivity studies:

1. For performance-assessment timescales, does the form and degree of the channel network discretization affect the final flow and transport predictions?

2. To what extent do factors such as node density and intersecting ('crossing') pipes affect retention in a feature of relatively limited complexity (such as Structures 1S and 4S)?

These questions were addressed through re-discretizations of the Task 6F DFN-CN models, with re-runs of both the flow and transport models. All of the additional Task 6 performance metrics (model geometry, β-factor distributions, water residence times, and tracer breakthrough data) were computed.

6.6.2 Task 6F2 CN Model Implementation

The JNC/Golder Task 6F simulations utilized the DFN models built for Task 6F on Structures 1S and 4S, as described in Chapter 6.2.1. No changes were made to the DFN model. Pipe discretization was performed using the PAWorks/Genpipe software package (Dershowitz et al, 2002). The DFN to CN discretization process is defined in detail in Chapter 3. The base Task 6F models used the following mesh discretization parameters:

1. CN pipes cannot cross each other; the pipes on a given fracture (such as 1S and 4S) will be created so that pipes do not cross. This, in theory, should prevent the simulation of additional rentention in 'intersection zones' within the plane of the test fracture.

2. The width of the 'pipes' that connect two nodes within a channel network were assigned based on the projected trace lengths of the intersecting fractures (see Figure 3-1). The pipe width (W_p) was biased towards the length of the smallest of the two traces, based on the following formula:

   $$W_p = (X_{min} * L_{min}) + (X_{max} * L_{max})$$

   where $X_{min} = 0.7$, $X_{max} = 0.3$, and L_{min}/L_{max} were the shorter and longer intersection trace lengths, respectively.

3. The CN mesh was discretized using an effective pipe factor of 2.0. The effective pipe factor is a mesh adjustment option designed to prevent Genpipes from producing excessively long and tortuous pathways (which, in a simplified model such as Task 6F, are unrealistic) through a single fracture. Genpipes will add additional nodes to the mesh that DO NOT lie on the intersection of two fractures so as to keep the tortuous distance between any two nodes in a fracture less than Cartesian distance multiplied by the effective pipe factor (Dershowitz et al., 2000).

For this sensitivity study, the only parameter that was changed was Parameter 1, the geometric relationships between CN pipes. PAWorks/Genpipes is capable of discretizing a CN mesh using several different pipe options (Dershowitz et al., 2000): Note that Task 6F2 was simulated with transport aperture assigned as 12.5% of hydraulic aperture.

- All Pipes ('_all'): This is the simplest method of pipe generation. Pipes connect every node (which is placed at the intersection of two fractures) to every other node. In addition, nodes are added where two pipes intersect. There are no geometric restrictions.

- Pipes cannot cross ('_default'): A new pipe may not cut across an existing pipe. This has been the standard for all Task 6 channel networks.

- Pipes cannot cross fracture traces ('_nct'): Pipes may not cut across existing pipes, nor can they cut across fracture traces. This option also enforces the additional restriction that each node must have at least one pipe connected to it.

- All pipes on a given fracture must be connected ('_conn'): This option will generate additional nodes and pipes so that all pipes on a single fracture are connected to each other.

- Include effective pipes ('_eff'): This is the same as the '_conn' option above, except that effective pipes are generated as per a user-specified threshold (see Parameter 3 above).

JNC/Golder Task 6F2 simulations used all of the above pipe generation options, in an attempt to further constrain the effects of network geometry on flow and transport parameters. New CN mesh files were generated from the Structure 1S DFN, sent to MAFIC for a steady-state head solution, sourced to PAWorks for pathway identification, and finally run through the LTG transport module to produce tracer breakthrough curves and time statistics. Table 6-14 describes the simulations completed, in terms of the number of nodes and pipes created during the CN discretization using different options. In general, fewer nodes and pipes lead to faster run times with less of a potential for numerical instability in LTG.

Table 6-14. Details of CN discretization of Task 6F2 DFN model (Structure 1S).

Model Case	# of Nodes	# of Pipes	Simulation Name
All Pipes	2606	90391	_all
Pipes Cannot Cross	2603	6665	_default
Pipes Cannot Cross Traces	2599	4340	_nct
All Pipes on Fracture Connected	2599	4405	_conn
Include Effective Pipes (EPP = 2.0)	2601	4958	_eff

6.6.3 Task 6F2 Sensitivity Study Results

The results of the JNC/Golder Task 6F2 sensitivity study were surprising. As indicated by Table 6-14, the different pipe discretization options had little effect on the number of nodes in the resulting 1D pipe mesh (see Figure 6-35 below).
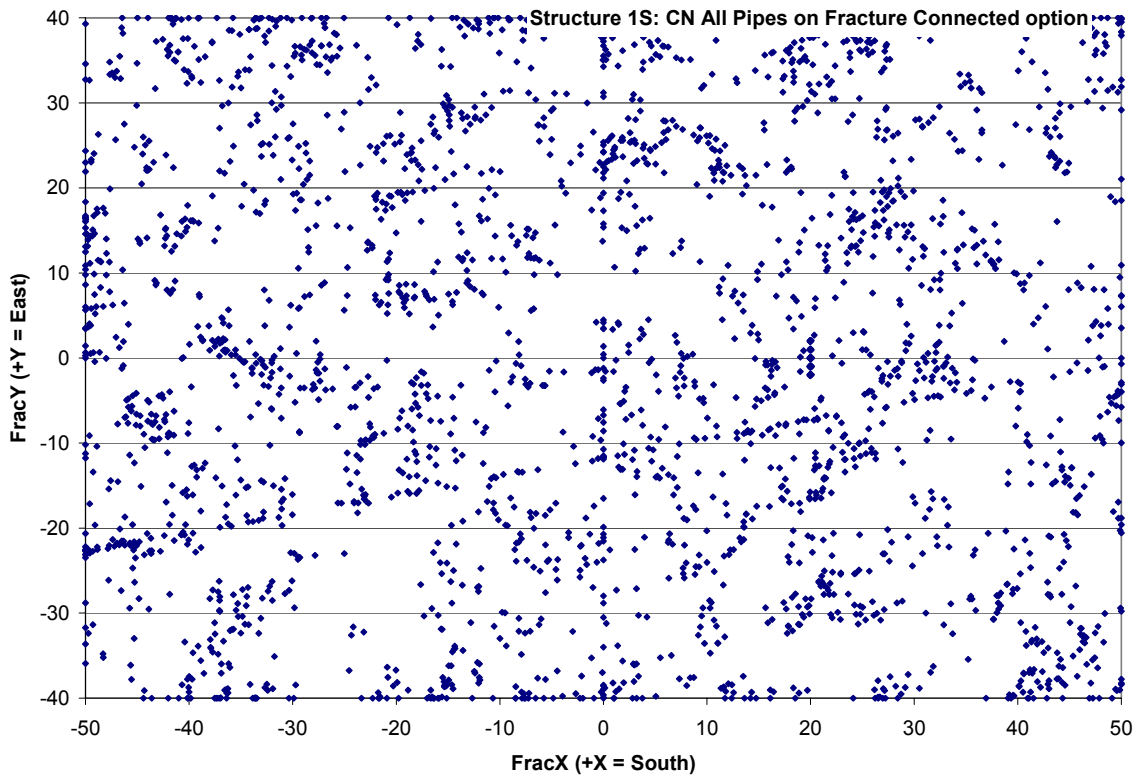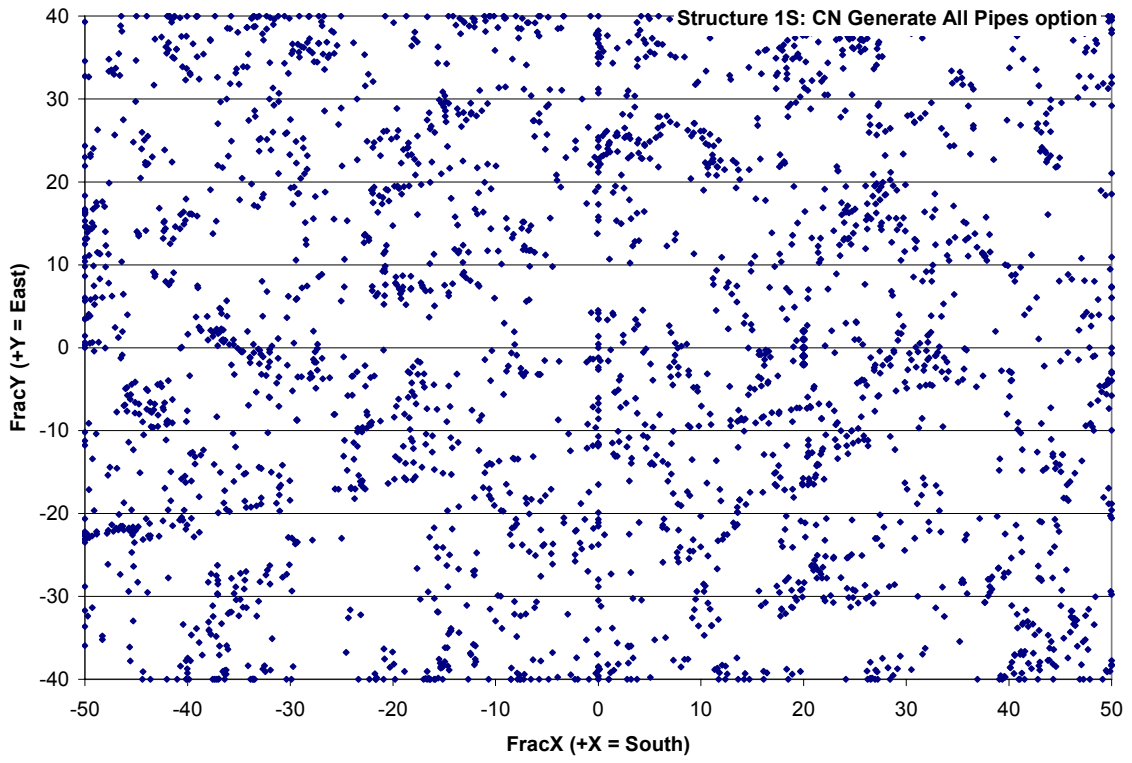
Figure 6-35. *Comparison of CN nodes produced using 'All Pipes' (top) and the 'All Pipes on Fracture Connected' options.*

However, the total number of pipes was highly variable. Especially surprising were the more than 90,000 pipes produced by the '_all' generation option. The '_all' pipes option significantly increased model computation times; in addition, both the MAFIC and LTG packages had difficulty converging on a solution using such an interconnected network. Significant dispersion of particles along the plane of Structure 1S was noted for model iterations using the 'All Pipes' option; in some cases, significant numbers of particles became 'stuck' down dead-end pathways near the no-flow edges of the Task 6F model regions. Figure 6-36 illustrates the difference between the two discretization options.
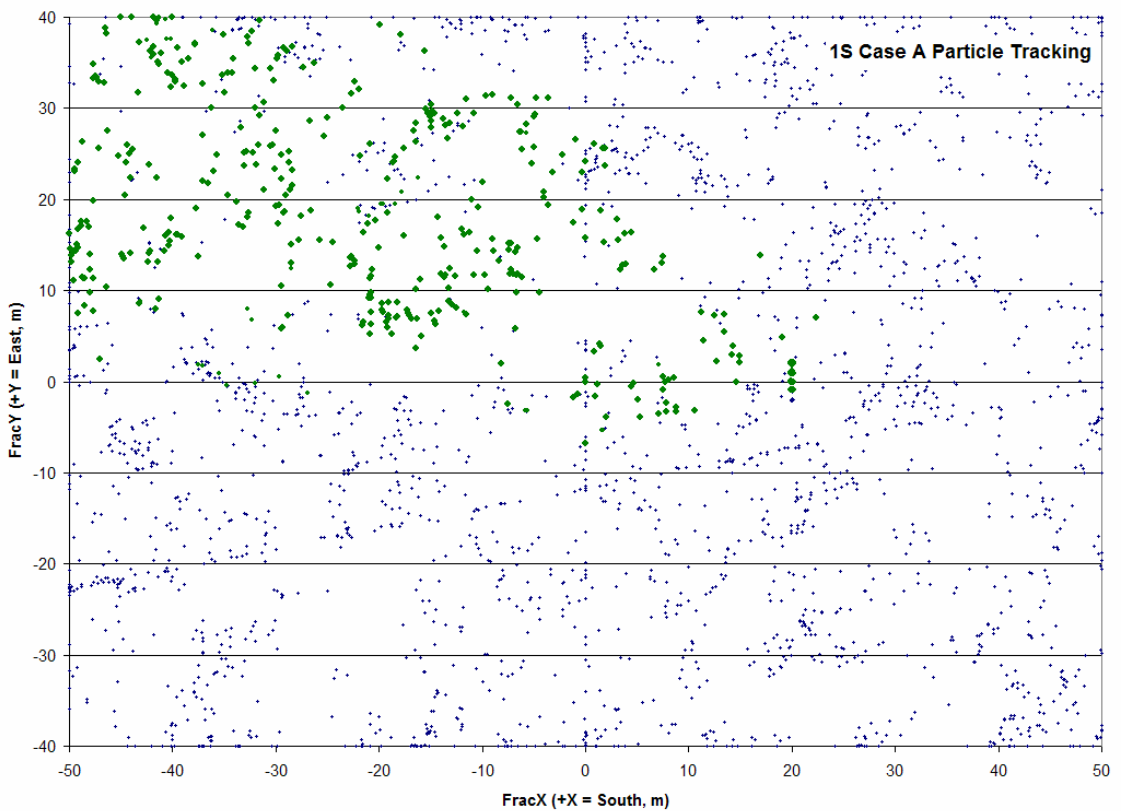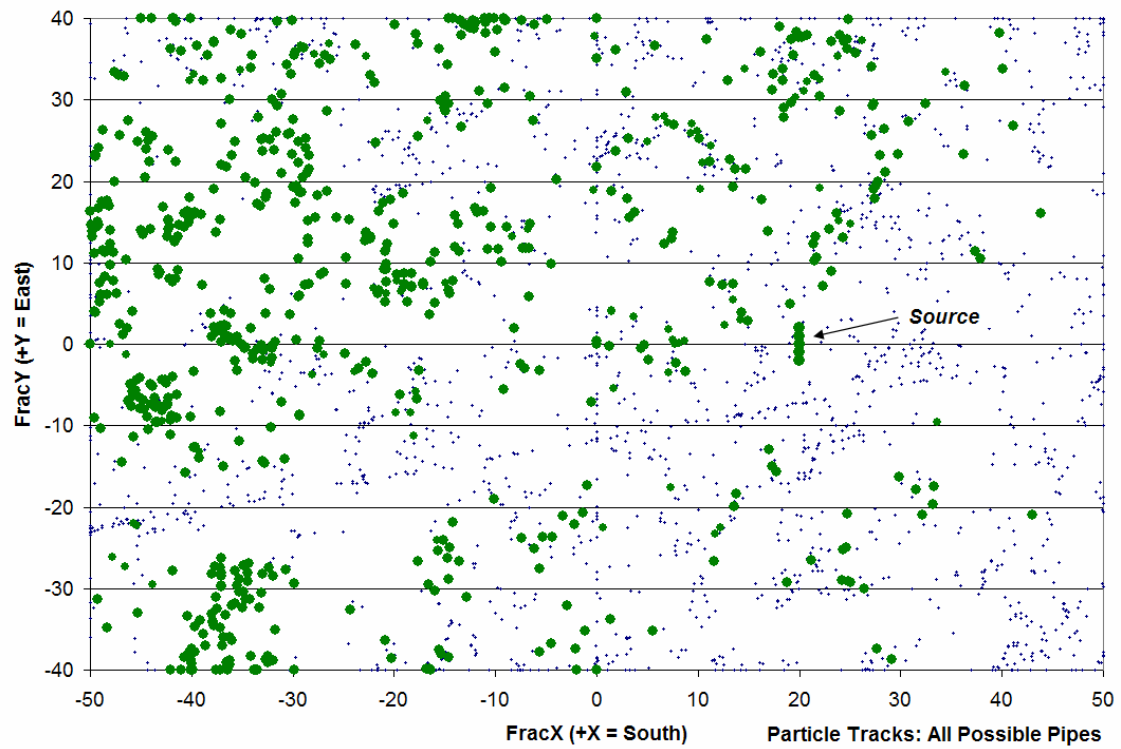
Figure 6-36. *Comparison of in-plane pathways identified through PAWorks particle tracking in the plane of Structure 1S. Top image is utilizing the 'All Pipes' option; note the significant dispersion and dead zones. Bottom image is using the 'No Crossing Pipes' option from Task 6F; note the lack of dispersion and confinement of the particles to the significant flow paths.*

A comparison of the 'No crossing pipes' and 'No crossing traces' options produced interesting results. It was expected that the 'No crossing traces' option might, on average, produce slightly longer potential pathways between the Task 6F sources and sinks. However, this was not the case. The 'no crossing traces' option produced, on average, slightly faster but longer pathways (see Table 6-15), resulting in a reduced β-factor distribution. However, the 'No crossing traces' option also produced several pathways that were significantly longer AND shorter that those identified during Task 6F. These new distributions are presented below as Figure 6-37. In general, both particle tracking and graph-theory searches suggested the 'No crossing traces' option produced pathways in Structure 1S with the shortest overall lengths and the fastest travel times. It is unknown, however, if this result is by itself significant, or is a consequence of a poorly-constrained steady-state head solution produced by a potential lack of connectivity in a 'no crossing traces' CN.
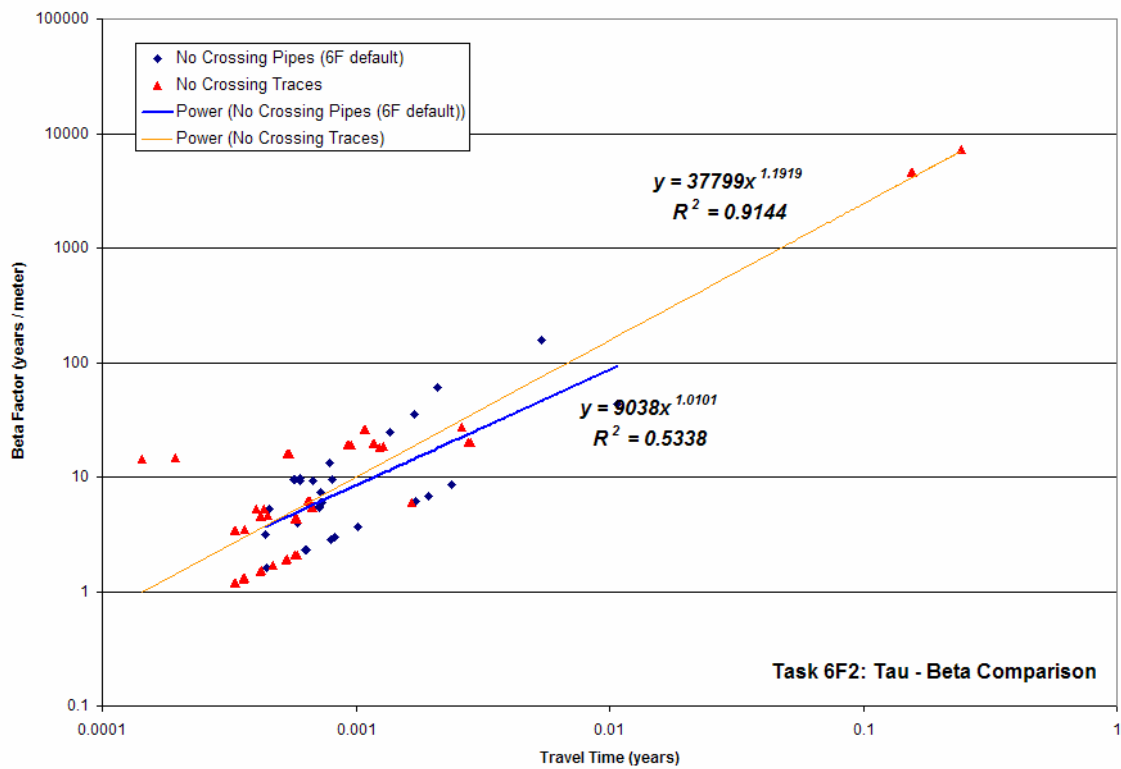
Figure 6-37. *Comparison of β-factor distributions for the 'No Crossing Pipes' and 'No Crossing Traces' CN discretization options.*
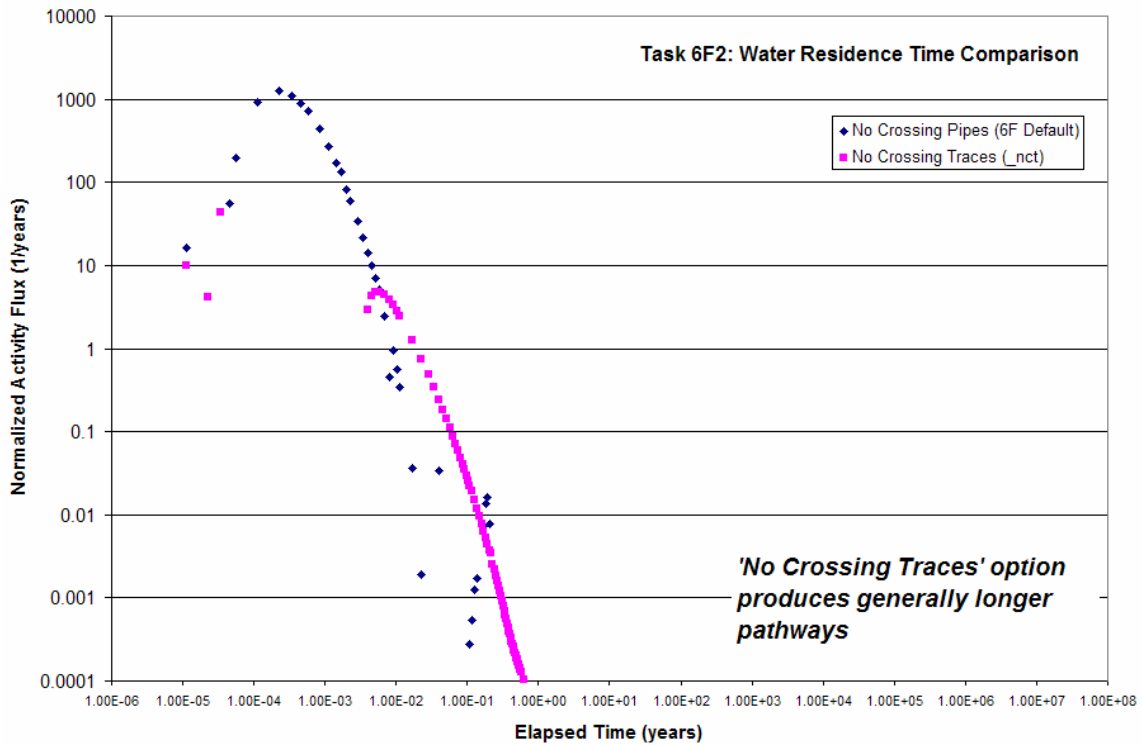
Figure 6-38. *Comparison of water residence time distributions (advection + dispersion) only) between the 'No Crossing Pipes' and the 'No Crossing Traces' CN discretization options.*

Table 6-15. Comparison of pathway statistics for the 'no crossing traces' and 'no crossing pipes' CN discretization options, JNC/Golder Task 6F2 modelling.

Particle Tracking Statistics (1000 particles released)			
Travel Times	**_all**	**_default**	**_nct**
Longest Path (years)	1.19E+02	1.80E+00	1.36E-02
Shortest Path (years)	4.89E-04	2.58E-04	1.44E-04
Mean (years)	1.57E+01	1.68E-01	6.29E-04
Std. Dev. (years)	1.78E+01	2.50E-01	1.07E-03
Geometric Pathway	**_all**	**_default**	**_nct**
Maximum # of Pipes Traversed	2999	715	19
Minimum # of Pipes Traversed	1	3	3
Mean # of Pipes Traversed	443	71	5
Std. Dev. (# of Pipes Traversed)	489	86	3

Structure #1: No Crossing Traces		
	Travel Time	**Beta**
	(yrs)	*(yrs / m)*
Mean	2.47E-02	7.19E+02
Std. Dev.	6.69E-02	1.99E+03
5%	3.34E-04	1.29E+00
50%	5.78E-04	5.41E+00
95%	2.44E-01	7.24E+03

Structure #1: No Crossing Pipes		
	Travel Time	**Beta**
	(yrs)	*(yrs / m)*
Mean	1.55E-03	1.79E+01
Std. Dev.	2.14E-03	3.19E+01
5%	4.45E-04	2.33E+00
50%	7.83E-04	7.41E+00
95%	5.40E-03	6.02E+01

Finally, the dense network of pipes on a Type I (fault) geologic structure produced by using the 'Generate All Pipes' was unsuitable for performance-assessment modelling using the current Task 6C microstructural model. Retention was drastically over-predicted, such that no tracer was ever detected crossing the channel network.

Slightly better results were obtained when using the 'No crossing pipes' (the default Task 6 settings) and the 'No crossing traces' discretization options. The 'No crossing traces' option produced faster breakthrough times than the 'No crossing pipes' option. Figure 6-39 suggests that no significant changes to the amount of retention caused by sorption or matrix diffusion was noted by using the 'No crossing pipes' option; this was a surprise, since the 'No crossing traces' option produced only two-thirds of the pipes that the 'No crossing pipes' option did. The reduced number of pipes should have resulted in a slight reduction in retention due to a lack of available surface area for sorption and diffusion. This suggests that both discretization methods produced similar hydraulically-significant pathways, and that the 'No crossing traces' option tended to discard non-hydraulically significant connections.
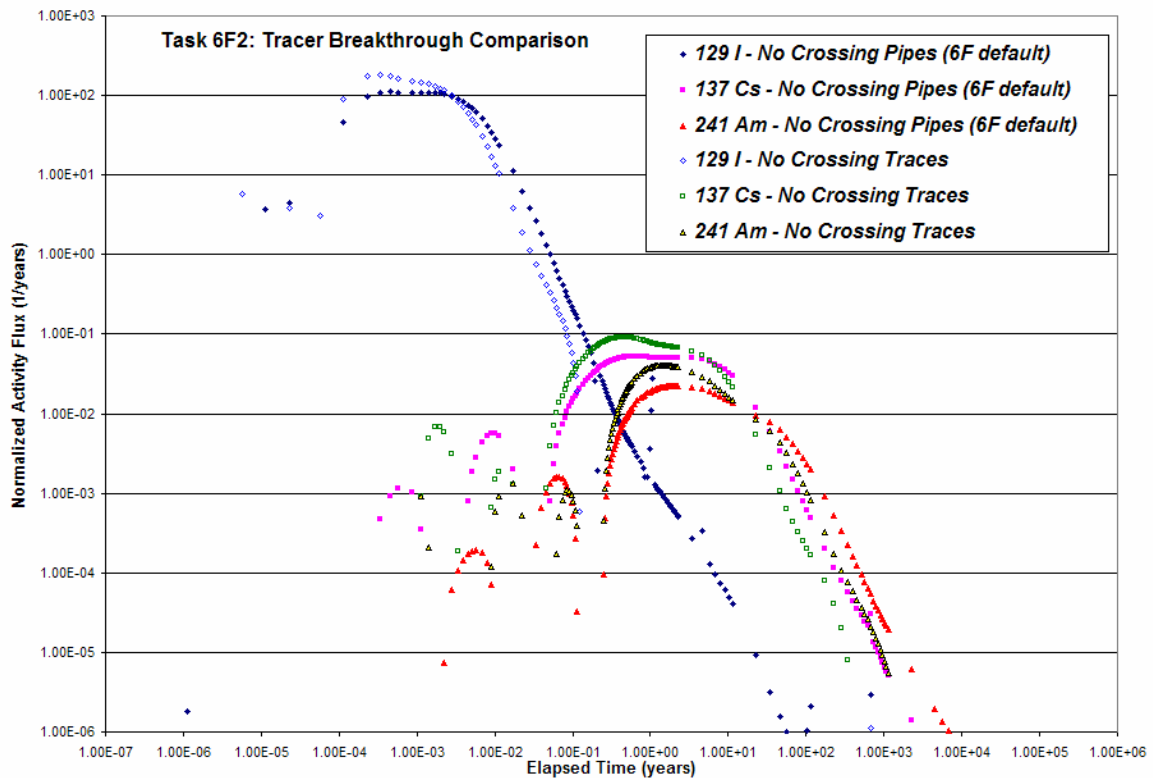

Figure 6-39. *Comparison of tracer breakthrough curves for different CN pipe discretization options, Task 6F2 sensitivity study.*

6.7   Task 6F and 6F2 Conclusions

The JNC/Golder team reached the following conclusions from the Task 6F and 6F2 modelling

1. While solute transport in fracture networks tends to be dominated by the pattern of fracture connectivity within the network, transport in single fractures depends on the discretization of the fracture into channels.

2. The discretization algorithms studied in Task 6F2 had a greater effect on pathway statistics than on the actual tracer transport results reported in e.g., Figure 6-39.

3. The PAWorks channel network modelling approach is optimized for evaluation of transport in complex networks, rather than for focusing on transport in single fractures as in Task 6F and 6F2. The plate element solute transport modelling used by Golder for modelling of Aspo Task Force Task 6B2 and similar approaches are more suited to this application.

4. Water residence time distributions for the three gradients modelling in Task 6F are similar, with simple scaling by gradient.

5. Sorbing solute transport behaviour, as indicated by the Tau-Beta relationship, and the Beta distribution are also similar between the three calses. Breakthrough curves for strongly sorbing tracers, however, do show increased retension for the slower flow flow rates.

7   Discussion and conclusions

7.1   Discussion of results

Task 6D and 6E are intended to study the differences between site characterization and performance assessment (PA) modelling at the scale of a rock block containing conductive fracture networks. As such the expected result was that the primary control on solute retention at the site characterization time frame is the more reactive, higher porosity, limited volume (gouge, fracture minerals) immobile zones, while the primary control on solute retention at the slower groundwater velocities of PA would be the larger volume, lower porosity, less reactive immobile zones of altered and intact rock.

Given that the JNC/Golder simulations were carried out under a microstructural model combining these two classes of immobile zones, it is not surprising that this pre-conception is confirmed by the simulations. Consequently, it is more in the sensitivity studies carried out than in the base cases of Tasks 6D, 6E, and 6F that insites are to be gained.

7.2   Main conclusions

The primary conclusion from Tasks 6D, E, F, and F2 are as follows:

1. Solute retention at site characterization and experimental time scales is controlled by different immobile zones, and consequently extrapolations from tracer testing to PA modelling must consider how the tracer testing constrains the transport processes and properties which apply to PA.

2. Fracture geometry (orientation, size, intensity) has a significant but not primary influence on solute transport at site characterization and PA time scales, provided connected transport pathways exist

3. Pathway geometry, and particularly path width strongly influence mobile zone/immobile zone interaction and therefore solute retention at both site characterization and PA time scales. Therefore, site characterization experiments are needed which improve the (currently poorly constrained) path width information

4. The fracture structure type and microstructural model provided a useful technique for defining immobile zone geometries and properties within the Task 6C fractured rock block conceptual model.

5. The fracture complexity factor concept has the potential to significantly increase solute retention at both site characterization and PA time scales, and therefore needs further study. In its current form, however, there is not sufficient geological and solute flow/transport information to make direct application of the complexity factor productive.

7.3 Lessons learned and implications for Task 6 objectives

The primary of objective of Task 6 was to provide a bridge between site characterization (SC) and performance assessment (PA) approaches to solute transport in fractured rock. Task 6D and 6E aimed to bridge the gap between PA and SC type models at "rock block" scale off approximately 100 m. This scale is both PA-type and SC-type models will be applied to tracer experiment considering both the experimental boundary conditions and boundary conditions for a PA scale.

Task 6D, 6E, 6F, and 6F2 directly supported these objectives, by providing a first comparison of modelling approaches for a well defined 100 m scale rock block.

- Modelling for 6D/E/F/F2 was based only on detailed modelling approaches generally reserved for site characterization. Therefore, the goal of utilizing PA modelling tools was not met. However, the simulation tools used in 6D/E/F/F2 were sufficiently numerically efficient to be used for PA, should this be desired in the future

- The difference between site characterization and PA modelling was defined in terms of boundary conditions, with the consequent effect on the relative importance of different immobile zones. If PA modelers accept this concept, then more detailed site characterization models, which better reflect site characterization data, could have increased applicability in PA studies

- Task 6A/B focused in part on how site characterization modelling constrains PA modelling. This was not studied in Task 6D/E/F/F2. Rather the 6D/E/F/F2 modelling was more concerned with how particular aspects of the fractured rock hydrostructural and microstructural models and model parameters potentially effect repository safety.

8 References

Andersson, P., Byegård, J., Holmqvist, M., Skålberg, M., Wass, E., and Widestrand, H. (2001): TRUE Block Scale Tracer Test Stage, Tracer test, Phase C, International Progress Report IPR-01-33, Svensk K AB (SBK), Stockholm, Sweden.

Andersson, P., Byegård, J., Doe, T., Hermanson, J., Meier, P., Tullborg, E-L., and Winberg, A. (2002a): TRUE Block Scale Project Final Report – 1. Characterization and model development, Technical Report TR-02-13, Svensk Kärnbränslehantering AB (SKB), Stockholm, Sweden.

Andersson, P, Byegård J., and Winberg, A. (2002b): TRUE Block Scale Project Final Report – 2. Tracer tests in the block scale, Technical Report TR-02-14, Svensk Kärnbränslehantering AB (SKB), Stockholm, Sweden.

Bear, J., (1972): Dynamics of Fluids in Porous Media, American Elsevier Publishing Co., New York, New York.

Byegård J. et al. (1992): Field and laboratory studies of the reduction and sorption of technetium(VII), Radiochim. Acta 58/59 239-244.

Cvetkovic, V., Selroos, J-O., and Cheng, H. (1999): Transport of reactive solute in single fractures, J. Fluid Mech. 318:335-356.

Deer, W., Howie, R., and Zussman, J. (1966): An Introduction to The Rock Forming Minerals, Halsted Press, John Wiley and Sons, New York.

Dershowitz, W., Foxford, T., Sudicky, E., Shuttle, D., Eiben, T., Ahlstrom, E. (2000): PAWorks: Pathways Analysis for Discrete Fracture Networks with LTG Solute Transport, User Documentation, Version 1.62, Golder Associates, Inc., Redmond, Washington.

Dershowitz, W., Winberg, A., Hermanson, J., Byegård, J., Tullborg, E-L., Andersson, P., and Mazurek, M. (2002): Task 6C - Construction of block scale semi-synthetic hydrostructural models and attribution of hydraulic and transport properties.

Elert, M. and Selroos, J-O. (2002): TASK 6D Modelling task specification, Version 1.0, Svensk Kärnbränslehantering AB (SKB), Stockholm, Sweden.

Elert, M. and Selroos, J-O. (2004a): TASK 6D Specification of additional performance measures, Version 1.0, February 2004, Svensk Kärnbränslehantering AB (SKB), Stockholm, Sweden.

Elert, M. and Selroos, J-O. (2004b): Task 6E Modelling task specification, Version 3.0, January 2004, Svensk Kärnbränslehantering AB (SKB), Stockholm, Sweden.

Elert, M., and Selroos, J-O. (2004c): Task 6F Sensitivity Analysis - Modelling task specification – Simplified "Test Bench" calculations, Version 3.0, December 2004, Svensk Kärnbränslehantering AB (SKB), Stockholm, Sweden.

Elert, M., and Selroos, J-O (2004d): Task 6F2 Sensitiviy Analysis – Modelling task specification – Additional Tasks, Version 1.0, December 2004, Svensk Kärnbränslehantering AB (SKB), Stockholm, Sweden.

Holmqvist, M., Andersson, P., Trick, T., Fierz, T., Eichinger, L., and Scholtis, A. (2000): Test of new possible non-reactive tracers - experimental description and evaluation, Äspö Hard Rock Laboratory, International Technical Document ITD-00-07, Svensk Kärnbränslehantering AB (SKB), Stockholm, Sweden.

Jansson, M. and Eriksen, T. (2001): CHEMLAB; A probe for in-situ radionuclide experiments, Technical Report TR-01-14, Svensk Kärnbränslehantering AB (SKB), Stockholm, Sweden.

Miller, I., Lee, G., Dershowitz, W. (2002): MAFIC: Matrix/Fracture Interaction Code with Heat and Solute Transport, User Documentation Version 1.712, Golder Associates, Inc., Redmond, Washington

Oda, M., (1984): Permeability Tensor for Discontinuous Rock Masses, Geotechnique, Vol. 35, pp. 483-495.

Sudicky, E., (1989): The Laplace Transform Galerkin technique: A time-continuous finite element theory and application to mass transport in groundwater, Water Resources Research, v. 18 no. 3, p. 1833-1846.

Sudicky, E., (1990): The Laplace Transform Galerkin technique for efficient time-continuous solution of solute transport in double-porosity media, Geoderma, v. 46, p. 209-232

Sudicky, E., and McLaren, R. (1992): The Laplace Transform Galerkin technique for large-scale simulation of mass transport in discretely fractured porous formations", Water Resources Research, v. 28 no 2, p. 499-514.

Systems Simulation Group, Golder Associates, Inc. (1999): GoldSim User's Guide, Version 6.01, Redmond, Washington.

Walker, D., and Gylling, B., (1998): Site-scale groundwater flow modelling of Aberg, Technical Report TR 98-23, Svensk Kärnbränslehantering AB (SKB), Stockholm, Sweden.